



NATIONAL INSTITUTE FOR CONGESTION REDUCTION

FINAL REPORT

31st July 2021

Proactive Congestion Management

Sisinnio Concas

Mohsen Kamrani

Vishal C. Kummetha

For:

National Institute for Congestion Reduction

University of South Florida

Center for Urban Transportation Research | University of South Florida



NICR
NATIONAL INSTITUTE FOR
CONGESTION REDUCTION

DISCLAIMER

The contents of this report reflect the views of the authors, who are responsible for the facts and the accuracy of the information presented herein. This document is disseminated in the interest of information exchange. The report is funded, partially or entirely, by a grant from the U.S. Department of Transportation's University Transportation Centers Program. However, the U.S. Government assumes no liability for the contents or use thereof.

Technical Report Documentation Page

1. Report No.	2. Government Accession No.	3. Recipient's Catalog No.	
4. Title and Subtitle Proactive Congestion Management		5. Report Date November 23, 2021	
		6. Performing Organization Code	
7. Author(s) Vishal Kummetha, Sisinnio Concas, Mohsen Kamrani		8. Performing Organization Report No.	
9. Performing Organization Name and Address Center for Urban Transportation Research University of South Florida 4202 E. Fowler Ave, CUT 100 Tampa, FL 33620		10. Work Unit No. (TRAIS)	
		11. Contract or Grant No. 69A3551947136	
12. Sponsoring Organization Name and Address U.S. Department of Transportation, University Transportation Centers 1200 New Jersey Avenue, SE Washington, DC 20590 United States		13. Type of Report and Period Covered	
		14. Sponsoring Agency Code	
15. Supplementary Notes			
16. Abstract <p>This report details the development and implementation of a method to proactively detect and mitigate congestion on freeways and arterials. To accomplish this goal, the research utilizes data fusion between conventional sources, such as radar detectors and traditional probe-based data, with newer sources, such as Bluetooth and connected vehicle (CV) data, to identify conditions that signal impending congestion. Data-driven and signal processing techniques are explored and developed to produce an algorithm that relies on near-real- or real-time traffic measurements capable of generating predictions proactively, using complex and often subtle factors that trigger congestion. The algorithm is validated and calibrated using traffic and other relevant data from comparable roadway facilities located in Florida and Texas. The algorithm is robust enough to function on both traditional and CV-based datasets and provides distinction between four intensity levels of congestion. The algorithm is applied within a microsimulation model to test the effectiveness of congestion mitigation strategies ranging from speed harmonization to dynamic rerouting, implemented individually and simultaneously. Performance measurement benchmarks show how these strategies prove to be effective in proactively reducing recurring and non-recurring congestion while providing additional safety benefits. Finally, this project demonstrates the clear advantage of using CV-based travel time estimates to calibrate microsimulation models over fixed point-based derivations of travel time from spot speeds.</p>			
17. Key Words Proactive management, recurring congestion, non-recurring congestion		18. Distribution Statement	
19. Security Classification (of this report) Unclassified.	20. Security Classification (of this page) Unclassified.	21. No. of Pages 77	22. Price

Table of Contents

DISCLAIMER.....	ii
Table of Contents	iv
Tables	vi
Figures	vi
List of Abbreviations.....	viii
Executive Summary	1
1. Introduction.....	2
1.1. Objectives.....	2
1.2. Outline.....	3
2. Literature Review	3
2.1. Congestion on Freeways	3
2.2. Real-time Congestion Prediction.....	10
2.3. Active Traffic and Demand Management (ATDM) Strategies.....	13
2.3.1. Driver Alerts.....	13
2.3.2. Speed Harmonization	14
2.3.3. Variable Message Signs (VMS)	14
2.3.4. Ramp Metering.....	14
2.3.5. Incident Detection.....	15
2.3.6. Dynamic Re-routing and Pre-travel Information	15
2.3.7. Speed Feedback Signs	16
3. Methodology	16
3.1. Data Compatibility and Preprocessing	16
3.2. Facility Description	19
3.2.1. Florida.....	19
3.2.2. Texas.....	21
3.3. Data Fusion.....	22
3.4. Developing the Congestion Detection Algorithm	25
4. Results and Discussion	31
4.1. Congestion Detection Algorithm.....	31
4.1.1. Algorithm Validation	31

4.1.2.	Approach Limitations	35
4.2.	Microsimulation	36
4.2.1.	Baseline Geometry	36
4.2.2.	Simulation Calibration	37
4.2.3.	Congestion Mitigation	42
4.2.4.	Approach Limitations	51
5.	Conclusions.....	52
6.	Future Research	53
	References.....	53
	Appendix A: Algorithm Validation	57
	Appendix B: Recurring Calibration	64
	Appendix C: Non-recurring Calibration	66

Tables

Table 2-1. Summary of the performance measures in HCM	5
Table 2-2. Commonly used performance measures of congestion	6
Table 2-3. Further breakdown of LOS F	9
Table 3-1. Definitions used	16
Table 3-2. Geometric properties of the Selmon Expressway.....	20
Table 3-3. Traffic statistics of the Westbound segments of the Selmon Expressway (2019).....	20
Table 3-4. Facility/segment matching criteria	20
Table 3-5. Geometric properties of the matched segments in Texas.....	21
Table 3-6. Traffic statistics of the matched segments in Texas	22
Table 3-7. Levels of congestion	29
Table 4-1. Confusion matrix for the congestion detection algorithm	32
Table 4-2. Established manual validation error rules by case.....	33
Table 4-3. Summary of Incident validation	34
Table 4-4. Desired speed distributions for individual road classes.....	39
Table 4-5. Car-following model selection and modified parameters for recurring conditions	39
Table 4-6. Car-following model selection and modified parameters for non-recurring conditions.....	41
Table 4-7. Location of recurring congestion estimated from average section speed on seed day	42
Table 4-8. Selected speed advisories for recurring congestion	43
Table 4-9. Summary of recurring TT improvements during 7 AM – 9 AM by section	44
Table 4-10. Summary of recurring TT improvements during 5 AM – 10 AM by section	44
Table 4-11. Location of incident-related congestion estimated from average section speed on seed day	47
Table 4-12. Selected speed advisories for incident-related congestion	48
Table 4-13. Summary of incident-related TT improvements during 7 AM – 9 AM by section	48
Table 4-14. Summary of incident-related TT improvements during 5 AM – 10 AM by section	49
Table 4-15. Summary of TT improvements obtained from microsimulation models	51

Figures

Figure 2-1. Greenshields speed, flow, and density relationships (Greenshields, 1935).....	4
Figure 2-2. Influence areas of segments	7
Figure 2-3. Density, speed, and LOS thresholds (HCM 2010 : highway capacity manual, 2010)	8
Figure 2-4. Fuzzy input subsets (Tseng et al., 2018)	11
Figure 3-1. Test corridor for TT comparison between BSMs and Bluetooth nodes	17
Figure 3-2. Bluetooth-based AM TTs by day	18
Figure 3-3. BSM-based AM TTs by day	18
Figure 3-4. Scatter plots of TTs obtained via BSMs and Bluetooth.....	19
Figure 3-5. RSU locations closest to the Selmon Expressway in Tampa, FL.....	19
Figure 3-6. Snapshot of the 6-point Excel matching table for 3 lane segments	21
Figure 3-7. Data fusion flow diagram for facilities in Texas	23
Figure 3-8. Two-mile segment split of the Selmon Expressway in Tampa, FL	23
Figure 3-9. TT generation using BSMs in Tampa, FL	24

Figure 3-10. Data fusion flow diagram for Selmon Expressway in Tampa, FL25

Figure 3-11. Density plots of TTI and b1 metric by segment26

Figure 3-12. Exponential moving average (EMA) applied to b1 metric26

Figure 3-13. Second order Butterworth filter output27

Figure 3-14. Density plots of Butterworth filter output by segment.....27

Figure 3-15. Cumulative density function (CDF) depicting the Butterworth filter differences in congestion types28

Figure 3-16. Butterworth filter thresholds of various levels of congestion29

Figure 3-17. Congestion detection algorithm development and validation framework (Kummetha et al., 2021)30

Figure 4-1. Distributions for maximum TTI during morning congestion32

Figure 4-2. Location of virtual detectors used to estimate TTs36

Figure 4-3. 2D facility layout in the WB direction36

Figure 4-4. BSMS-observed TT in minutes across the 0.5-mile sections for the recurring seed day.....38

Figure 4-5. NRMSE and MAPE results for calibration of recurring conditions.....40

Figure 4-6. BSMS-observed TT in minutes across the 0.5-mile sections for the incident seed day41

Figure 4-7. NRMSE and MAPE results for calibration of incident-related congestion.....41

Figure 4-8. Single vehicle speed profiles through various recurring congestion mitigation strategies45

Figure 4-9. Space-time charts showing the impact of mitigation strategies as applied to recurring congestion (red zones indicate congestion)46

Figure 4-10. Single vehicle speed profiles through various non-recurring congestion mitigation strategies.....49

Figure 4-11. Space-time charts showing the impact of mitigation strategies as applied to non-recurring congestion50

List of Abbreviations

AADT	Annual Average Daily Traffic
API	Application Programming Interface
ATDM	Active Traffic and Demand Management
AWAM	Anonymous Wireless Address Matching
BSM	Basic Safety Message
CAVs	Connected and Autonomous Vehicles
CCTV	Closed-Circuit Television
CDF	Cumulative Distribution Function
COVID	Corona Virus Disease
CUTR	Center for Urban Transportation Research
CV	Connected Vehicle
DDHF	Directional Design Hour Flow
DDHV	Directional Design Hour Volume
DR	Dynamic Rerouting
DSRC	Dedicated Short Range Communications
EEBL	Electronic Emergency Brake Light
EMA	Exponential Moving Average
ERDW	End of Ramp Deceleration Warning
FCW	Forward Collision Warning
FFS	Free flow Speed
FIR	Finite Impulse Response
FN	False Negative
FP	False Positive
GPS	Global Positioning System
HCM	Highway Capacity Manual
HMI	Human Machine Interface
I2I	Infrastructure to Infrastructure
IIR	Infinite Impulse Response
LOS	Level of Service
MAPE	Mean Absolute Percentage Error
NICR	National Institute for Congestion Reduction
NRMSE	Normalized Root Mean Square Error
OBU	On-board Unit
OD	Origin-Destination
PHD	Person-Hours of Delay
PHT	Person-Hours Traveled
PMT	Person-Miles Traveled
PTI	Planning Time Index
RSU	Roadside Unit
SD	Standard Deviation

SH	Speed Harmonization
TIM	Traveler Information Message
TN	True Negative
TP	True Positive
TT	Travel Time
TTI	Travel Time Index
V2I	Vehicle to Infrastructure
V2V	Vehicle to Vehicle
V2X	Vehicle to Everything
VMS	Variable Message Signs
VRC	Vehicle-to-Roadside Communication

Executive Summary

Traffic congestion is a phenomenon that has been extensively explored by researchers. However, the negative safety and economic impacts resulting from traffic congestion remain at large and can occur on any roadway at any moment. This research utilizes data fusion between conventional sources, such as radar detectors and traditional probe-based data, with newer sources, such as Bluetooth and connected vehicle (CV) data, to identify conditions that signal impending congestion. The goal is to develop a method to proactively detect and mitigate congestion on freeways and arterials.

Data-driven and signal processing techniques are explored and developed to produce an algorithm that relies on near-real- or real-time traffic measurements capable of generating predictions proactively, using complex and often subtle factors that trigger congestion. The algorithm is validated and calibrated using traffic and other relevant data from comparable roadway facilities located in Florida and Texas.

The algorithm is robust enough to function on both traditional and CV-based datasets and discerns between four intensity levels of congestion. The algorithm is applied within a microsimulation model to test the effectiveness of congestion mitigation strategies ranging from speed harmonization to dynamic rerouting, implemented individually and simultaneously. The simulated mitigation strategies prove to be effective in proactively reducing recurring and non-recurring congestion while providing additional safety benefits.

The project also demonstrates the clear advantage of using CV-based travel time estimates to calibrate microsimulation models over fixed point-based derivations of travel time from spot speeds. The ability to calibrate simulation models based on individual sections of shorter lengths (less than or equal to 0.5 miles) allows more detailed replications of real-world conditions.

1. Introduction

Congestion management is an area of traffic research aimed towards reducing the impact of various forms of congestion. Typically, most congestion management solutions focus on reactive rather than proactive approaches. Proactive approaches to congestion management, unlike reactive, seek to apply algorithms and mathematical models to identify early indicators that might potentially lead to traffic congestion using available data sources such as radar sensors, loop detectors, probe or connected vehicles (CVs), and appropriately deploying mitigation strategies to optimize traffic flow and reduce delays (Abdel-Aty, Pande, & Hsia, 2010; Pan, Khan, Popa, Zeitouni, & Borcea, 2012).

This project is applicable to congestion management on corridors, both with and without managed lanes. The project utilizes data fusion between traditional sources, such as radar and loop detector data, with newer sources, such as Bluetooth and CV data, to identify conditions that signal impending congestion. The main goal is to establish a data driven methodology to signal the likely occurrence of both recurring and non-recurring congestion, irrespective of the data source. Traffic and other-relevant data from two states, Texas and Florida, in the United States are collected and analyzed. The collected data include both traditional traffic measures and high frequency CV data. Big data and signal processing techniques are explored to understand and differentiate various levels of recurring and non-recurring congestion within the collected data.

Congestion mitigation strategies that could be deployed within the study area (i.e., ramp metering, speed harmonization, and dynamic re-routing) in conjunction with the predicted type/level of congestion are simulated in TransModeler (Caliper-Corporation, 2020) to examine potential benefits, especially in terms of delaying the onset of congestion thereby reducing its duration and impact.

Further, a parallel effort focusing on developing a confluence platform for transportation agencies to visualize the benefits and costs associated with proactive congestion management strategies is being undertaken by the Texas A&M Transportation Institute. The results and findings from this research will supplement their extensive literature search by using real-world data to simulate the efficacy of select congestion mitigation strategies.

1.1. Objectives

The overall aim of this project is to utilize aggregate data available from traditional traffic monitoring sources coupled with CV data and other geospatial information to build a more robust congestion detection algorithm for freeways. The robustness (compatibility of use with traditional and/or newer data sources) and proactive capabilities of the algorithm are prioritized to effectively test and deploy congestion mitigation strategies in the study area. More specific objectives of this project are to:

- Conduct a thorough literature review on existing measures of congestion and near real-time congestion management/mitigation strategies.
- Develop a congestion detection methodology applicable to both traditional (i.e., radar, loop detectors, Bluetooth) and CV-based data sources, originating from different geographic locations.
- Utilize the depth of low penetration CV-data along with traditional measures of traffic congestion to develop and validate a congestion detection algorithm.
- Highlight the versatility of CV-based infrastructure even at low market penetration, when compared to other traffic data sources.

- Use TransModeler to simulate recurring and non-recurring congestion on the Tampa Hillsborough Expressway Authority (THEA) Selmon Expressway in Tampa, FL. Further, apply and simulate congestion mitigation strategies based on the predictions of the congestion detection algorithm to demonstrate potential traffic and safety benefits.

1.2. Outline

The report starts by providing a brief introduction along with the specific project objectives. Chapter 2 presents a comprehensive literature review detailing similar research efforts and potential gaps that could be addressed. Chapter 3 focuses on the methodology and details the study locations, the data collection and data fusion processes, and the development of the congestion detection algorithm. Chapter 4 presents and discusses the results of applying the congestion detection algorithm and microsimulation. The results section also details any limitations to the methodological approach. Chapter 5 concludes by providing recommendations for future research.

2. Literature Review

Congestion, simply stated, is a phenomenon that occurs when demand (*volume of roadway traffic*) is greater than or equal to supply (*optimum roadway capacity at a given time*). The highway capacity manual (HCM) defines it as “the difference between the highway performance experienced by the users and how the system actually performs” (*HCM 2010 : highway capacity manual, 2010*). Traffic congestion typically entails periods of decreased or nonuniform travel speed, increased vehicle density, increased delays or travel times, and long queue lengths. Severe congestion known as “unacceptable congestion” consists of delays in excess of the acceptable/agreed-upon norms after accounting for the time of day, geographic location, mode of travel, and type of transportation facility (Lomax et al., 1997). Congestion can also be further divided into recurring and non-recurring. Recurring congestion takes place at a specific time period every day and is usually associated with peak commute hours (Lomax et al., 1997). Non-recurring congestion, on the other hand, could be a result of incidents, weather, lane closures, and other unforeseen capacity reductions or increase in traffic demand (i.e., special events).

Factors that lead to traffic congestion have been extensively studied by researchers all over the world. This review of existing literature summarizes the frequently used measures to define and measure congestion. Several algorithms and approaches previously derived by researchers are discussed in detail. The literature review also discusses the various types of traffic management strategies (reactive and proactive) and their validity from past research.

2.1. Congestion on Freeways

One of the first studies documented to demonstrate breakdown of traffic flow resulting from oversaturated conditions (congestion) is conducted by Greenshields in 1935. Greenshields suggested a linear decrease in space mean speed with an increase in traffic density (defined as the number of vehicles per mile per lane on a roadway). At an optimum speed (S_0) resulting in the density (D_0), the roadway provides the maximum flow- V_m (defined as the number of vehicles passing through a given point per unit time) following a parabolic curve.

Exceeding the D_o threshold signals oversaturated conditions and the start of congestion as shown in Figure 2-1 (Salter, 1976). Researchers have further refined this relationship through large traffic studies across various locations to show a discontinuous relationship when approaching D_o , identifying oversaturated conditions (HCM 2010 : highway capacity manual, 2010).

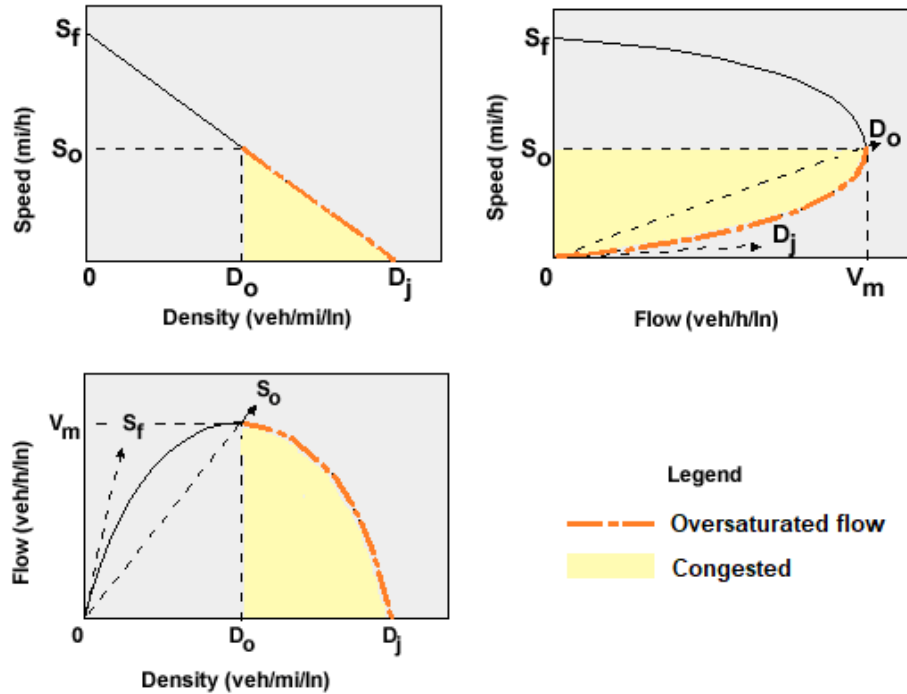


Figure 2-1. Greenshields speed, flow, and density relationships (Greenshields, 1935).

These speed-flow-density relationships have been used to develop several tools and methodologies to pinpoint the start and progression of congestion. The Greenshields approach is known to be more accurate for density/speed/flow estimation at the beginning and end of the concentration curves and less accurate in the middle region (maxima). A lot of the density estimation techniques used in studies provide and follow a reactive approach to solving congestion i.e., by relying on historical data to deliver informed mitigation strategies. However, in most cases the recommended control strategies apply to fixed or previously documented experiences of recurring congestion (Pan et al., 2012). The control strategies are usually not transferrable to other locations, not even to those with similar characteristics. Recent studies have considered this limitation of reactive approaches and are more focused on proactive approaches that could, in near-real time, predict congestion and trigger mitigation strategies to optimize the flow of traffic using connected vehicle infrastructure.

Typical performance measures obtained from the HCM that classify the extent of congestion include:

- **Quantity of service** – determined by the number of people using the system, the distance they travel i.e., person-miles traveled (PMT), and the time spent traveling i.e., person-hours of travel (PHT). The mean trip speed for the roadway/segment is obtained by dividing the PMT by the PHT.
- **Intensity of congestion** – number of hours of congestion (person-hours of delay); mean delay per person-trip; volume/demand-to-capacity ratio.

- **Duration of congestion** – Total time that the demand exceeds the discharge capacity of the freeway segment.
- **Extent of congestion** – directional miles of congested facility (or queue lengths).
- **Variability** – probability of occurrence (recurring or nonrecurring).
- **Accessibility** – system effectiveness in terms of persons able to accomplish their travel goal within the anticipated timeframe (*HCM 2010 : highway capacity manual*, 2010; Lomax et al., 1997).
- **Other frequently used variables** – travel time index (ratio of actual travel time to ideal travel time at free-flow speed) where a travel time index of 1.5 usually indicates congestion (*HCM 2010 : highway capacity manual*, 2010); planning time index (ratio of the 95th percentile travel time index to free-flow travel time (Transportation Research Board & NASEM, 2014a)); level of service (LOS) of the segment.

Table 2-1. Summary of the performance measures in HCM

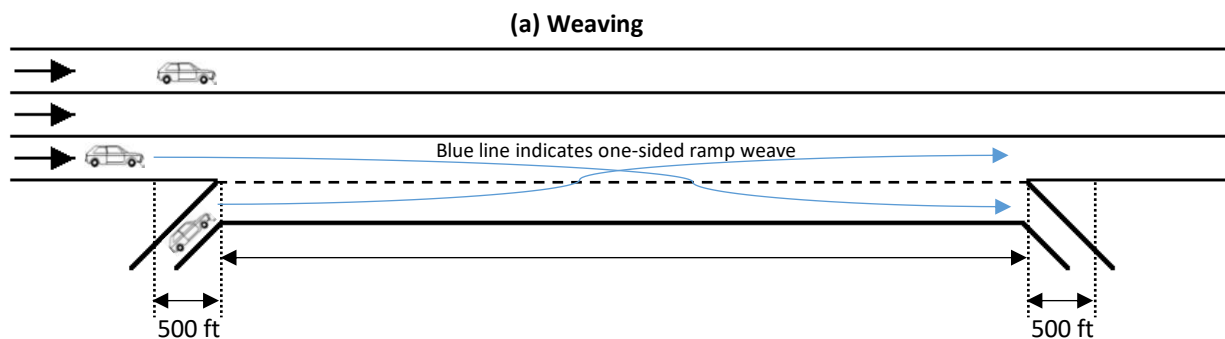
Category	Performance Measure
Quantity of service	Person-miles traveled (PMT) Person-hours of travel (PHT) Mean trip speed
Intensity of congestion	Person-hours of delay (PHD) Mean delay per person-trip Volume-to-capacity ratio Demand-to-capacity ratio
Duration of congestion	Total time
Extent of congestion	Directional miles of congested facility (queue lengths)
Variability	Probability of occurrence
Accessibility	Persons able to accomplish their travel goal within the anticipated timeframe
Other variables	Travel time index (TTI) Planning time index (PTI) Level of service (LOS): A to F

Other performance measures typically used when identifying congestion mitigation strategies are detailed by Lomax et al. (1997) and they include: travel rate (ratio of travel time to segment length), delay rate (*difference between actual and acceptable travel rate*), delay ratio (*ratio of delay rate to actual travel rate*), congested roadway (*total sum of congested segment lengths*), speed reduction index (*percentage reduction in average speed from free-flow speed divided by 10 and ranges between 0 to 10, with values exceeding 5 indicating congestion*) and congested travel (*sum of the product of all individual congested segment length and traffic volume*) (Lomax et al., 1997). These performance measures have been typically used as aggregate reactive measures for congestion studies. Estimating more predictive measures such as probability of occurrence has not been explicitly defined as other measures in the HCM. This could be due to several constraints but mostly because of lacking infrastructure to routinely collect and analyze high resolution traffic data. A more detailed overview of commonly used congestion measures is presented in Table 2-1.

Table 2-2. Commonly used performance measures of congestion

Variable	Performance Measure	Facts
Travel time	TTI Travel time reliability Travel rate Delay rate Mean delay per person trip Delay ratio Planning time index (PTI)	Frequently used Check-in/out approach Both space and speed are considered Accuracy depends on equipment Easy to compare to ideal conditions Roadway characteristics not required Continuous in most cases
Speed	Mean trip speed Speed reduction index Spot speed	Relatively easy to obtain Free-flow speed acts as a good baseline Usually based on space-mean-speed Easy to compare to ideal conditions Continuous measure
LOS (A-F)	Density	6 levels based on ranges of traffic density at corresponding free-flow speeds Complex to obtain Segment characteristics required Discontinuous in nature Does not provide any information on oversaturated traffic flow
Other	Total congestion time Queue length Volume/capacity ratio Demand/capacity ratio Congested travel	Continuous Difficult to estimate accurate queue lengths Queue length is an easy measure to understand Traffic demand is difficult to estimate

The HCM methodology provides guidelines for determining levels of congestion within a freeway facility (*defined as a portion of the freeway with multiple segments selected for analysis*) by splitting it into three types of segments i.e., weaving, merge and diverge, and basic, as these segment types have shown to vary in traffic behavior and characteristics. Each of these segments have influence areas as shown in Figure 2-2, derived from the HCM 2010. Impact of interacting traffic varies substantially between these types of segments and so do the applicable methodologies for traffic density estimation.



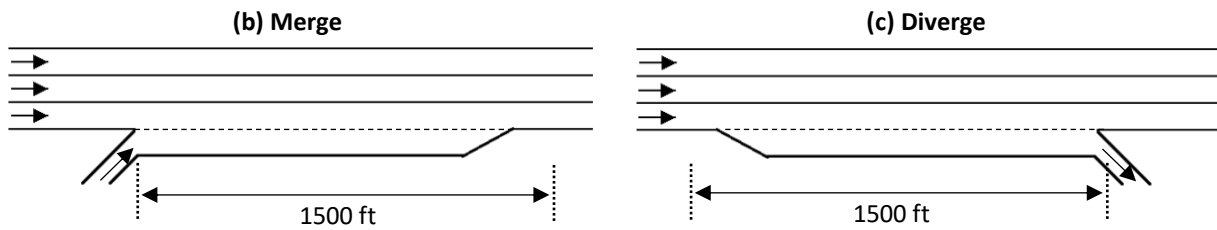


Figure 2-2. Influence areas of segments

The HCM methodology is heavily reliant on establishing the demand (defined as the number of vehicles desiring to use a given facility within a time period) and capacity (*defined as the maximum sustainable hourly flow rate at which vehicles pass through a section of the roadway under the existing traffic conditions*) of a facility (HCM 2010 : highway capacity manual, 2010). To establish current conditions, free flow speed (FFS) must first be established either by carrying out a spot speed study or using Equation 2.1. The HCM recommends measuring a sample of at least 100 passenger cars (pc) during flow rates of less than 1000 pc/h/ln by isolating speeds of every tenth car in a particular lane. Establishing FFS also helps determining ideal and true travel times and their reliability.

$$FFS = 75.4 - f_{LW} - f_{LC} - 3.22TRD^{0.84} \quad (2.1)$$

Where,

FFS = free flow speed (mph)

f_{LW} = lane width adjustment (Exhibit 11-8 HCM)

f_{LC} = right-side lateral clearance adjustment (Exhibit 11-9 HCM)

TRD = total ramp density (ramps/mile): 3 miles up and downstream of the facility.

The HCM methodology then requires a demand adjustment based on the peak hour factor (defined as the hourly flow during the maximum-volume hour during the 24-hour period divided by the maximum 15-minute flow rate within the peak hour). This aspect restricts the methodology to be applied to proactive congestion detection as knowing traffic volume for the entire peak period is a prerequisite. Other adjustment factors (i.e., heavy vehicles, unfamiliar drivers, etc.) demand to further calibrate to existing conditions might pose more challenges. Additionally, establishing true demand of a facility is complex and usually adjusted during calibration but cannot be accurately measured as it is affected by upstream conditions (*HCM 2010 : highway capacity manual, 2010*). Figure 2-3 shows the corresponding density thresholds for a particular level of service (LOS), given the FFS. The HCM also does not provide any further analysis of the intensity or progression of congestion once LOS F has been exceeded. An increase in the deployment of connected and autonomous vehicles (CAVs) technology might provide more insights into the initial identifiers of congestion and how to predict their occurrence by providing access to high frequency continuous datasets that can be used in precision mapping of changing traffic conditions such as travel times, queues, expected delays, and potential incidents.

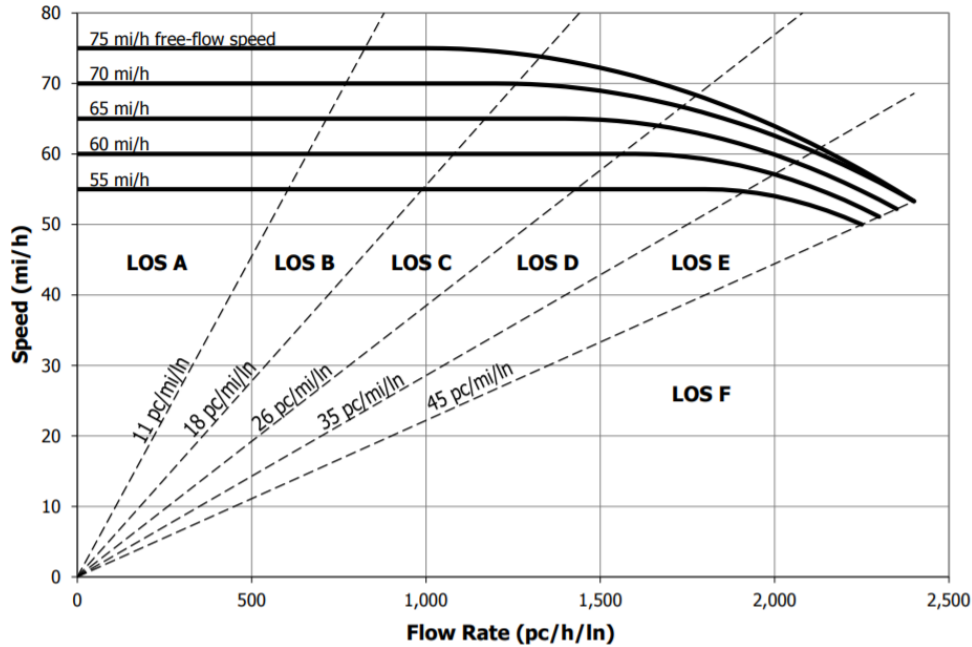


Figure 2-3. Density, speed, and LOS thresholds (HCM 2010 : highway capacity manual, 2010)

Researchers using probe-vehicle, simulated CV, and real-world CV data have utilized alternative but comparable approaches to the HCM for estimating traffic density more readily with less complexity (Anand, Ramadurai, & Vanajakshi, 2014; Anand, Vanajakshi, & Subramanian, 2011; Grumert & Tapani, 2018; Khan, Dey, & Chowdhury, 2017; Qiu, Lu, Chow, & Shladover, 2010; Rahman, Chowdhury, & McClendon, 2018). A frequently used alternative to the HCM is proposed by May in 1990. This approach estimates density using the percentage occupancy (% OCC: defined as the percent of time a section of the roadway is occupied) per lane as shown in Equation 2.2 (May, 1990).

$$k = \frac{52.8}{\bar{L}_V + L_D} \times \% OCC \quad (2.2)$$

Where,

k = density (vehicles/lane/mile)

\bar{L}_V = average vehicle length (feet)

L_D = detection zone length (feet)

% OCC = percent occupancy

Although this methodology used thresholds from the 1985 HCM for density to determine LOS, newer thresholds can be substituted from the HCM 2010. Percent occupancy can be established using Equations 2.3 and 2.4. Density can then be obtained using Equation 2.2.

$$\% OCC = \frac{N}{T} \left(\frac{100}{\bar{\mu}_{SMS}} \right) \frac{\bar{L}_V + L_D}{5280} \quad (2.3)$$

$$\bar{\mu}_{SMS} = \frac{3600}{5280} \left(\frac{\bar{L}_V + L_D}{\bar{t}_0} \right) \quad (2.4)$$

Where,

N = number of vehicles passing over a point in time period T

T = time period of observations (hours)

t_0 = individual vehicle occupancy time (seconds)

$\bar{\mu}_{SMS}$ = space mean speed at time period T

These methodologies for establishing density are heavily reliant on historical trends and numerous variables that increase the complexity when applied to a predictive model. The type of segment also introduces more checks and adjustment factors within the methodology. Further, the HCM or May (1990) do not categorize what happens within each LOS band. This is especially useful when establishing the level of congestion due to oversaturated flow. A more precise breakdown of LOS F is detailed by a traffic quality study of the metropolitan Washington area (Bauza & Gozalvez, 2013; Skycomp, 2009). The breakdown is summarized in Table 2-3. Table 2-3 also provides an insight into speed ranges for various levels of congestion. This provides a good baseline for distinguishing between recurring and non-recurring congestion.

Table 2-3. Further breakdown of LOS F

	Severity	Description	Observed Speed, mph	Density, pc/mi/ln
LOS F	1	Minor slowing	30 – 50	46 – 59
	2	Further slowing	15 – 40	60 – 79
	3	Congested flow with some stopping	10 – 25	80 – 99
	4	Severe congestion with stop-and-go flow	< 10	100 – 119
	5	Possible incident, crash, lane closure, etc.	< 10	> 119

* With a spacing of 20 feet between vehicles, a theoretical value of 260 pc/mi/ln can be estimated for jam density. However, in practical conditions, jam density is usually around 180 to 190 pc/mi/ln.

Apart from computing existing traffic conditions, the HCM methodology has been adopted into software tools such as FREEVAL and highway capacity software capable of computing travel time reliability and impacts of incidents such as work zones to freeway capacity (Jolovic, Stevanovic, Sajjadi, & Martin, 2016). FREEVAL is also capable of utilizing inbuilt historical weather data to determine adjustment factors but at a very aggregate level. However, these tools are not optimized for real-time prediction, require heavy calibration, and lack the ability to utilize dynamic information such as incidents or even changing weather conditions.

From the above information, a few limitations of traditional measures of congestion to near real-time applicability are summarized below:

- Many variables are required to be collected for estimating existing conditions and bottlenecks.

- Based on a seed day and process must be repeated/alterd for any slight change in traffic, geometric, or climatic conditions to achieve higher accuracy. Complicated and labor intensive to repeat the process for a large period.
- Computing densities is usually an approximation and true conditions over a small-time frame might have high variability (Anand et al., 2014; Hall, 1996).
- Oversaturated flow conditions are not sufficiently captured.
- Using space mean speed (defined as the harmonic average speed in the HCM) has limitations when applied to congested conditions as speeds at segment vertices might not capture conditions within the segment. A possible solution would be to use average travel speed (determined by dividing the segment length by average travel time) (Hall, 1996).
- Extensive calibration efforts are required to bridge HCM estimates to real-world observations via several capacity and speed adjustment factors.
- Weather and incident information is usually applied as an aggregate value (per day) and not within a period.
- Great for estimating existing conditions but lacks the ability to dynamically predict any future conditions (*HCM 2010 : highway capacity manual, 2010*).

Apart from traditional data sources such as traffic volume counts and spot speeds, emerging technologies add more depth by estimating travel times and in some cases high frequency vehicle trajectories. The next section provides an overview of some commonly used technologies.

2.2. Real-time Congestion Prediction

Real-time congestion prediction strategies using CV-data have been previously explored (Grumert & Tapani, 2018; Rahman et al., 2018). However, most of the studies use simulations and lack real-world data. In the past five years, USDOT has tried to make more CV datasets publicly available to researchers through the USDOT Intelligent Transportation Systems (ITS) Joint Program Office (JPO) Data Hub. CV pilot deployment sites providing valuable data include Tampa, Wyoming, and New York City. Before the availability of such detailed datasets, a common source of publicly available vehicle trajectory data used by researchers to model CV behavior is the Next Generation SIMulation (NGSIM). NGSIM data are captured using a series of synchronized video cameras on freeways and processing algorithms without relying on CAV infrastructure (Punzo, Borzacchiello, & Ciuffo, 2011; Rahman et al., 2018). However, these datasets require heavy filtering and consistency checks to isolate trajectories especially in oversaturated conditions with stop-and-go traffic (Punzo et al., 2011). Utilizing these datasets alone would not result in efficient models, so researchers employ data fusion to combine information (Anand et al., 2014; Anand et al., 2011; Grumert & Tapani, 2018; Khan et al., 2017; Papacharalampous, Cats, Lankhaar, Daamen, & Lint, 2016; Qiu et al., 2010; Rahman et al., 2018). Data fusion in transportation involves utilizing multiple sources (i.e., cell phones, Bluetooth, loop detectors, video, radar detectors, RFID readers, toll tags, CV, GPS, probe vehicles, social media reports, DOTs, weather APIs) measurement techniques, and analytics to generate more complete datasets.

Rahman et al. (2018) utilize NGSIM datasets to predict traffic flow at low CV penetration. However, the authors assume each NGSIM data timestep (10HZ) to approximate/represent a Basic Safety Message (BSM) sent by a CV. The authors examine several recurring neural network models to capture temporal variations in time-series datasets (vehicle trajectories). The Long Short-Term Memory (LSTM) neural network is coupled with either the moving average model, standard Kalman filter model, or Rauch-Tung-Striebel (RTS) model at various

penetration rates given that the NGSIM data are assumed to provide 100% penetration over the several 500 m collection zones (Rahman et al., 2018). The results suggest an accurate prediction of speed and space headways when the LSTM is coupled with the RTS model even at low penetration rates of 5% (Rahman et al., 2018). The computational time for future predictions is estimated at 80 milliseconds. It should be noted that these predictions are solely based on past trajectories and no other external factors such as geometry, weather, incidents, and closures are evaluated. Also, the individual highway sections considered are relatively small and the performance of the prediction algorithm might vary significantly if a longer facility is considered. Although the model does not predict congestion status, estimating future speeds and space headway can provide insight into roadway capacity and flow.

Tseng et al. (2018) utilize data from select Taiwan regions to develop a real-time congestion prediction model using the Apache Storm open-source computing system. To develop the Support Vector Machine (SVM) model, they use several open data sources such as traffic, weather, and social media traffic status updates. The traffic data consist of volume counts, observed densities, and lane speeds. Fuzzy thresholds are developed for the various parameters to easily classify existing conditions as shown in Figure 2-4. The defuzzification is based on the center of area method to estimate levels of congestion shown in Figure 2-4(e). The levels of congestion are then used by the SVM model to effectively predict speeds for the immediate future time period (Tseng et al., 2018).

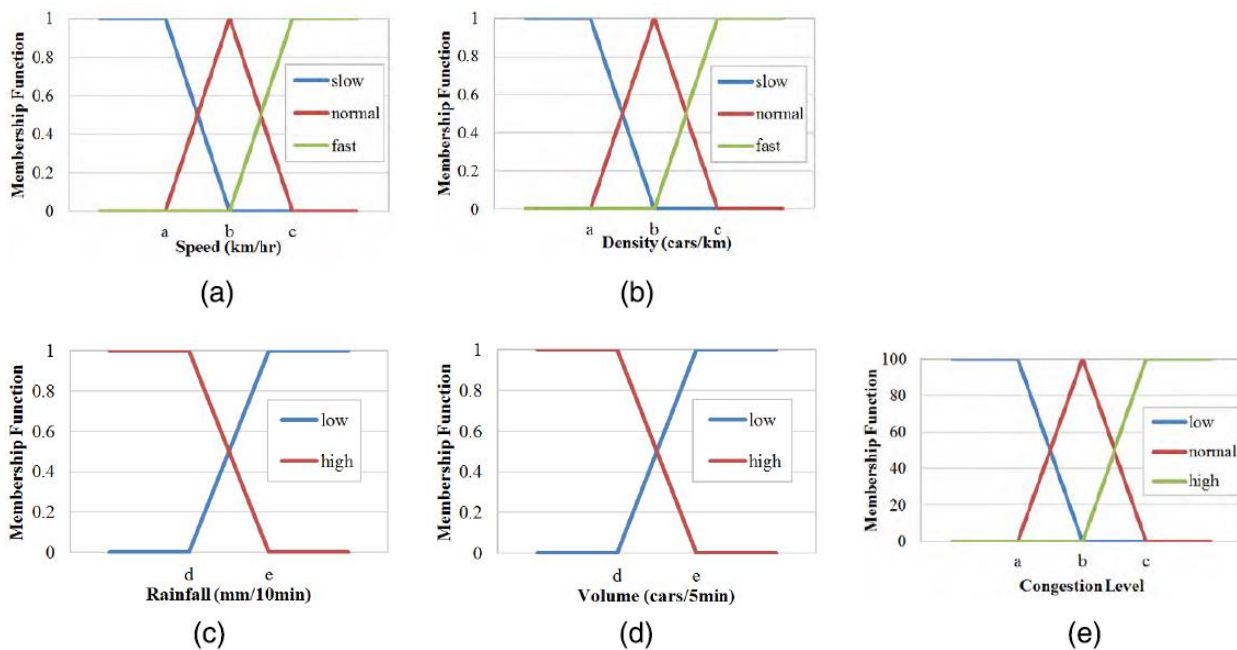


Figure 2-4. Fuzzy input subsets (Tseng et al., 2018)

Another widely used metric for congestion classification is travel time. Several technologies that collect such information already exist and they include: automatic vehicle identification (electronic tolls, RFID tags, license plate recognition), radar, Bluetooth, and probe vehicles (Hargrove, Lim, Han, & Freeze, 2016; Puckett & Vickich, 2010). Although most of these technologies are interchangeably used by DOTs, they are being overshadowed by Bluetooth detectors that are cost effective, maintain anonymity, and provide reliable data (Friesen & McLeod, 2015; Karatsoli, Margreiter, & Spangler, 2017; Margreiter, Spangler, Zeh, & Carstensen, 2015; Puckett & Vickich, 2010). Margreiter et al. (2015) showed that travel time from Bluetooth detectors could be used as a

substitute for traditional tolling or loop detectors estimates. Incidents and changes in average speed are captured with relatively good precision and small sample size. Hargrove et al. (2016) compare several of these technologies using the license plate recognition as ground truth and found similar travel time results, though Bluetooth is not very efficient in estimating traffic volumes. The study also shows that travel time estimates match ground truth when the time intervals used are not widely spaced i.e., 1 min or 5 min intervals. Using larger time intervals results in a larger variance and over smoothing (Hargrove et al., 2016). It should also be noted that Bluetooth data have several limitations such as establishing true location of congestion, sample loss due to designated check-in/check-out zones, wide detection zones sometimes introducing false data, dependency introduced due to TT estimates arising from multiple devices within a single vehicle, and poor traffic volume correlation.

As previously mentioned, another emerging source of detailed traffic-related data is CV infrastructure. CV technologies utilize one or more of the following communications, such as vehicle to vehicle (V2V), vehicle to infrastructure (V2I), infrastructure to vehicle (I2V), infrastructure to infrastructure (I2I), and vehicle to everything (V2X), to facilitate information transmission between roadway users and surrounding systems ("J2735_201603: Dedicated Short Range Communications (DSRC) Message Set Dictionary," 2016; Kishimoto, Yamada, & Jinno, 2014; LeBlanc, 2006). Communication across these systems can be achieved via land mobile radios, commercial mobile radio services, radio frequency identifiers, infrared tags and beacons, WiFi, dedicated short range communications (DSRC), cellular vehicle-to everything (C-V2X), and Bluetooth (LeBlanc, 2006). The three CV pilots in Tampa, Wyoming, and New York City rely on DSRC (802.11 p-based wireless communication that operates in the 5.9 GHz band whilst enabling high-speed, low-latency, and secure communication between vehicles and infrastructure, without cellular support). BSMs are the primary source of CV data shared across these communication protocols and consist of information pertaining to the type, location, longitudinal/lateral control, and state of the CV equipped with an on-board unit (OBU). Individual OBUs broadcast BSMs continually to the roadside units (RSUs) along the roadway, which in turn facilitate V2X communications.

Bauza and Gozalvez (2013) present a novel approach to cooperative traffic congestion detection (CoTEC) based on V2V communications in the iTETRIS simulation platform. CoTEC utilizes a fuzzy-based congestion detection mechanism based on more aggregate thresholds of speed and density developed by Skycomp (2009) as shown in Table 3. However, density estimation is based on an assumption of 100% penetration with vehicles being able to estimate distance between themselves thus approximating the number of neighboring vehicles (Bauza & Gozalvez, 2013). Although this approach works in theory, the applicability to real-world situations with penetration rates far from 100% is very limited. When the penetration rates are further modified to 75% and 50% in the simulations, the models ability to predict diminishes substantially by up to 50% and 80%, respectively (Bauza & Gozalvez, 2013). Grumert and Tapani (2018) propose estimating traffic state with respect to density using a similar approach within SUMO microsimulation. Traffic state estimates vary significantly if short time periods are used together with low penetration rates. It is also noted that inhomogeneous traffic conditions further compromise the density predictions (Grumert & Tapani, 2018).

Overall, literature indicates that congestion prediction models/algorithms are substantially more efficient with high CV penetration rates. CV-data based algorithms are highly complex and not easily transferrable. And as evident from the literature, they are largely modeled under simulation platforms and make several assumptions towards real-world conditions. Also, existing models almost always use multiple sources such as volume counts, speeds, and densities, requiring more infrastructure than relying on any one individual technique.

In summary, the review finds that:

- Using data fusion of traditional TT measures to enrich BSM-based TT especially in terms of incident and weather information has not been extensively explored.
- The models do not adequately distinguish between recurring and non-recurring congestion.
- The models also tend to calculate traffic densities using the Greenshields method, which is known for being easy to apply but not very accurate when compared to the HCM. Applying other parameters that can be more readily obtained, unlike density, could be beneficial.
- A universally applicable approach that could work on both traditional and BSM-based datasets with low penetration rates has not been extensively researched. Also, most models/algorithms use a conspicuous number of variables (live data feed) and validate using simulation platforms thus affecting their real-world validity.

2.3. Active Traffic and Demand Management (ATDM) Strategies

The usefulness of individual ATDM strategies is being extensively researched. However, their effectiveness on demand, speed, capacity, and travel time is highly variable and in most cases condition-specific. This section discusses some strategies that can be coupled with CV infrastructure for real-time traffic management.

2.3.1. Driver Alerts

These comprise of non-conventional short messages or warnings, displayed via HMIs, set to alert the driver of impending congestion with the overall goal of improving safety and easing the progression of congestion by reducing start-stop traffic (Concas, Kourtellis, Reich, & Authority, 2019). A few examples of driver alerts that have been previously applied with CV infrastructure, as detailed below.

2.3.1.1. Emergency Electronic Brake Light (EEBL)

EEBL is a V2V application that alerts drivers to hard braking events occurring in downstream traffic. This alert is transmitted by a CV currently engaged in an emergency braking event (remote vehicle) to other nearby CVs not immediately behind or out of line of sight (Concas et al., 2019). The application acts as a signal of impending congestion and could be coupled with speed advisories.

2.3.1.2. Queue Warning/End of Ramp Deceleration Warning (ERDW)

The ERDW is a V2I application typically used to detect queue lengths in a specific zone and transmit information back to the RSU. The RSU then issues a traveler information message (TIM) that suggests traveling speeds when the driver is approaching the end of the queue by estimating a safe stopping distance. The application serves the dual purpose of improving safety and mobility to users.

2.3.1.3. Forward Collision Warning (FCW)

Forward Collision Warning (FCW) is a V2V application that alerts the host vehicle driver of an impending threat ahead and in line of sight. The overall goal of the alert is to reduce the severity of crashes typically rear end by taking into account the time to collision (Concas et al., 2019). These alerts could train drivers to maintain a safe following distance while decreasing the effect of stop-and-go traffic.

2.3.2. Speed Harmonization

Speed harmonization entails implementing variable speed limits in relation to the traffic conditions downstream of a roadway, to reduce speed differentials (Hale et al., 2016; Malikopoulos, Hong, Park, Lee, & Ryu, 2019). There are several benefits of speed harmonization, particularly in terms of improved safety (less stop-go traffic) and mitigating loss of highway performance (travel times, and speeds). Speed harmonization algorithms have been extensively researched, however, practical implementation varies based on several geometric and traffic factors (Hale et al., 2016). The application of speed harmonization can be done using speed- or density-based algorithms. Equation 2.5 shows an example of a simple speed-based harmonization algorithm used to output a speed advisory.

$$u_m(k) = a_m \times \bar{v}_m(k) \quad (2.5)$$

Where,

$u_m(k)$ = Suggested speed advisory at time interval k in bottleneck

a_m = proportional control in bottleneck (adjust factor, default = 1.3)

$\bar{v}_m(k)$ = measured speed in the bottleneck

The established speed advisories can be communicated using variable/dynamic message signs. Emerging research has also shown possibilities of communicating speed advisories in near-real time using CV-infrastructure coupled with driver alerts (Hale et al., 2016). An example is the use of the ERDW and EEBL applications in the THEA CV Pilot (Concas, Kourtellis, Kamrani, & Dokur, 2021).

2.3.3. Variable Message Signs (VMS)

This strategy uses dynamic reprogrammable signs to display messages to roadway users. Messages involving road closures, incidents, optimized speed limits, bad weather, travel time delays, and possible work zones can be displayed (Mahmassani et al., 2014). The idea is to prepare drivers and possibly modify driving behavior by providing an insight on what to expect.

These signs have been used widely in many states in the United States and United Kingdom. However, there is no accurate data on their effectiveness as an ATDM strategy. Effectiveness of such strategies depends on several factors such as location, purpose, sign size, and other factors (Gopalakrishna, Cluett, Kitchener, & Balke, 2011). However, these signs can be used in tandem with CV infrastructure to not only display what to expect but also to state recommendations such as speed advisories to minimize travel times by decreasing delays incurred due to stop-and-go conditions.

2.3.4. Ramp Metering

Ramp meters have been in use since late 1950's in several cities across the United States. Ramp metering involves controlling traffic merging onto the freeway by using a traffic signal situated near merge points. It restricts vehicles entering the freeway to optimize freeway capacity and free flow speeds. Ramp metering can be devised based on upstream and downstream traffic conditions or at pretimed intervals. Ramp meters can be programmed to release vehicles as a platoon or on a one-at-a-time basis (Jacobson, Stribiak, Nelson, & Sallman, 2006). Installing ramp meters depends on several factors other than freeway traffic conditions, such as the

availability of queue storage on ramps, queue detectors on the ramp to facilitate timing adjustment, geographical extent, and impact on surrounding arterials (Jacobson et al., 2006).

In multiple traffic studies carried out by State DOTs and research centers, ramp metering has shown to increase vehicle speeds, increase vehicle flow, and improve roadway capacity. Safety improvements such as reduced crashes have also been observed by up to 50% in some cases (Jacobson et al., 2006). However, negative impacts such as potential traffic diversion to other arterials without ramp meters and possible shift of congestion zones are theorized.

2.3.5. Incident Detection

Incidents are a major cause of travel delays and other crashes on freeways. A commonly used incident detection strategy by most DOTs in the United States is a network of closed-circuit television cameras (CCTVs). These cameras are monitored by operators in real-time to determine location of incidents and assist dispatchers in responding promptly. However, manual or semi-automated processes are not as prompt in mitigating crashes as automated real-time strategies. Automated incident detection algorithms have been developed for decades using loop detector data to predict unexpected travel time delays (Houbraken et al., 2017; Wang, Xie, Liu, Fang, & Ragland, 2016; Weil, Wootton, & Garcia-Ortiz, 1998). However, they are prone to limitations such as poor spatial coverage, data blind spots between the detectors, missed check-in points, and mechanical failures. Houbraken et al. (2017) propose utilizing floating car data coupled with loop detector estimates of average speeds for validation. The study considers two travel routes, one consisting of a more access-controlled location (route A58: 19 km long from Tilburg to Eindhoven in Netherlands) and one consisting of several at-grade intersections (route A27: 37 km long from Utrecht to Gorinchem in Netherlands). The methodology divides congestion into two states (ON/OFF) based on a speed (< 40 mph) and acceleration threshold. The results show that floating car estimates of possible incidents (indicated by lower average speeds) are more accurate under the access-controlled setting. Overall, floating car data only produce 4-5% of false negatives when compared to the loop detectors (Houbraken et al., 2017).

Another common hazard experienced by roadway users is debris. Debris on freeways is a major concern as it results in crashes or damage to vehicles. Between 2011 and 2014 there are an estimated 243,413 crashes attributed to debris in the United States (Tefft, 2016). Further, in 2018 over 2,900 crashes are attributed to debris in the State of Florida alone (Concas & Kamrani, 2019). Typically, these obstructions are usually reported by roadway users (toll-free numbers), maintenance vehicles, and CCTV operators. However, similar to incident detection, immediate traffic cannot be alerted swiftly. Concas and Kamrani (2019) established an algorithm capable of identifying potential locations with debris by modeling individual lane changes from BSMs. The algorithm had a high accuracy of 96% in estimating the true location of the debris (Kamrani, Concas, & Kourtellis, 2021). Similar techniques could also be applied towards traffic incidents and even non-recurring congestion.

2.3.6. Dynamic Re-routing and Pre-travel Information

Dynamic rerouting is a traffic management strategy that provides road users alternative routes when their preferred route is congested due to recurring or non-recurring traffic conditions (Mirshahi et al., 2007). This strategy can be applied during or before trip-making. The former requires the presence of roadway infrastructure such as VMS, V2X capabilities, radio broadcasts, to relay prevailing conditions detected by the traffic management center to the driver. Dynamic rerouting could also be combined with pre-traveler information to better inform users about prevailing traffic-related conditions before choosing their route and

mode of travel, thus allowing for a less stressful trip (Mirshahi et al., 2007). It includes information such as congestion zones, bad weather, work zones, incident delays, and several other trip-specific information.

2.3.7. Speed Feedback Signs

This strategy involves a speed camera and a monitor. The speed camera tracks the speed of the oncoming vehicle and displays it on the monitor. The idea of this strategy is to inform drivers of their current speed to make them comply with the roadway speed limit. CV infrastructure can also be used to communicate speed warnings over the air via on-board human-machine interfaces to ensure driver compliance.

3. Methodology

This section describes the preliminary assessment of data compatibility between Bluetooth and CV-based datasets, properties of selected roadway facilities, data fusion protocols for the two geographic locations, and the development of the congestion detection algorithm. Table 3-1 outlines a few commonly used definitions when describing the study areas.

Table 3-1. Definitions used

Term	Definition
Facility	The mainline roadway spanning the study area
Segment	A portion of the facility comprising consistent geometric/traffic properties (i.e., number of lanes, AADTs, speed limits)
Section	Smaller portions than segments, established to determine TTs between two points or virtual sensors.
Travel time (TT)	Time taken to traverse a section of roadway
Travel Time Index (TTI)	Ratio of actual TT to ideal TT at free-flow speed (FFS)

3.1. Data Compatibility and Preprocessing

Preliminary testing is first carried out to compare TT estimates generated from BSMs and Bluetooth to ensure data compatibility for development of the congestion detection algorithm. A small study location in Tampa, FL, comprising of RSUs and Bluetooth detectors is used to test compatibility of TT measurements across the equipment. TTs are compared across these devices during the morning peak period (6 AM to 10 AM) for an entire year (1st January 2019 to 31st December 2019). Figure 3-1 shows the 0.27-mile test corridor (AB) along with the location of Bluetooth nodes and RSUs.

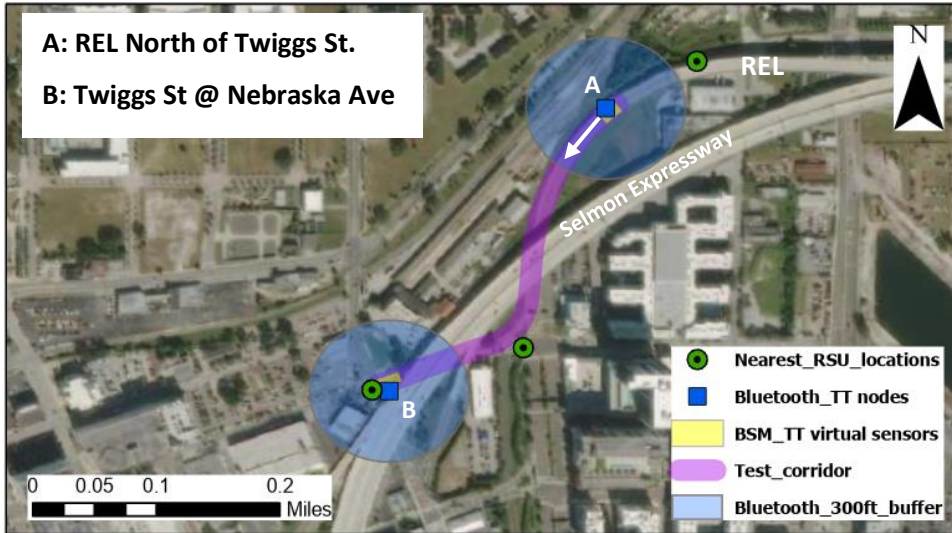


Figure 3-1. Test corridor for TT comparison between BSMs and Bluetooth nodes

Using BSMs generated multiples times per second (up to 10 Hertz) by up to 964 active participant (closely split between males and females) vehicles equipped with after-market OBUs, geo-spatial information is processed via virtual sensors (indicated in yellow) to flag check-in and check-out times of individual vehicles using a unique static identifier assigned during participant recruitment. Using Equation 3.1, average penetration rates are computed over a one-month period (July) across the two data generation sources (Friesen & McLeod, 2015). Average CV penetration rates during the morning peak period are computed to average 0.44% (with hourly highs of up to 1.2%) while Bluetooth penetration is computed to average 4% (with hourly highs of up to 7%).

$$\text{Average penetration rate} = \frac{100\%}{n} \times \sum_{i=1}^n \frac{X_i}{C_i} \quad (3.1)$$

Where,

n = Number of days in July (31 days)

X_i = Daily count of observations used for TT match during morning peak period

C_i = Daily vehicle count estimate during the morning peak period, extracted from the electronic toll counts

Figure 3-2 and Figure 3-3 show a comparison of TTs and daily AM averages established from Bluetooth and BSMs. The observed daily AM TT average pattern across the two estimates is similar but the TTs obtained from BSMs are consistently higher. The scatter plot shown in Figure 3-4 indicates a high correlation (*Pearson's coefficient* = 0.811) between the TTs obtained from BSMs and Bluetooth nodes. The difference in actual TTs for a specific 5-minute period could be attributed to the relatively large detection zones (200 ft-400 ft) of the Bluetooth nodes that further vary by type/connectivity range of Bluetooth device detected. The high correlation suggests that the two estimates of TT are compatible for use in TT-based congestion algorithm development and validation.

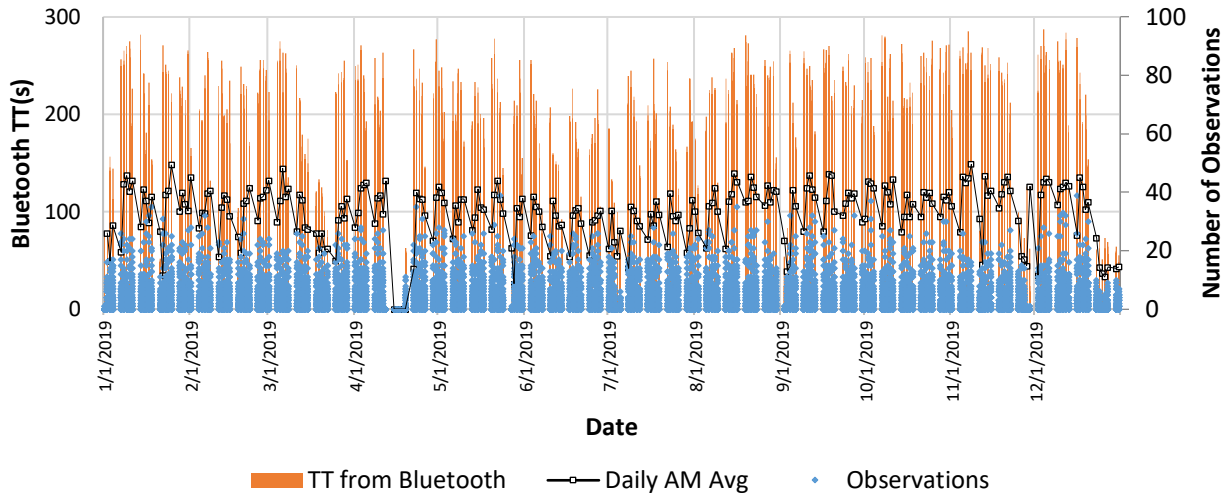


Figure 3-2. Bluetooth-based AM TTs by day

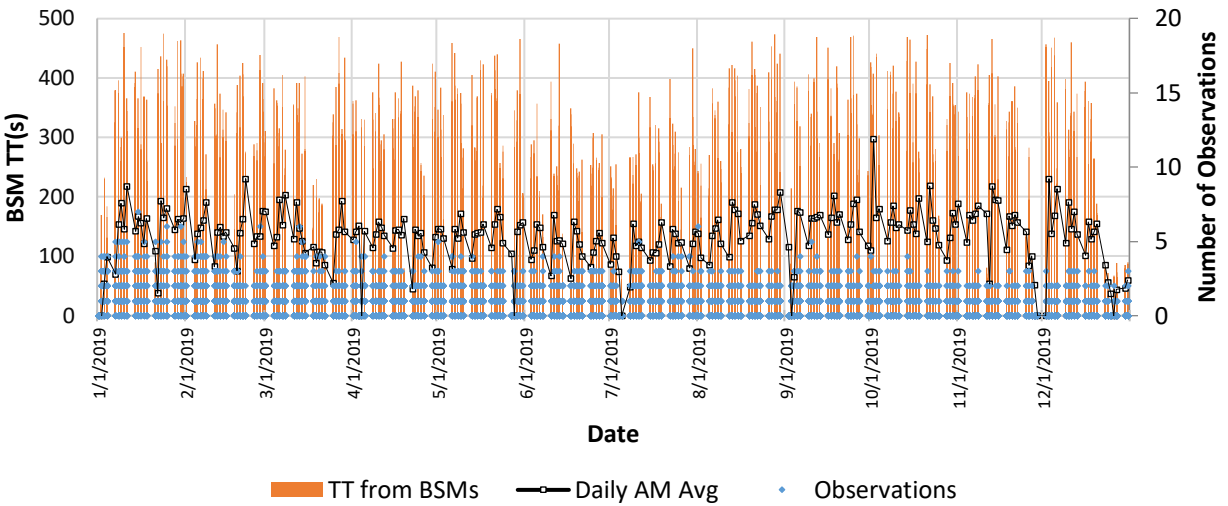


Figure 3-3. BSM-based AM TTs by day

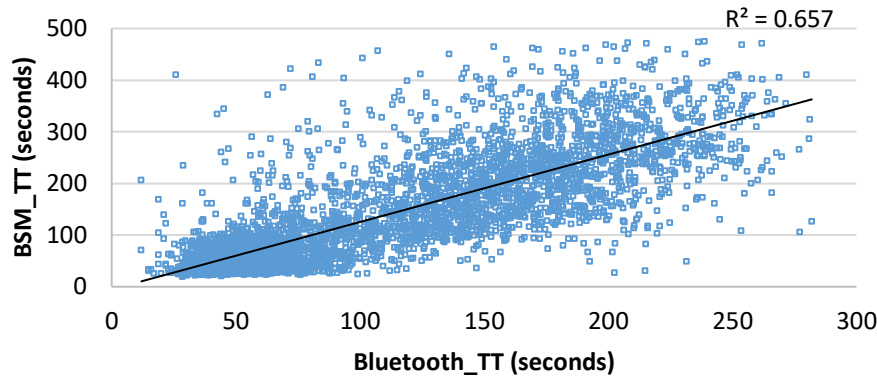


Figure 3-4. Scatter plots of TTs obtained via BSMs and Bluetooth

3.2. Facility Description

The first step is to select freeway facilities from the pooled databases of the project research teams, with similar traffic and geometric properties across the two states, Florida and Texas, in Unites States.

3.2.1. Florida

The primary facility consists of a seven mile stretch of the Selmon Expressway in Tampa equipped with multiple RSUs generating data from 834 unique connected vehicles. This facility is further divided into two three-lane and one two-lane segments in the westbound direction, as shown in Figure 3-5. The study focuses on the westbound direction due to the higher penetration of CV-equipped commuters traveling towards downtown, Tampa. A unique feature of the Selmon Expressway is the ability to access the reversible express lanes (REL) system located on the upper deck of the freeway. The REL changes operation by day of week and time of day (AM, mid-day, PM) to efficiently move traffic in/out of Tampa.

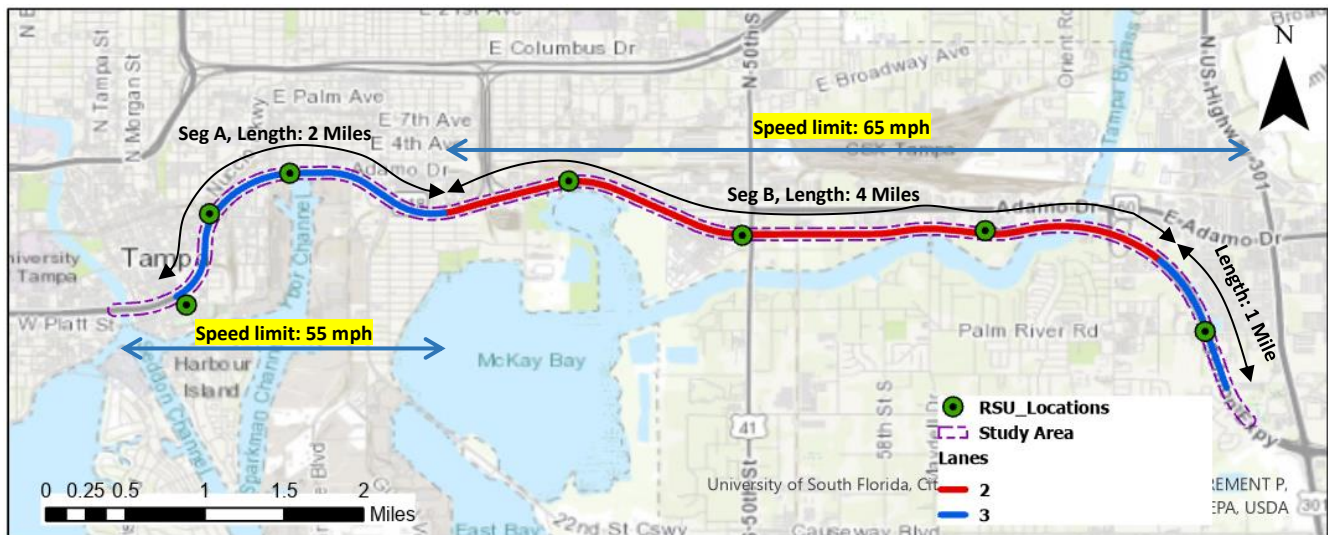


Figure 3-5. RSU locations closest to the Selmon Expressway in Tampa, FL

Table 3-2 and Table 3-3 provide geometric and traffic statistics for the Selmon Expressway. The facility has two speed limit zones of 55 mph and 65 mph. However, both zones exhibit similar free flow speeds (FFS) of 73 mph and 75 mph, respectively.

Table 3-2. Geometric properties of the Selmon Expressway

Seg ID	Location	Zip	Lanes	Length/ miles	Speed Limit/ mph	AADT (vehicles)	% Heavy vehicles
A	N 26 th St to S Morgan St	33605	3	2.0	55	80,000	5%
B	S 78 th St to N 26 th St	33619	2	4.0	65	80,000	5%

Table 3-3. Traffic statistics of the Westbound segments of the Selmon Expressway (2019)

Seg ID	Direction	HCM FFS/ mph	*85 th Percentile FFS/ mph	50 th Percentile TTI	85 th Percentile TTI	95 th Percentile TTI
A	WB	69.6	73	1.09	1.21	1.34
B	WB	69.6	75	1.08	1.18	1.57

*85th percentile FFS is derived by computing TTs under known normal traffic conditions (i.e., 10 PM to 5 AM)

Data from different geographic locations are used to develop and validate a robust congestion detection algorithm. A 6-point checklist based on the principles of the HCM is developed in Microsoft Excel to identify facilities/segments in Texas that are comparable to the Selmon Expressway as shown in Table 3-4. The six variables used include: Number of lanes, Median type, HCM free flow speed (FFS), Annual Average Daily Traffic (AADT), directional design hour volume (DDHV) in vehicles per hour, and directional design hour flow (DDHF) in passenger car equivalent per hour per lane. Matches are performed with respect to the two distinct segments A and B. An ideal match would comprise an entire 6-point match. However, due to the limited availability of travel time and vehicle volume collection equipment at short segment intervals (i.e., 2 miles or less) in Texas, three levels of matching are ultimately established to ease selection criteria. A “Good Match” requires 4 or more variable matches (shown in Figure 3-6) while a “Poor Match” requires at least 3 variable matches. A “Failed Match” is recorded when less than 3 variables are adequately matched. The matching process significantly improves the identification and selection of facilities while accounting for traffic and geometric properties.

Table 3-4. Facility/segment matching criteria

Variable	Criteria for Match
Number of lanes	2 or 3 lane segments
Median type	Concrete barrier
HCM FFS	+/- 5 mph
AADT	+/- 10,000 vehicles
DDHV	+/- 300 veh/h
DDHF	+/- 150 passenger cars/h/ln

Characteristics	CUTR	Select option to determine FFS/DDHV	
Name	Selmon Expressway	North Sam Houston Tollway - Wilson Rd to W Lake Houston Parkway (Houston)	
Approx lat/long: START	27.9516475, -82.4299771	29.934670, -95.249719	
Approx lat/long: STOP	27.9460426, -82.4522997	29.89691, -95.204143	6-point Check
Number of lanes per direction	3	3	a) MATCH
Speed limit (mph)	55 mph	65	
Average lane width (ft)	12 ft	12	
Lateral clearance	≥6 ft	≥6	
Total Ramp Density (ramps/mile) (from HCM)	2 ramps/mile	2	
Freeway Facility type	Urban radial	Suburban circumferential	
D-Factor	0.7	0.52	
Median type	Concrete barrier	Concrete barrier	b) MATCH
Free flow speeds (mph)	69.6 mph	69.6	c) MATCH
Terrain (90% of the time)	Level	Level	
% Heavy Vehicles (HV)	≤ 5%	10%	
AADT (both directions)	80,000	80,000	d) MATCH
K-factor	0.091	0.091	
DDHV (veh/h)	5,100	3,790	e) NO MATCH
DDHV flow (pc/h/ln)	1,750	1,330	f) NO MATCH
			GOOD MATCH

Figure 3-6. Snapshot of the 6-point Excel matching table for 3 lane segments

3.2.2. Texas

The matching process identified 5 facilities, with four located in Houston and one in Prairie Dell on Interstate-35. Table 3-5 and

Table 3-6 provide the geometric and traffic properties of the matched segments with respect to the direction of travel. Each segment comprises two Bluetooth sensors for travel time estimation and at least one radar detector for volumes and spot speeds, located within the segment. Segments 1 and 2 match segment A in Tampa while segments 3, 4, and 5, match segment B.

Table 3-5. Geometric properties of the matched segments in Texas

Seg ID	Location	Zip	Lanes	Length/ miles	Speed Limit/ mph	AADT (vehicles)	% Heavy vehicles
1	North Sam Houston Tollway – Wilson Rd to W Lake Houston Parkway	77049	3	2.0	65	80,000	10%
2	I-35 – Prairie Dell to FM-2115	76571	3	1.4	75	80,000	25%
3	SH-99 – Cinco Ranch Blvd to Kingsland	77494	2	2.0	70	95,000	5%
4	SH-288 County Rd 58 to County Rd 101	77578	2	1.4	65	70,000	20%
5	SH-288 County Rd 101 to County Rd 518	77578	2	1.9	65	70,000	20%

Table 3-6. Traffic statistics of the matched segments in Texas

Seg ID	Direction	HCM FFS/ mph	*85 th Percentile FFS/ mph	50 th Percentile TTI	85 th Percentile TTI	95 th Percentile TTI
1	EB	69.6	64	1.08	1.27	1.53
	WB		71	1.05	1.13	1.31
2	NB	67.7	70	1.01	1.07	1.11
	SB		69	1.01	1.07	1.12
3	NB	67.3	68	1.12	2.17	2.56
	SB		76	1.16	1.64	3.22
4	NB	69.6	67	0.94	1.10	1.17
	SB		72	0.98	1.17	1.22
5	NB	69.6	72	1.09	1.17	1.24
	SB		71	1.07	1.14	1.20

*85th percentile FFS is derived by computing travel times under known normal traffic conditions (i.e., 10 PM to 5 AM)

3.3. Data Fusion

Data fusion methods are employed to establish a complete dataset consisting of various segment-specific traffic-related variables. This step is carried out independently for the roadway segments in Florida and Texas. The complete process of data fusion is shown in Figure 3-7.

Data fusion is first applied to the Texas segments to facilitate the development of the congestion detection algorithm. Texas raw data consist of five main sources i.e., Bluetooth (Anonymous wireless address matching-AWAM), radar (at least one radar location), planned road closure records, incident records, and historical weather collected from January 2018 to March 2020 (790 days). Although more recent traffic data are available, the project team selected this timeframe to control for impact of the Corona Virus Disease 2019 (COVID-19) on travel behavior.

The AWAM and radar data are available in 5-minute increments. Planned road closures are extracted based on the start/end datetime and flagged every 5-minutes until elapsed. Similarly, incidents are flagged based on confirmed/cleared datetimes. To further investigate traffic progression during incident-related congestion, time buffers are placed one-hour prior the confirmed incident times and two hours post cleared times. Only incidents within one mile upstream/downstream of the segment are included. Historical weather data are available in one-hour increments from an application programming interface (API) using the closest zip code of the segment. Following data merging across these sources, FFS (85th percentile speed computed using average speeds from 10 PM and 5 AM), travel rate, and TTI, are computed. In time-period with no TT estimates, TT from the last known period is applied.

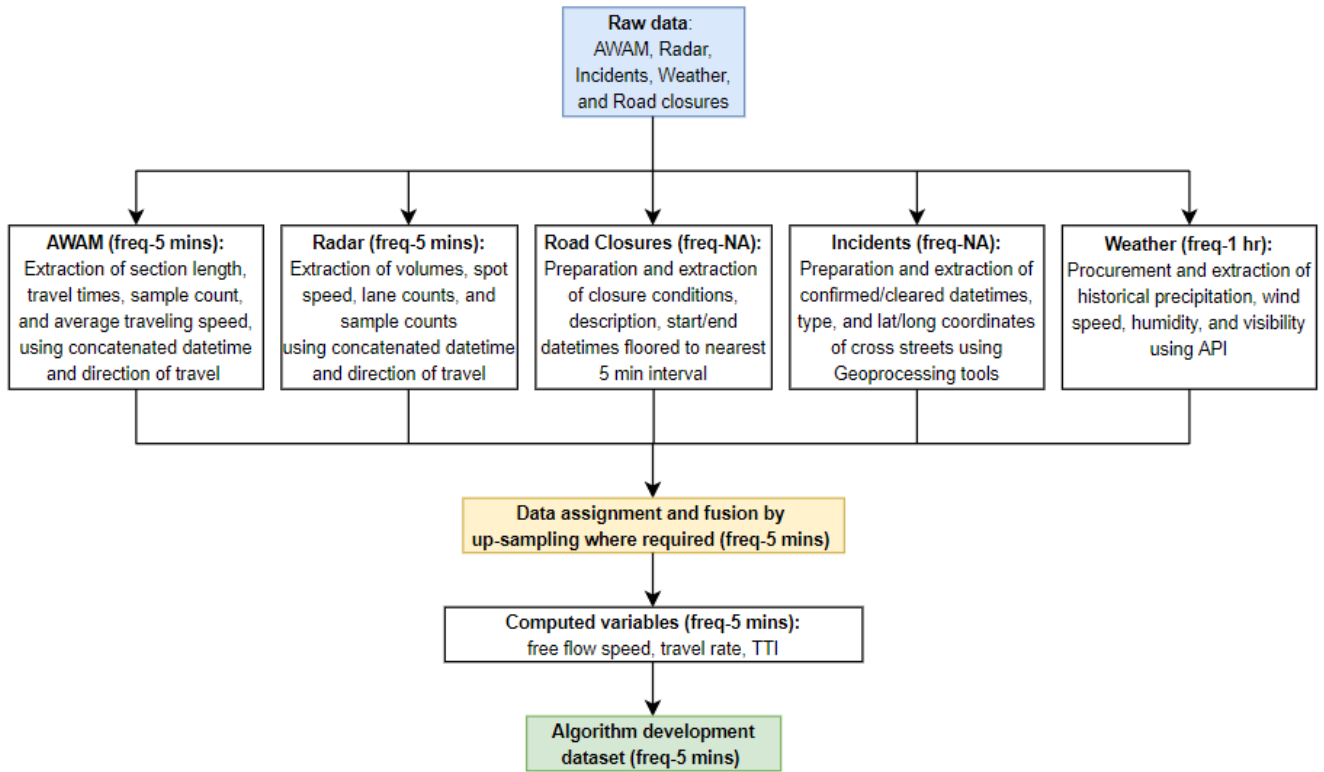


Figure 3-7. Data fusion flow diagram for facilities in Texas

A similar data fusion process is used to create the Florida dataset. Segment lengths across the two geographic locations is set to a maximum of two miles to identify and potentially mitigate sources of congestion. Segment B from the Selmon Expressway is divided into two 2-mile segments shown in Figure 3-8.



Figure 3-8. Two-mile segment split of the Selmon Expressway in Tampa, FL

There are several advantages of using CV infrastructure to determine TTs. This research capitalizes on the spatial-temporal precision of BSMs and limited TT estimate loss due to incomplete check in/out vehicle identifiers especially when involving segments with multiple access points. To continually estimate TTs at low CV penetration rates, multiple intermediate virtual sensors are positioned half-mile apart in ArcGIS as polygon shape files, 100 ft in length, and later referenced in R scripts (Pebesma, 2018) to determine intersecting BSM trajectories.

TTs are then extracted for sections between two consecutive virtual sensors in 5-minute aggregates. Figure 3-9 shows the trajectory of a single vehicle. In the event two BSMs are present within the virtual sensor as shown by 1 & 2 or 3 & 4, deduplication is applied to only select the earliest BSM. TT for this section would then be estimated between the two BSMs, 1 and 3. If multiple vehicles are present within a 5-minute interval, average TT would be computed for the section. This process is applied to periodically estimate TTs of the three segments by summing TTs between consecutive 0.5-mile virtual sensors within the bounds of the selected segment. TT data cover one year starting on 21st February 2019 and ending on 21st February 2020.

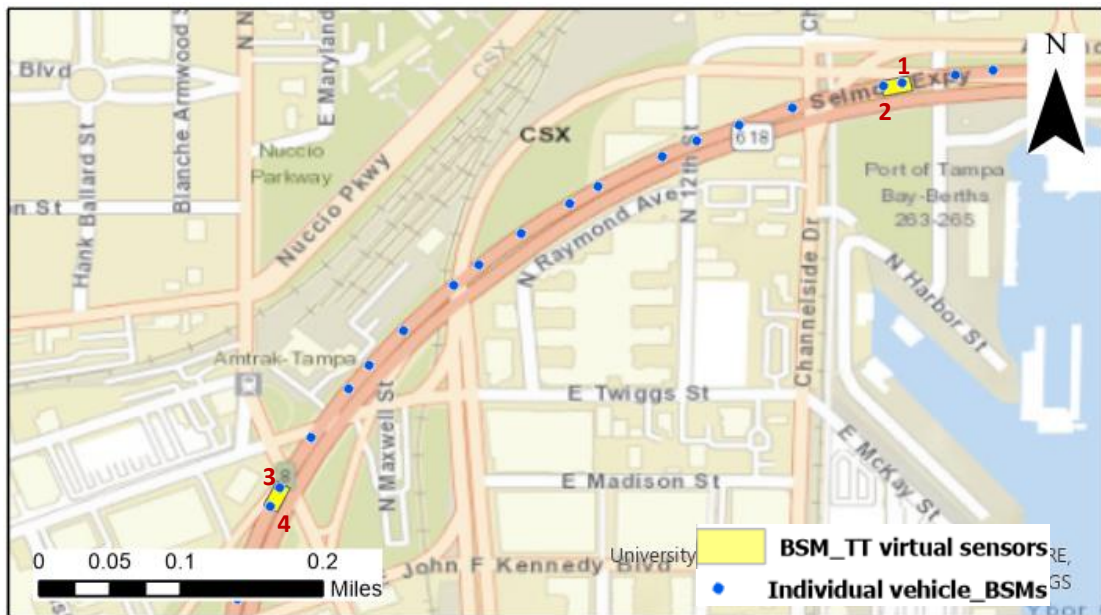


Figure 3-9. TT generation using BSMs in Tampa, FL

The Incident records are from the Florida Department of Transportation (FDOT) open data hub (FDOT-Safety-Office, 2020). However, incident cleared times are not available in the database, so the Florida 2019-2020 reported average incident clearance time (one hour) is added as a congestion buffer. Only incidents within one-mile upstream/downstream of the segment are included. Historical weather data are collected in 10-minute intervals from an API starting on 21st February 2019. Unfortunately, road closure information is not readily available to the project team for validation. Figure 3-10 shows the data fusion steps.

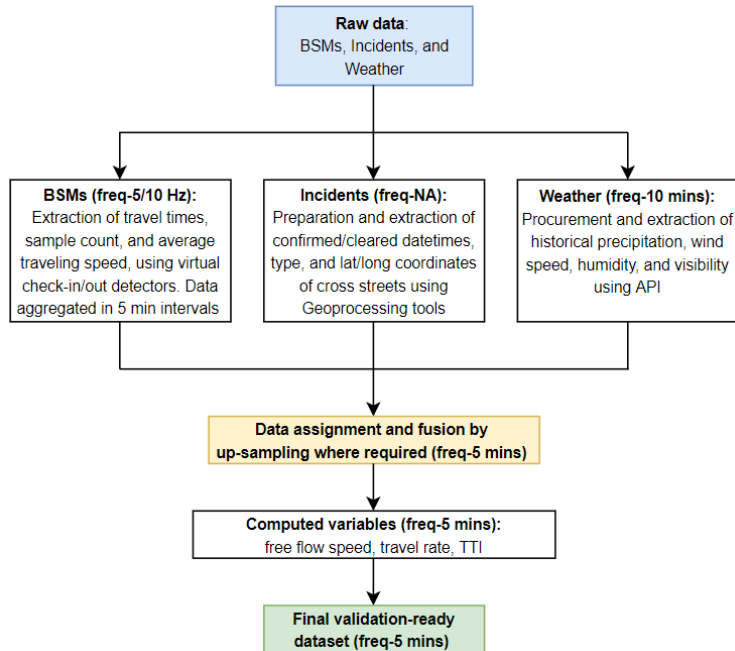


Figure 3-10. Data fusion flow diagram for Selmon Expressway in Tampa, FL

3.4. Developing the Congestion Detection Algorithm

Based on the objective of this research project on being able to apply the developed congestion detection algorithm to any data source with TT estimates, the algorithm is first applied to the Texas dataset (due to more segment diversity and completeness in terms of logging non-recurring events) and is later tested on the CV-based Florida dataset (Kummetha, Kamrani, & Concas, 2021).

After performing data fusion, a universal parameter is required to ensure the robustness of the congestion detection algorithm. The b1 metric is established to simply compute change in TTI intensity between two successive time-steps, as shown in Equation 3.2. This metric makes direct comparisons between distinct segments to establish static zones of various types of congestion.

$$b1 = \frac{TTI_t - TTI_{t-1}}{TTI_{t-1}} \tag{3.2}$$

Where,

TTI_t = TTI at time step t

TTI_{t-1} = TTI at the immediate previous time step (5 minutes prior)

Figure 3-11 shows the result of using the b1 metric instead of directly applying TTI across the various segments. Figure 3-11(a) clearly depicts the failure of TTI as a universal threshold due to the wide variety of traffic conditions across segments within similar geographic locations. Figure 3-11(b) shows the applicability of the b1 metric as a universal approach to setting static thresholds, as the density plots are more normally distributed around a common mean.

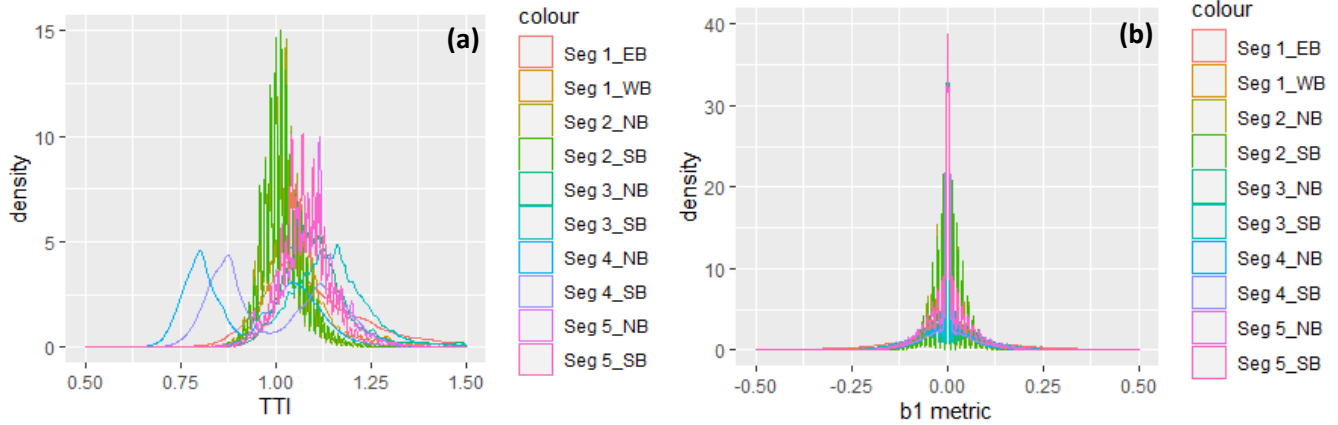


Figure 3-11. Density plots of TTI and b1 metric by segment¹

Although using the b1 metric proves to unify the distributions, high variability between time points is observed, as shown in Figure 3-12. The high variability would result in discontinuous and frequent prediction fluctuations without any clear insights into the type or intensity of congestion. The research team applied several smoothing functions to reduce the variability of the b1 metric, including simple moving average and exponential moving average (EMA) with varying window sizes. While the functions can reduce the high variability, they do not sufficiently smooth the b1 metric and are still susceptible to averaging the highs and lows. As a result, they are not able to highlight key congestion peaks/points.

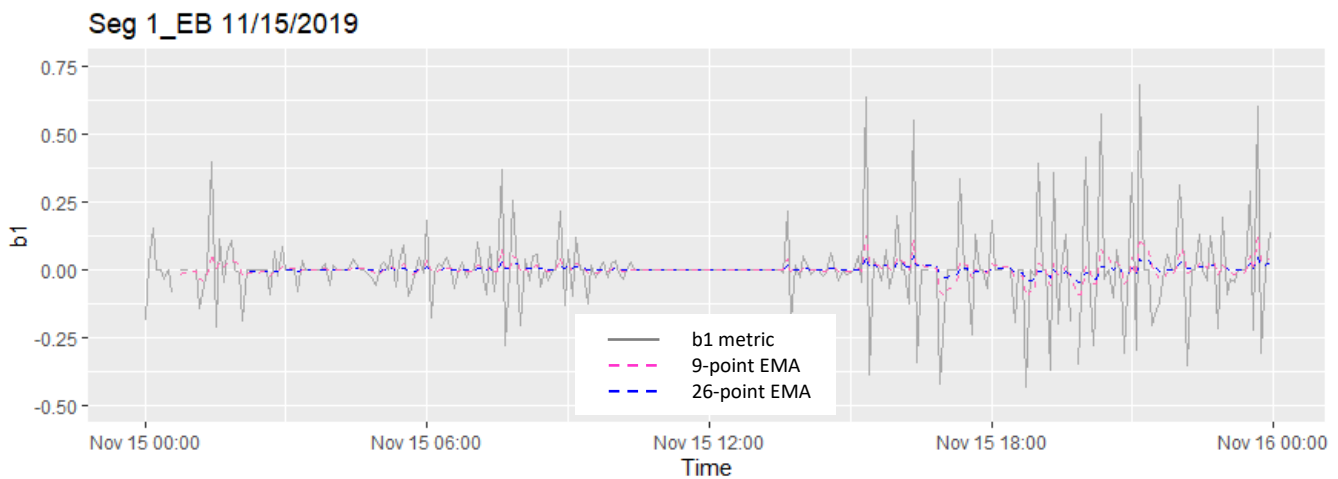


Figure 3-12. Exponential moving average (EMA) applied to b1 metric

The next approach is to apply signal processing algorithms and assess the outcomes. Finite Impulse Response (FIR) and Infinite Impulse Response (IIR) filters are examined. The proposed congestion detection algorithm would benefit from faster processing power due to near real-time processing of data and more consistent

¹ Where, EB = Eastbound, WB = Westbound, NB = Northbound, and SB = Southbound, directions of travel

outputs resulting from feedback circuitry. A commonly used filter in signal processing known for efficiently rejecting unwanted signal frequencies (low ripples in the processed signal) while maintaining uniform sensitivity towards the key frequencies is the Butterworth filter (Roberts & Roberts, 1978). The Butterworth IIR filter is selected with a bandpass ranging from 0 to 0.1 (0% to 10% change in b1)(Developers, 2014; Jagtap & Uplane, 2012). This is done to ensure that large highs followed by steep lows in the b1 metric (signaling volatile recovery) would be minimized without affecting the overall observed trend. Also, as the goal is congestion prediction, negative b1 values are treated as noise and filtered accordingly. Several orders of the Butterworth filter are examined, but the second order achieved sufficient smoothing without excessive signal lag. Figure 3-13 shows the results of the application of the second order Butterworth filter.

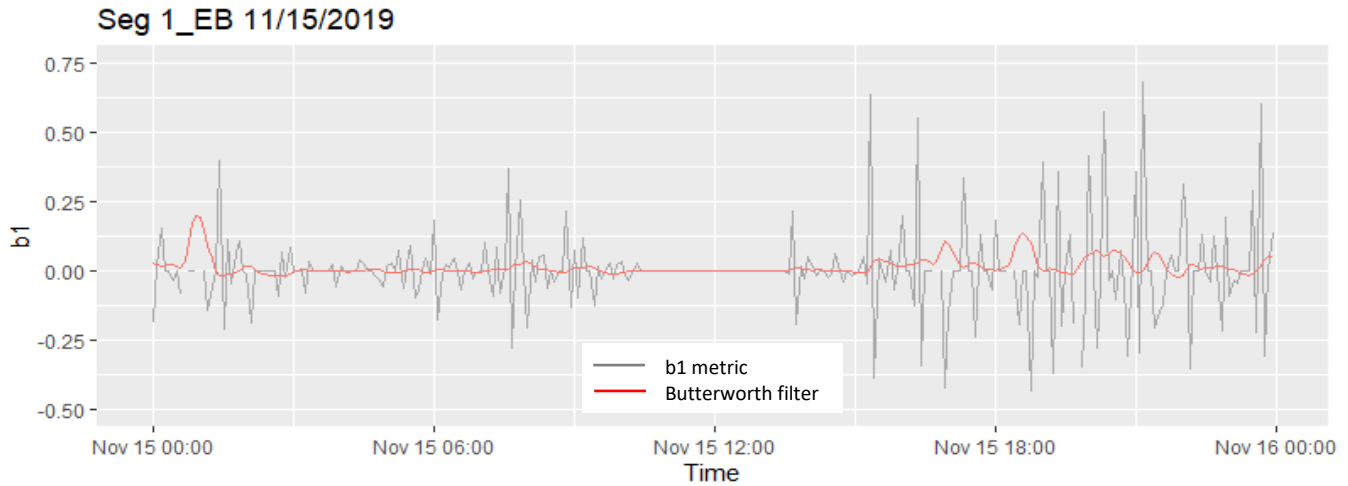


Figure 3-13. Second order Butterworth filter output

Density plots are re-examined to ensure that the application of the signal processing algorithm does not significantly shift the distribution of the segments. Figure 3-14 shows the distributions is still centered around the origin.

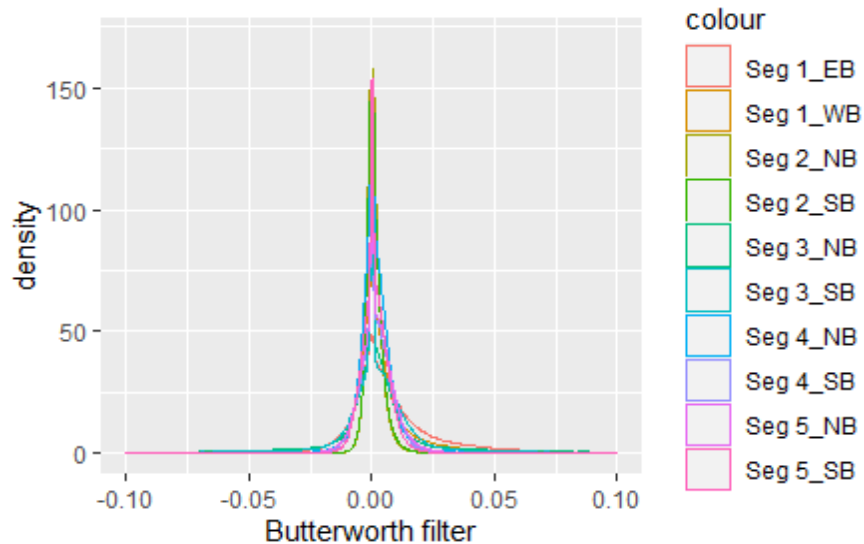


Figure 3-14. Density plots of Butterworth filter output by segment

After establishing the merit of using Butterworth filter, data from the five segments are combined and processed to establish thresholds for various types of congestion. The types of congestion are determined by tracking some of the more common causes of congestion within the pooled dataset i.e., recurring, weather, road closures, and incidents.

To begin, normal conditions must be established for the Butterworth filter output. This is done by filtering out time periods showing the presence of adverse conditions such as incidents, road closures, and weather. Public holidays are also excluded from the normal conditions as research has shown non-recurring congestion patterns during these periods (Transportation Research Board & NASEM, 2014a, 2014b). Also, normal conditions are assumed to occur after 10 PM and before 5 AM of any given day. However, constant time thresholds over this time period are established across all five segments to generalize hours of daily recurring congestion without individual inference to account for high variability of recurring periods within/between segments and day of week. Due to not being able to fully isolate recurring congestion, this category is classified as “Normal + Recurring.”

Weather-related congestion is assessed in detail by identifying congestion peaks in the pooled dataset. The two main weather-related variables contributing to congestion are identified to be precipitation and visibility. Further data processing signal higher congestion if precipitation is present or visibility is less than 4 miles. As adverse weather during late night/early hours would not significantly affect the traffic flow due to inherently low volumes, data from 5 AM to 10 PM are used to determine the Butterworth filter thresholds. Incident and road closure-related congestion thresholds are established within the same time period.

The quantiles for all five cases are computed and are shown in Figure 3-15. Based on these quantiles, the 95 percentiles are used to classify congestion as depicted in Figure 3-16. Figure 3-15 and Figure 3-16 show that the quantiles for recurring and weather-related congestion are similar and cannot be fully distinguished from each other.

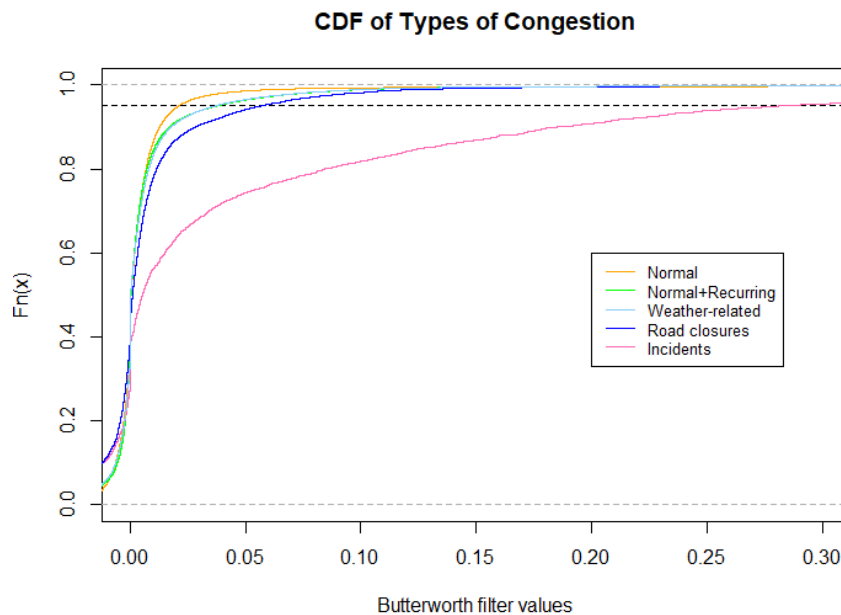


Figure 3-15. Cumulative density function (CDF) depicting the Butterworth filter differences in congestion types

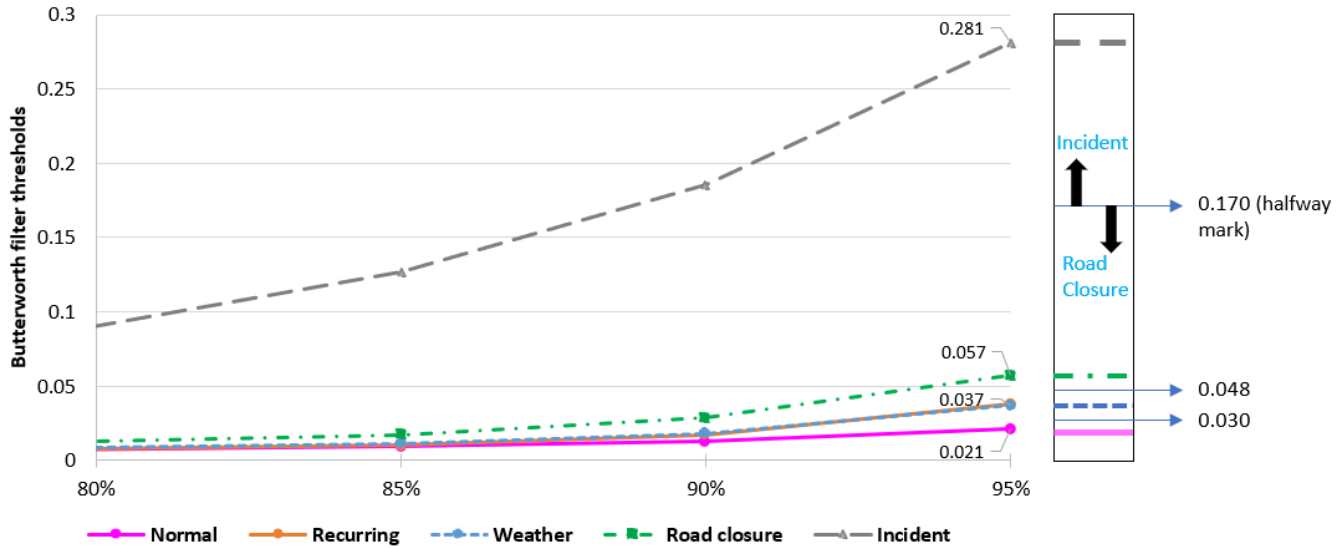


Figure 3-16. Butterworth filter thresholds of various levels of congestion

As the thresholds for “Normal” condition are established, the clear difference in 95th percentile Butterworth thresholds when compared to “Normal + Recurring” imply that this could be directly attributed to recurring congestion. Although five types of congestion are analyzed, the similarities between the intensities of recurring and weather-related congestion warrant the congestion detection algorithm to combine them. The output of the algorithm provides four levels of congestion and follows the conditions shown in Table 3-7 (as evident from Figure 3-16).

Table 3-7. Levels of congestion

Congestion Type	Condition	Predicted Congestion Level
Normal	$y \leq 0.030$	1
Recurring OR Weather	$0.030 < y \leq 0.048$	2
Other Non-Recurring (including planned road closures)	$0.048 < y \leq 0.170$	3
Incident	$y > 0.170$	4

*y = Butterworth filter value at time, t

Figure 3-17 shows the steps followed during algorithm development and validation.

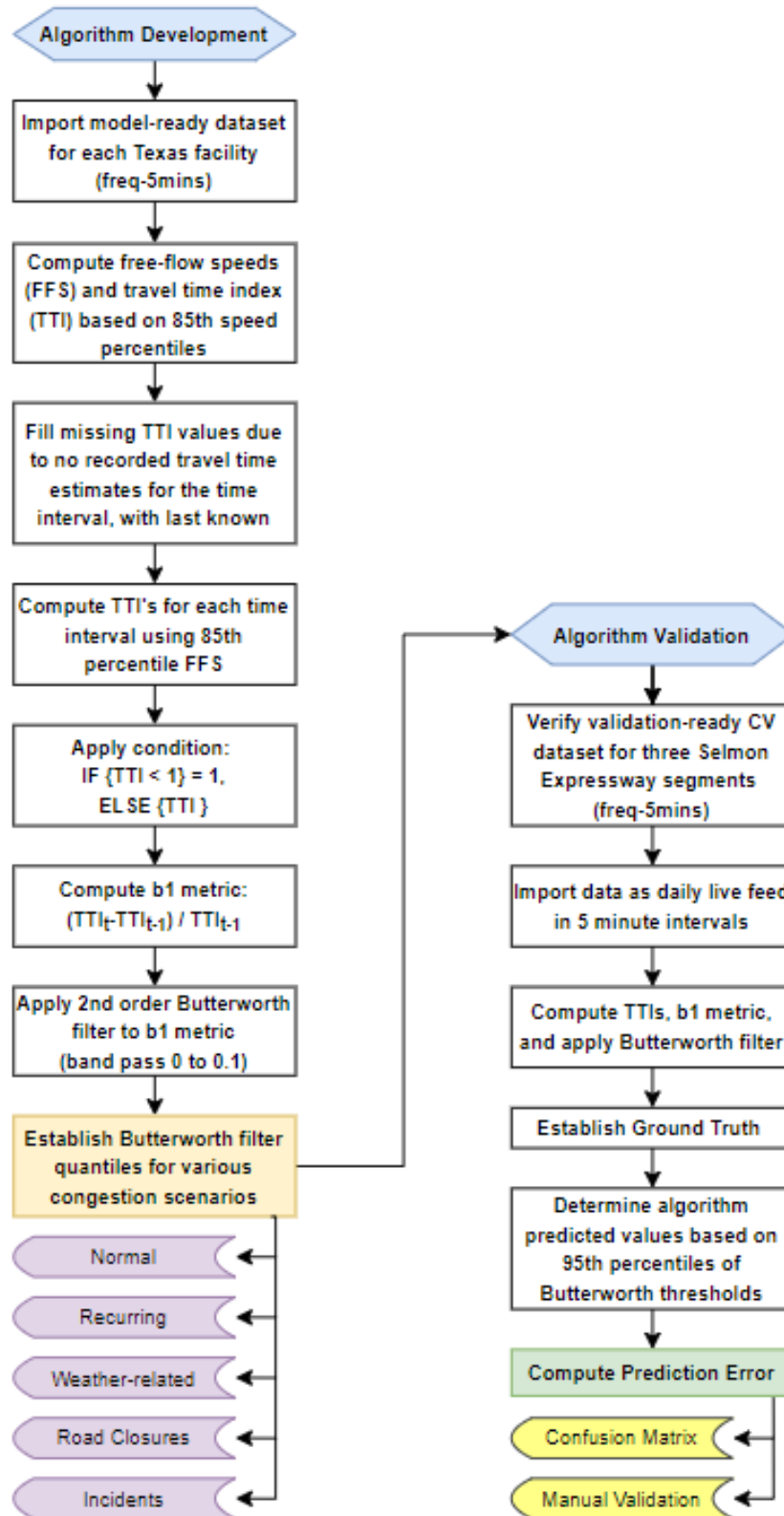


Figure 3-17. Congestion detection algorithm development and validation framework (Kummetha et al., 2021)

4. Results and Discussion

4.1. Congestion Detection Algorithm

The development of a robust congestion detection algorithm capable of functioning without extensive evaluation of geographic/segment-specific traffic thresholds is the primary objective of this project. The next few sections discuss the validation of the congestion detection algorithm, along with the encountered limitations to the approach.

4.1.1. Algorithm Validation

The validation dataset is inspected and imported as a daily live feed in 5-minute intervals. The second order Butterworth filter requires at least two hours (24 5-minute time steps) of data prior to the beginning of prediction. During the validation, daily data from 12 AM to 2 AM are used as prediction warm-up time. The Butterworth filter is applied after every 5-minute TT import. Due to the use of a TT dataset generated from low CV penetration, jumps in TT intervals are observed. To correct for this, the 95th percentile within a one-hour moving window of the Butterworth filter is used. The prediction time and level of congestion are noted accordingly.

Establishing ground truth for the validation dataset is based on a few assumptions as accurately classifying historical data is not possible. All time periods are initially assumed to exhibit normal congestion (level 1) unless an incident (level 4) or weather (level 2) event is reported. Any time periods with average travel speeds less than the posted speed limit of the segment and not satisfying incident or weather conditions are treated as possible cases of non-recurring congestion (level 3).

Recurring congestion (level 2) is established based on a series of normal distributions established from the pattern of morning peak traffic for each of the three segments (A, B-1, and B-2). Figure 4-1 shows the density plots of TTI for weekday morning peak time period. During the evaluation timeframe, the facility did not exhibit afternoon peak hour traffic in the Westbound direction. To establish morning recurring congestion start/end times on a particular day of a segment, a random value is drawn from the normal distribution of that particular segment and offset by an hour to set the start of recurring congestion for that particular day. Since the standard deviation of the plots is approximately 1 hour, a fixed value of 2 hours is used as the duration of recurring congestion.

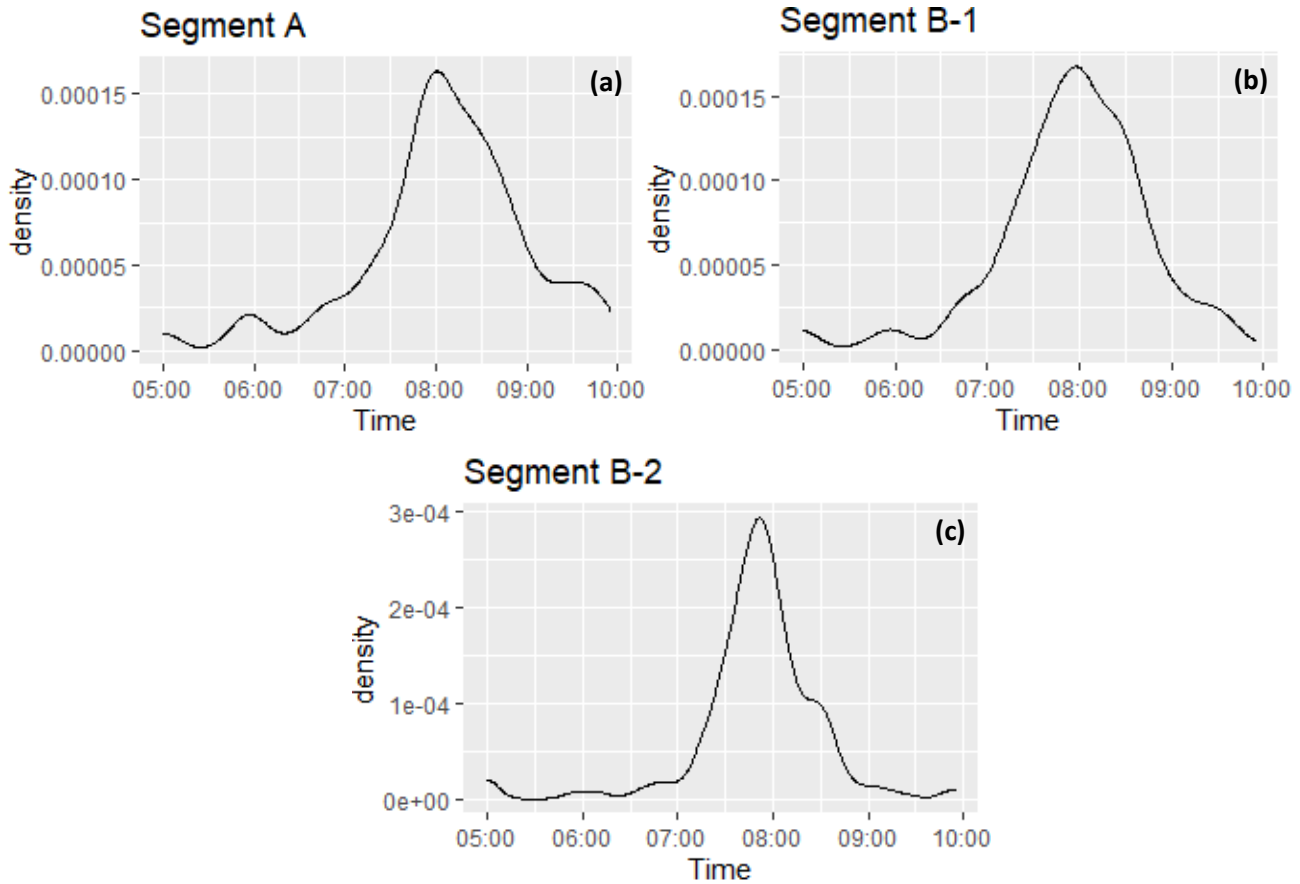


Figure 4-1. Distributions for maximum TTI during morning congestion

4.1.1.1. Confusion Matrix

Prediction error computation is first established by creating a confusion matrix, as shown in Table 4-1. However, due to the presence of time lags (proactive or delayed) and varying levels of congestion prediction, a one-on-one match might only be appropriate for the normal condition (level 1). The confusion matrix is further aggregated for level 1, to establish the precision, recall, and error in the prediction.

Table 4-1. Confusion matrix for the congestion detection algorithm

		Predicted				
		Levels	1	2	3	4
Ground Truth	1	209295	2907	2973	1825	217000
	2	31594	3892	6356	941	42783
	3	19699	2174	2592	1568	26033
	4	55	11	18	12	96
	Total	260643	8984	11939	4346	285912

Level 1	Positive	Negative
Positive	TP = 209295	FN = 7705
Negative	FP = 51348	TN = 17564

Precision = 0.803

Recall = 0.964

Error = 20.7%

The results indicate a relatively good precision, recall, and low error (20.7%) in establishing normal conditions. However, to evaluate other levels, manual validation is warranted.

4.1.1.2. Manual Validation

Manual validation is performed by considering the congestion prediction time and level. Prediction errors are equally allocated between the proactive nature of the algorithm (0.5) and the accuracy of the level of congestion being predicted (0.5). The sum of the prediction errors attributed to the proactive and predicted levels are then computed, to establish total prediction error (shown in Table 4-2). The congestion detection algorithm is only penalized for a predicted level lower than the intensity of the ground truth (i.e., a case with ground truth of level 3 congestion would only be penalized if the predicted congestion level is level 2 or 1, level 3 or 4 would not be penalized). A failed prediction would result in an error of 1.

Table 4-2. Established manual validation error rules by case

Case	Description	Applied Error Rules	
		Proactive component (max = 0.5)	Congestion level component (max = 0.5)
1	Full proactive – with sufficient congestion prediction before ground truth.	0	0
2	Partially proactive – prediction starts before ground truth, but sufficient prediction is only reached after ground truth.	0	$ LP-LG \times 0.5/3$ [3 indicates the maximum possible difference in congestion levels]
3	Delayed – prediction starts after ground truth, but sufficient prediction is achieved within 30 minutes (six 5 -minute periods).	$(TP-TG) \times 0.1$ [0.1 accounts for the 30-minute allowable delay]	$ LP-LG \times 0.5/3$
4	Failed – prediction starts after 30 minutes of ground truth.	0.5	0.5

*LP = Accepted level of predicted congestion, LG = Level established from ground truth, TP = Time of prediction, TG =Time of congestion as established form the ground truth

$$Mean\ error = 100\% \times \frac{\sum_i^N \varepsilon_i}{N} \quad (4.1)$$

Where,

N = Total number of cases examined

ε_i = Established error for a single case, i

The validation summaries by congestion types are discussed below.

Recurring Congestion Validation

A total of 100 cases of recurring congestion are randomly selected and examined across the three segments. The mean error is computed to be 29.7% using Equation 4.1. All examined cases are presented in Appendix A.

Other Non-recurring Congestion Validation

A total of 75 cases of non-recurring congestion are examined across the three segments. The mean error is computed to be 32.2%. Summarized metrics are presented in Appendix A.

Weather-related congestion Validation

A total of 45 cases are examined for weather-related congestion. Changes to traffic state arising from weather cannot be detected by the congestion detection algorithm due to overlapping thresholds with recurring congestion (level 2), hence the need for an external weather data source providing the ground truth for validation. The selected cases comprise of speed changes coupled with flags of adverse weather conditions (i.e., onset of precipitation or drop in visibility) to establish the algorithm’s accuracy in capturing weather influenced changes to traffic conditions. The mean error for the 45 cases is computed to be 33.3% (shown in Appendix A).

Incident Validation

The number of incidents validated are relatively low over the selected validation time frame. Overall, seven incidents are validated as shown in Table 4-3. The mean error is found to be 43.2%. However, excluding incidents that occur on weekends as changes to traffic state (average speed/TT) are not readily detected resulted in a mean error of 35.1%.

Table 4-3. Summary of Incident validation

Date	Confirm Time	Seg ID	Location	Day of Week	Prediction Start Time	Level Match Time	Prediction Error
3/22/2019	4:25	A	Downstream	Fri	*NA	NA	1.00
10/30/2019	10:35	A	Upstream	Wed	7:25	7:25	0.00
11/13/2019	7:00	A	Within	Wed	6:50	NA	0.13
10/30/2019	10:35	B-1	Within	Wed	7:15	8:05	0.00
11/13/2019	7:00	B-1	Upstream	Wed	6:50	NA	0.25
11/23/2019	8:50	B-1	Within	Sat	NA	NA	1.00
7/16/2019	18:45	B-2	Upstream	Tue	19:15	19:20	1.00
11/13/2019	7:00	B-2	Within	Wed	6:40	7:25	0.08
Mean Error							0.432
Mean Error without Weekends							0.351

*NA indicates prediction did not start or intensity level is not matched within 30 minutes of ground truth

In general, the developed congestion detection algorithm is moderately effective in predicting the onset of congestion and its intensity level. The overall prediction error across all congestion types is averaged to 30.2%. However, the process followed to compute the prediction error heavily penalizes the algorithm especially in instances where the ground truth cannot be fully verified to the nearest 5-minute time period, i.e., time logs from incident reports could be filed as a derivation of officer arrival time and not actual crash time. This also applies to the estimation of recurring congestion which is based on historical distribution plots and not observed ground truth. Also, since the number of incident-related congestion events were small (seven), evaluation of the algorithm with future crash logs could provide better validation.

4.1.2. Approach Limitations

A few limitations of the developed congestion detection algorithm are discussed below:

- One of the main limitations of using BSM-based TT estimates are the high rate of discontinuous data within successive 5-minute intervals, resulting from low CV penetration rates. However, this is expected to significantly improve in the near future due to ongoing commuter recruitment and original equipment manufacturer (OEM) partnerships in Tampa, FL (Concas, Kourtellis, & Kamrani, 2021).
- The congestion detection algorithm is developed and validated using data from only two geographic locations. Adding more geographic variability could further improve the overall robustness.
- Computing free flow speeds using 85th percentile estimates from 10 PM to 5 AM results in some errors especially in facilities with high night-time truck traffic.
- The methodology does not distinguish between more than one type of congestion occurring simultaneously. However, the suggested mitigation strategy will still be valid based on the predicted congestion level.
- The validation metrics of the algorithm are not universally applicable and there are cases where the implemented error rules aggressively penalized the algorithm due to approximation of the ground truth.

4.2. Microsimulation

A key goal of this research is to proactively detect congestion and its intensity level. This section discusses the process followed to establish representative microsimulation models of recurring and non-recurring congestion in the lower decks of the Selmon Expressway in Tampa, FL. The purpose of this exercise is to simulate the types of congestion (recurring and non-recurring) and potential strategies that could be applied based on the four predicted congestion levels from the algorithm. The goal is to identify and evaluate mitigation strategies that could be applied in real-world conditions to alleviate the intensity of congestion based on the congestion detection algorithm's output.

4.2.1. Baseline Geometry

Figure 4-2 and Figure 4-3 show the geometry and location of virtual sensors used to compute section-wise TTs along the westbound Selmon Expressway. During the AM hours, the Selmon Expressway provides an on-ramp access to the REL in the direction towards downtown Tampa (shown in Figure 4-3). The virtual sensors are strategically positioned in ArcGIS as polygon shape files, 100 ft in length, and later referenced in R scripts to determine intersecting BSM trajectories.

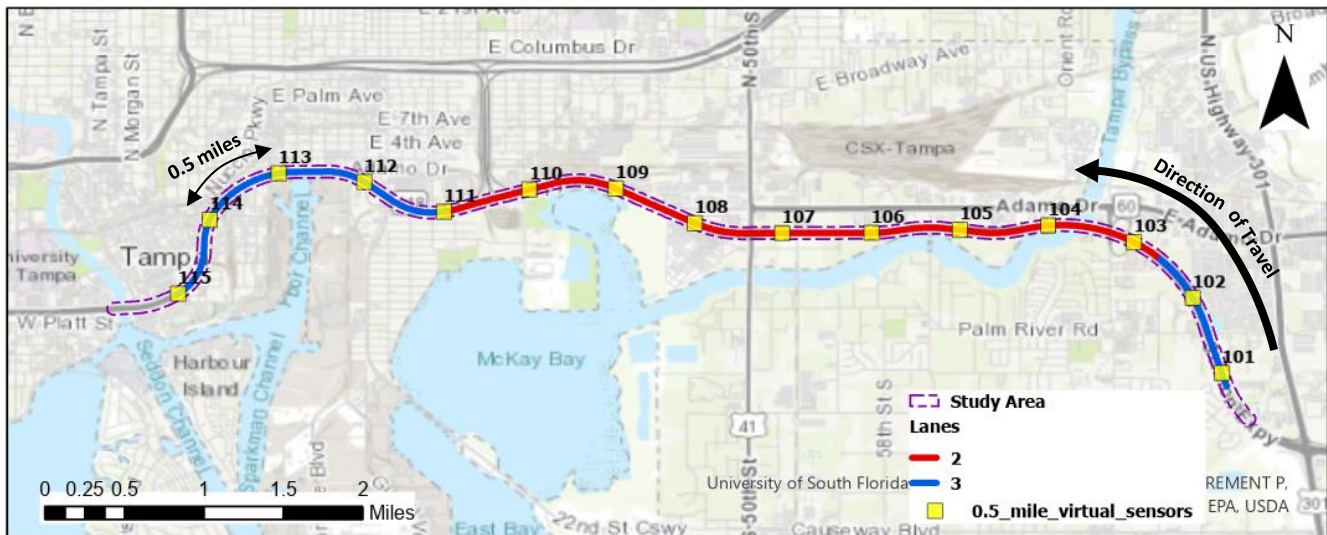


Figure 4-2. Location of virtual detectors used to estimate TTs



Figure 4-3. 2D facility layout in the WB direction

The simulation model, run using TransModeler, utilizes the GIS-based coordinates of virtual sensors to assign the positions of vehicle-to-roadside communication (VRC) sensors. The VRC sensors track unique vehicle IDs, sensor IDs, detection time, speed, origin point, and destination point, as they traverse through the simulation network. This simulation calibration approach takes full advantage of CV trajectory data while minimizing missing data points due to low penetration rates and multiple access points.

4.2.2. Simulation Calibration

Systematic simulation calibrations of real-world conditions involving recurring and non-recurring congestion are performed. This section describes all the steps followed and the establishes goodness of fit metrics.

4.2.2.1. Recurring Conditions

Recurring traffic conditions depict the existing conditions experienced by commuters using this facility. Traffic volumes are obtained from the Iteris dashboard for the mainline and surrounding on/off ramps in the westbound direction of the Selmon Expressway (Iteris, 2021). This is because the Selmon Expressway does not have sensor-based volume counts. Iteris generates hourly volume estimates using a combination of Texas Transportation Institute AADT to volume profile methodology and available probe/traffic sensor data. Origin-destination (OD) matrices for traffic volumes are developed in hourly increments as that is the highest level of granularity available.

A weekday (April 8, 2019) is selected as seed day after confirming the absence of non-recurring sources of congestion such as public holiday, incidents, precipitation, and poor visibility. TTs for the seed day during morning peak hours are obtained by geo-spatially extracting time stamps and vehicle IDs in BSMs detected within the virtual sensors shown in Figure 4-2. The virtual sensors are placed half-a-mile apart along the westbound 7-mile section of the Selmon Expressway. TTs are extracted for sections between two consecutive virtual sensors at 5-minute intervals, starting from 5 AM to 10 AM. The following steps are taken to generate more complete data:

- Missing data due to lack of BSMs generated within the 5-minute interval are populated with the last known travel time for that section.
- BSMs that miss checking in/out of one or more consecutive virtual sensors due to GPS signal loss are identified and also used to generate TTs by extrapolating individual 0.5-mile section TTs from average speeds.
- Where multiple vehicles IDs are detected within a single 5-minute interval and section, average TTs are computed respectively.

The project team acknowledges these assumptions/short-comings and attributes them to the current low CV penetration rates. However, current plans to increase enrolling vehicles would improve penetration rates and significantly reduce the need for extrapolation. Figure 4-4 shows the real-world (BSMs) travel times observed for the recurring conditions seed day. For reference, typical free-flow TTs across individual 0.5-mile sections are recorded to be between 0.40 and 0.42 minutes.

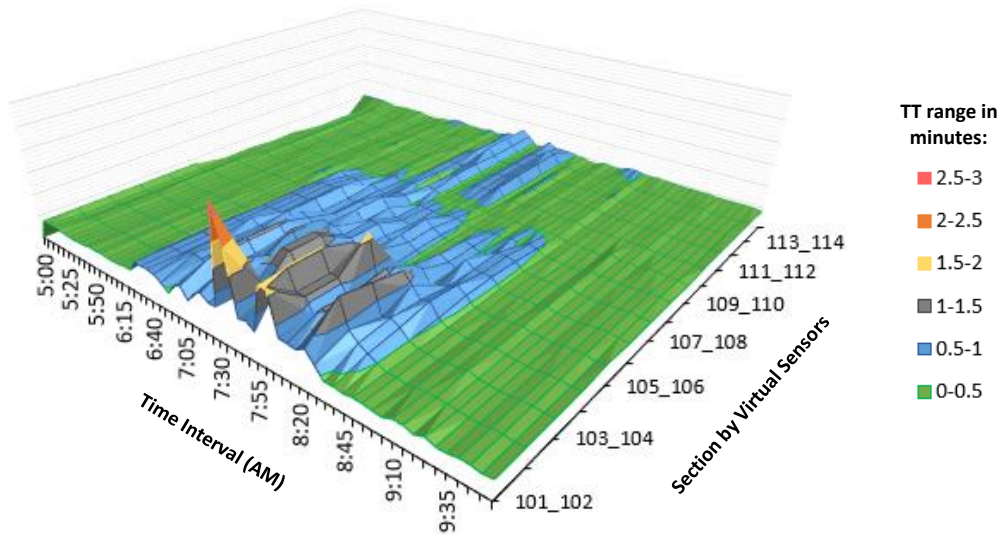


Figure 4-4. BSMs-observed TT in minutes across the 0.5-mile sections for the recurring seed day

After computing the observed TTs, the simulation is setup to match facility specific conditions by setting the vehicle class distribution to include 5% heavy vehicles and applying the appropriate speed limits to the respective road classes. Prior to making any calibration changes, all network links are set to follow the default Wiedemann 74 parameters for car-following and Neighboring lane model for lane changing. A 20-minute simulation warm-up period, prior to the start of data collection (4:40 AM to 5:00 AM) is set by accounting for the TTs to traverse the facility at the speed-limits. Traffic volumes are input in hourly intervals using OD matrices and a standard deviation of 5% is used to introduce some variability within the volumes.

The baseline simulation is then batch-processed 10 times to obtain the standard deviation from the results. Equation 4.2 shows the number of simulation runs required to achieve 95% confidence with an allowable error (ϵ) of 10-percent. The mean (μ) of the 0.5-mile section with the largest standard deviation (SD) in TTs is used for the calculation. A total of 25 runs are chosen as the optimum required number (Kamrani, Abadi, & Golroudbary, 2014).

$$t_{\alpha/2} = 2.262 \text{ (} df = 9, \text{alpha} = 0.05\text{)}$$

$$N \geq \left[\frac{SD \times t_{\alpha}}{\mu \times \epsilon} \right]^2 \tag{4.2}$$

$$\left[\frac{6.3 \times 2.262}{29.4 \times 10\%} \right]^2 = \mathbf{24 \text{ runs required} \sim 25 \text{ runs}}$$

Two measures, the normalized root mean square error (NRMSE) and mean absolute percentage error (MAPE) shown in Equations 4.3 and 4.4, are used to compute the goodness of fit between the observed and simulated travel times for the entire facility. A pre-liminary target of achieving both NRMSE and MAPE scores of less than

25% for the entire facility (from virtual sensor 101 to 115) is set. Further, individual 0.5-mile section targets of less than 30% for either NRMSE or MAPE are also set to ensure sufficient localized calibration.

$$\% \text{ NRMSE} = \frac{\sqrt{\sum_{t=1}^n (\hat{y}_t - y_t)^2 / n}}{y_{max} - y_{min}} \times 100 \% \quad (4.3)$$

$$\text{MAPE} = \frac{100 \%}{n} \sum_{t=1}^n \left| \frac{y_t - \hat{y}_t}{y_t} \right| \quad (4.4)$$

Where,

\hat{y}_t represents the estimated TT values output from TransModeler at time t

y_t represents the actual value of the TT (from BSMs) at time t

n represents the number of individual time points (5-second time steps)

y_{max} is the maximum value of y_t from t = 1 to t = n

y_{min} is the minimum value of y_t from t = 1 to t = n

The simulation model for recurring conditions is calibrated over several iterations. The initial iterations observed that the free-flow TTs did not match real-world conditions. To fix this, desired speed distributions are modified for both the sections of the facility with existing speed limits of 55 mph and 65 mph. It is noted that average and free-flow speeds within the two distinct speed-limit segments are identical and much higher than the posted speed limits. Free-flow TTs are closely matched by adjusting the speed distributions shown in Table 4-4.

Table 4-4. Desired speed distributions for individual road classes

Speed Deviation (mph)	-10	-5	0	5	10	15	20	25
Driver % for 55 mph segment	0	1	5	5	10	43	35	1
Driver % for 65 mph segment	1	2	15	25	50	5	2	0

Following the calibration of free-flow TTs, further iterations are performed to replicate the onset of recurring congestion, as shown in Figure 4-4. Driver behavioral parameters, shown in Table 4-5, with respect to car-following are then adjusted until the desired calibration thresholds of NRMSE or MAPE are reached (Kondyli, Chrysikou, & Kummetha, 2020). Batch simulations of 25 runs are then completed to generate the outputs.

Table 4-5. Car-following model selection and modified parameters for recurring conditions

		Wiedemann-74				Wiedemann-99		
From virtual sensor	To virtual sensor	AX _{add} (ft)	AX _{mult} (ft)	BX _{add} (ft)	BX _{mult} (ft)	CC0 (ft)	CC1 (s)	CC2 (ft)
101	109	8.00	0.98	8.00	9.84	-		

109	110	-				4.92	0.90	13.12
110	115	8.00	0.98	8.00	9.84	-		

The output from TransModeler’s VRC vehicle/sensor reports are then post-processed in R to compute TTs in 5-minute intervals for individual sections. The comparison charts showing seed day versus calibrated TTs are reported in Appendix B. Figure 4-5 shows a breakdown of the goodness-of-fit scores by section. Facility-wide NRMSE and MAPE averages are 22.7% and 16.8%, respectively.

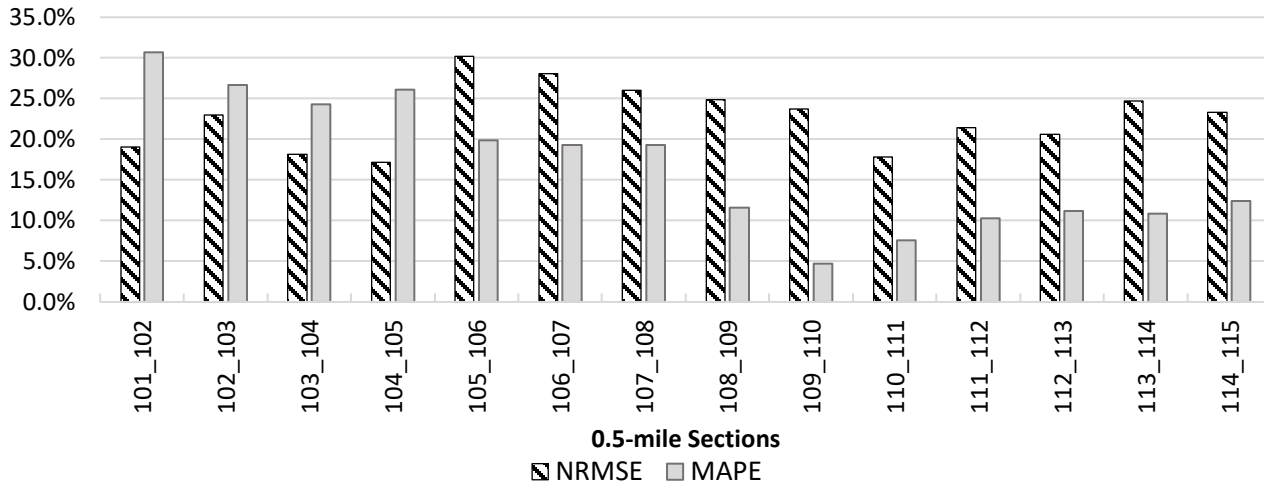


Figure 4-5. NRMSE and MAPE results for calibration of recurring conditions

4.2.2.2. Non-recurring Conditions

Like modeling recurring conditions, a seed day for incident-related congestion is identified along the facility. The chosen seed day, 13th November 2019, involved a two-vehicle crash heading westbound, close to the 78th street interchange on the Selmon Expressway. The crash is reported to have occurred at 7:02 AM and resulted in severe congestion as shown by the increase in TTs in Figure 4-6.

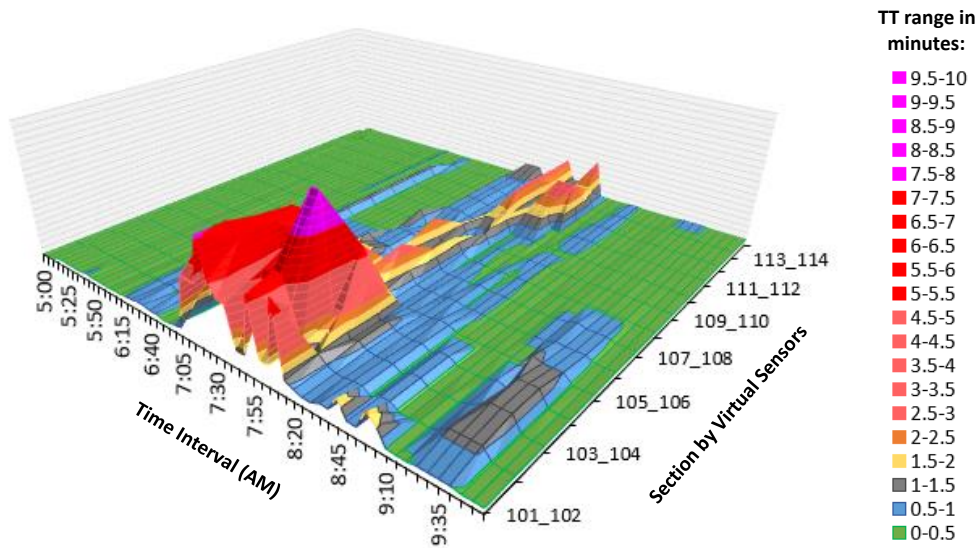


Figure 4-6. BSMs-observed TT in minutes across the 0.5-mile sections for the incident seed day

Calibration is performed by first trying to identify congestion patterns in the TTs obtained from the BSMs. Several iterations of calibration are attempted using speed and driver behavior adjustments. However, due to the impact of the incident, sufficient calibration is only achieved by applying a controlled lane closure between section 105 and 107 for a duration of 50 minutes. Table 4-6 shows the fine-tuned parameters of the car-following models used to achieve sufficient calibration.

Table 4-6. Car-following model selection and modified parameters for non-recurring conditions

From virtual sensor	To virtual sensor	Wiedemann-74				Wiedemann-99		
		AX _{add} (ft)	AX _{mult} (ft)	BX _{add} (ft)	BX _{mult} (ft)	CC0 (ft)	CC1 (s)	CC2 (ft)
101	102	6.00	1.00	6.00	3.00	-		
102	103	-				12.00	1.00	30.00
103	113	6.00	1.00	6.00	3.00	-		
113	114	-				12.00	1.00	30.00
114	115	6.00	1.00	6.00	3.00	-		

The comparison charts showing seed day versus calibrated TTs by section are reported in Appendix C. Figure 4-7 shows a breakdown of the goodness-of-fit scores by section after 25 batch runs. Facility-wide NRMSE and MAPE averages are 20.6% and 26.9%, respectively. Individual section goodness-of-fit scores are greater in MAPE than NRMSE. However, NRMSE satisfies the initial calibration threshold of less than 30% error per section.

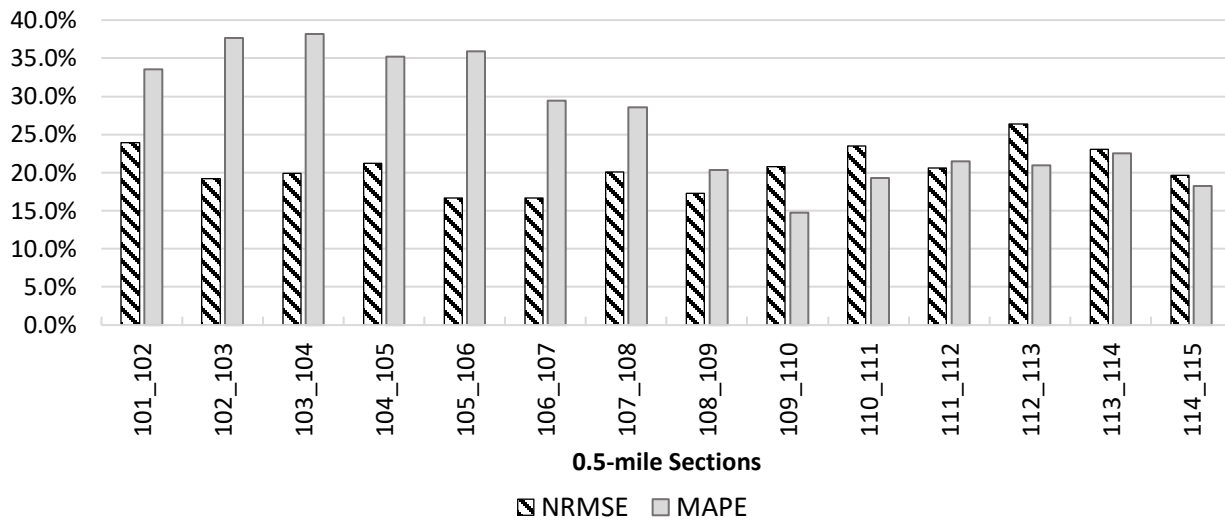


Figure 4-7. NRMSE and MAPE results for calibration of incident-related congestion

4.2.3. Congestion Mitigation

After performing sufficient calibration, both recurring and non-recurring simulation models are subjected to congestion mitigation strategies relevant to the study area: speed harmonization, dynamic rerouting, and combination of both. The next subsections present the findings in comparison to the calibrated seed-day conditions.

4.2.3.1. Recurring Congestion

No Strategy

The no strategy reflects the output of the calibrated recurring conditions on the seed day.

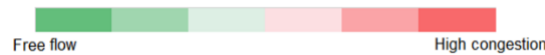
Speed Harmonization

A combination of iterative speed advisories and a speed-based algorithm (Hale et al., 2016) are used to select the most efficient speed advisories within an upstream of the identified bottleneck sections. The developed congestion detection algorithm can predict congestion with a level match (level 2-recurring) by 6:50 AM. The calibrated seed day simulation model indicates a similar starting point for congestion, shown by the yellow border in

Table 4-7. The bottleneck location is determined by identifying consecutive average section speeds lower than the posted speed limits.

Table 4-7. Location of recurring congestion estimated from average section speed on seed day

From	To	65 MPH										55 MPH			
		101_102	102_103	103_104	104_105	105_106	106_107	107_108	108_109	109_110	110_111	111_112	112_113	113_114	114_115
6:30	6:35	70.4	69.5	67.6	65.9	68.3	65.5	66.3	68.1	67.1	67.7	74.0	70.9	74.3	70.7
6:35	6:40	70.5	69.8	67.9	65.9	68.9	66.3	66.8	68.9	67.4	68.2	73.7	70.8	73.6	70.9
6:40	6:45	70.6	70.1	68.0	65.9	68.7	66.0	66.8	68.8	67.1	68.2	74.7	71.3	73.8	70.9
6:45	6:50	70.4	69.8	67.9	65.8	68.5	66.1	66.7	68.7	67.2	68.6	74.7	71.3	74.3	70.9
6:50	6:55	70.3	69.8	67.8	66.2	68.7	65.9	66.7	68.4	67.2	68.1	74.3	70.8	74.1	71.2
6:55	7:00	70.2	69.6	67.7	65.9	69.0	66.0	66.9	68.7	67.1	68.4	74.6	70.8	74.3	71.0
7:00	7:05	68.3	55.7	53.4	55.9	63.7	64.2	65.7	67.9	66.4	68.2	74.0	71.1	74.0	70.8
7:05	7:10	68.2	44.0	39.8	41.6	50.8	53.9	57.8	63.4	61.9	66.5	70.1	69.1	71.8	70.4
7:10	7:15	67.7	40.9	34.6	35.7	45.4	47.6	51.4	60.6	58.8	65.1	68.5	68.6	71.3	70.3
7:15	7:20	67.8	42.4	31.4	32.6	40.6	43.7	48.3	59.6	57.5	64.1	68.9	67.4	70.2	70.3
7:20	7:25	68.2	41.3	30.9	30.9	37.4	41.2	44.5	57.8	56.4	63.4	66.9	67.2	70.4	69.9
7:25	7:30	68.3	41.6	30.5	30.0	35.3	39.7	42.3	56.7	54.4	62.3	66.5	66.7	69.6	69.8
7:30	7:35	68.1	41.3	29.9	29.5	34.4	36.6	42.8	56.5	54.1	62.2	65.2	66.9	69.6	69.8
7:35	7:40	68.0	41.9	29.8	28.9	33.4	35.6	39.7	56.1	55.3	62.5	65.3	66.4	70.1	69.8
7:40	7:45	67.9	41.7	29.9	28.4	32.4	35.3	39.5	55.2	53.5	62.8	64.9	66.5	69.3	69.7
7:45	7:50	68.3	39.9	29.9	28.8	32.6	33.8	38.9	56.1	53.7	62.4	65.2	65.9	69.0	69.5
7:50	7:55	68.3	40.1	29.3	28.8	32.7	34.1	36.7	55.5	54.4	62.0	64.4	66.9	69.6	69.8
7:55	8:00	68.2	40.2	29.1	28.6	32.8	34.5	37.1	54.6	53.8	60.9	63.1	65.7	69.7	69.7
8:00	8:05	69.0	48.8	30.3	28.4	32.5	34.5	37.9	54.9	54.0	61.7	63.3	65.4	68.8	69.5
8:05	8:10	69.2	62.1	46.8	31.6	32.5	34.0	38.7	55.4	54.4	61.6	64.3	65.8	68.6	69.1
8:10	8:15	69.1	62.1	55.4	46.6	41.2	35.3	38.2	54.9	53.7	62.1	64.8	66.3	69.0	69.8
8:15	8:20	69.2	61.6	54.5	49.9	56.5	50.9	43.5	56.5	55.2	61.1	64.1	66.7	68.9	69.7
8:20	8:25	69.3	62.7	54.8	49.6	56.4	56.9	58.4	62.2	58.8	64.1	66.7	66.5	69.7	69.9
8:25	8:30	69.2	62.4	55.2	50.6	55.6	57.7	57.5	63.6	60.9	66.2	69.6	68.5	71.8	70.4
8:30	8:35	69.2	63.0	54.8	51.0	55.9	57.7	59.1	63.2	61.4	65.7	69.2	68.3	71.3	70.2



Speed advisories are first computed for the bottleneck and upstream sections based on the speed-based algorithm in Equation 4.5 and are activated in TransModeler assuming a 10-minute implementation/user acceptance delay.

$$u_m(k) = a_m \times \bar{v}_m(k) \tag{4.5}$$

Where,

a_m = established by computing ratio of the posted speed limit to minimum observed speed = $65/53.4 = 1.22$

$\bar{v}_m(k) = (55.7 + 53.4 + 55.9)/3 = 55$ mph

$u_m(k)$ = speed advisory in bottleneck = $55 \times 1.22 = 67$ mph \sim **65 mph**

$u_{m-1}(k)$ = speed advisory upstream of bottleneck = $55 / 1.22 = 45$ mph

After implementing these advisories, minor TT and average speed improvements are observed from the simulation models. Since developing optimized speed advisory algorithms is out of this study, an iterative approach is used to optimize the best combination of upstream, within, and downstream speed advisories. A total of 87 iterations of varying speed and advisory durations are performed. The best improvements to TT resulted from the combination of the speed advisories shown in

Table 4-8, applied for a duration of one hour.

Table 4-8. Selected speed advisories for recurring congestion

Seg ID	102_103	103_104	104_105	105_106	106_107	107_111
Speed advisory (mph)	55	55	50	45	45	65
% TT improvement for 5-10 AM traffic	0.99	1.78	0.42	1.54	2.20	1.75

The overall facility wide improvements to TT resulting from speed harmonization are grouped by the peak congestion period (7 AM to 9 AM) and extended morning period (5 AM to 10 AM). Speed harmonization resulted in TT improvements of 0.51% and 1.09% for the peak congestion and extended morning periods, respectively. Although, these improvements are minimal, the safety benefits of applying speed harmonization with respect to reduction of stop-and-go traffic conditions are discussed in the following sections.

Dynamic Rerouting

As mentioned earlier, a unique feature of the Selmon Expressway is the ability to access the REL located on the upper deck of the freeway. Access ramps to the REL are available in select locations and change travel direction depending on the time of day. For this study, in instances where congestion is detected on the lower decks of the westbound Selmon expressway, simulated traffic is selectively re-routed onto the REL (in the same travel direction) to alleviate congestion. When implementing the dynamic rerouting in a real-world setting, commuters will be informed of the traffic conditions and rerouting choice via HMIs or dynamic message signs.

Dynamic rerouting is applied for a one-hour period from the first detection of congestion. Traffic volume is strategically reassigned to the REL in 5%, 10%, and 15% increments. Peak congestion period traffic for the facility improved by 3.84%, 6.15%, and 7.82%, respectively. Extended morning period traffic also improved by 1.62%, 2.53%, and 3.24%, respectively. A section wise breakdown of the improvements resulting from dynamic rerouting are shown in Table 4-9 and Table 4-10.

Dual Strategies

Finally, a combination of two mitigation strategies is tested by simultaneously implementing speed harmonization with three varying increments of traffic rerouting. Traffic is rerouted onto the REL in three volume increments i.e., 5%, 10%, and 15%. Peak congestion period traffic for the facility (sensor 101 to 115)

improved by 3.82%, 5.55%, and 7.00%, respectively. Extended morning period traffic improved by 2.49%, 3.19%, and 3.80%, respectively.

A summary of the applied strategies, their intensities, and percentage improvements to traffic conditions are shown in Table 4-9 and Table 4-10.

Table 4-9. Summary of recurring TT improvements during 7 AM – 9 AM by section

Strategy Name	Speed limit = 65 MPH										Speed limit = 55 MPH			
	101_102	102_103	103_104	104_105	105_106	106_107	107_108	108_109	109_110	110_111	111_112	112_113	113_114	114_115
Speed Harmonization (SH)	-0.12%	0.33%	1.46%	-1.39%	0.36%	1.54%	0.52%	0.99%	0.44%	1.94%	0.75%	0.22%	0.15%	-0.01%
Dynamic re-routing (DR) 5%	-0.22%	7.82%	10.97%	8.59%	7.29%	6.36%	6.11%	1.70%	1.62%	0.96%	1.26%	0.75%	0.35%	0.21%
DR 10%	-0.46%	11.53%	15.29%	12.94%	12.54%	11.47%	10.25%	3.25%	3.19%	1.79%	2.04%	1.00%	0.89%	0.31%
DR 15%	-0.82%	13.24%	18.46%	17.23%	16.10%	15.04%	13.25%	4.39%	4.29%	2.39%	3.12%	1.38%	1.10%	0.37%
SH + DR 5%	-0.42%	7.11%	11.71%	5.97%	5.57%	5.74%	6.57%	2.97%	2.10%	3.21%	1.83%	0.71%	0.37%	0.10%
SH + DR 10%	-0.65%	9.88%	15.17%	9.65%	8.22%	7.74%	10.75%	4.33%	3.78%	3.80%	2.78%	1.20%	0.77%	0.29%
SH + DR 15%	-0.89%	11.90%	18.40%	11.65%	10.06%	9.54%	14.29%	6.17%	5.22%	4.69%	3.80%	1.53%	1.17%	0.43%

Table 4-10. Summary of recurring TT improvements during 5 AM – 10 AM by section

Strategy Name	Speed limit = 65 MPH										Speed limit = 55 MPH			
	101_102	102_103	103_104	104_105	105_106	106_107	107_108	108_109	109_110	110_111	111_112	112_113	113_114	114_115
Speed Harmonization (SH)	-0.07%	0.99%	1.78%	0.42%	1.54%	2.20%	1.85%	1.86%	1.35%	1.94%	0.83%	0.34%	0.25%	0.03%
Dynamic re-routing (DR) 5%	-0.11%	3.26%	4.65%	3.57%	3.04%	2.61%	2.46%	0.71%	0.75%	0.43%	0.58%	0.40%	0.20%	0.09%
DR 10%	-0.22%	4.75%	6.29%	5.30%	5.24%	4.82%	4.24%	1.29%	1.27%	0.69%	0.80%	0.43%	0.37%	0.09%
DR 15%	-0.38%	5.46%	7.63%	7.14%	6.75%	6.28%	5.37%	1.73%	1.73%	0.98%	1.32%	0.65%	0.54%	0.14%
SH + DR 5%	-0.18%	3.83%	6.10%	3.43%	3.60%	4.00%	4.39%	2.71%	2.06%	2.49%	1.37%	0.50%	0.44%	0.09%
SH + DR 10%	-0.28%	4.98%	7.54%	4.97%	4.84%	4.74%	6.10%	3.22%	2.74%	2.69%	1.69%	0.75%	0.51%	0.13%
SH + DR 15%	-0.39%	5.82%	8.90%	5.80%	5.42%	5.51%	7.59%	4.02%	3.37%	3.10%	2.15%	0.89%	0.73%	0.23%

Further, Figure 4-8 shows the speed profiles of a single vehicle traversing through recurring congestion under previously outlined mitigation strategies. Speed harmonization strategy using speed advisories can be clearly associated with reduction of stop-and-go traffic flow, thus reducing possibilities of rear-ending. However, TTs are not significantly improved. Dynamic rerouting resulted in the greatest improvement to TTs, but little to no improvement is observed in terms of stop-and-go flow. Combining both speed harmonization and dynamic rerouting (10% traffic rerouting onto the REL) proved to be very effective in achieving both TT and safety improvements.

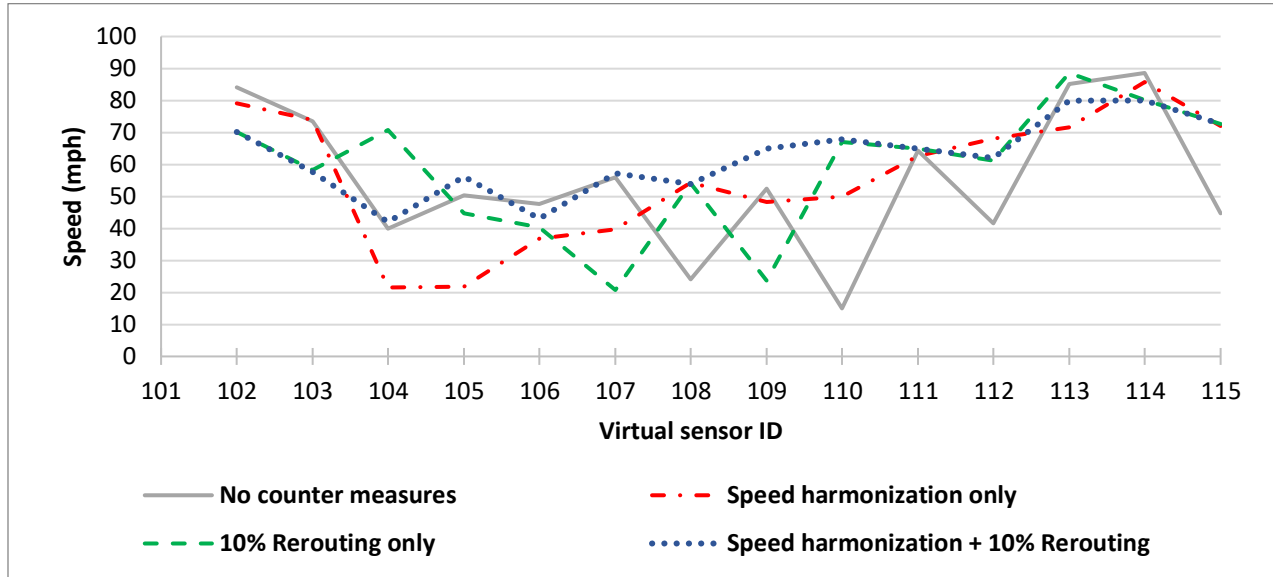
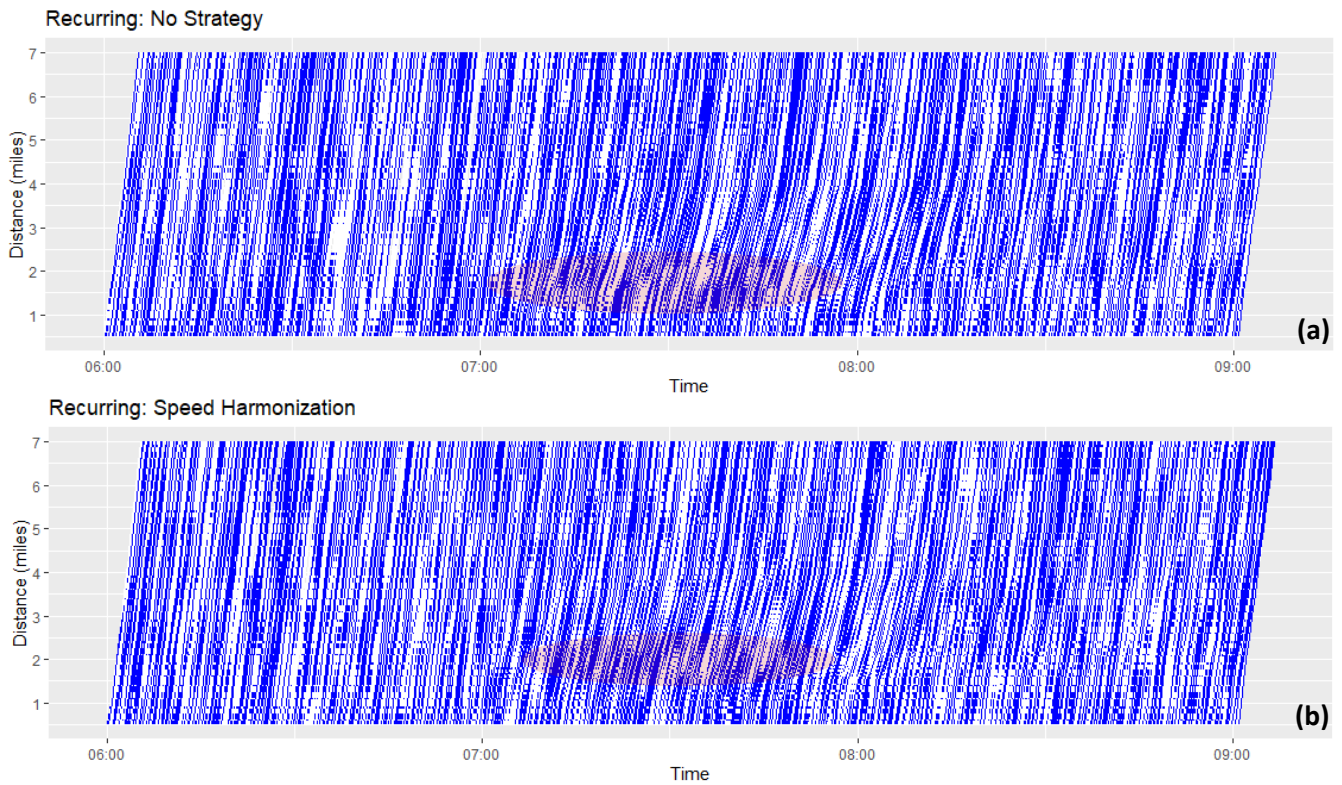


Figure 4-8. Single vehicle speed profiles through various recurring congestion mitigation strategies

Figure 4-9 shows space-time charts for a portion of the morning peak travel. The location and propagation of congestion is identified in red. Combining both speed harmonization and dynamic rerouting results in minimal disruption to overall traffic flow.



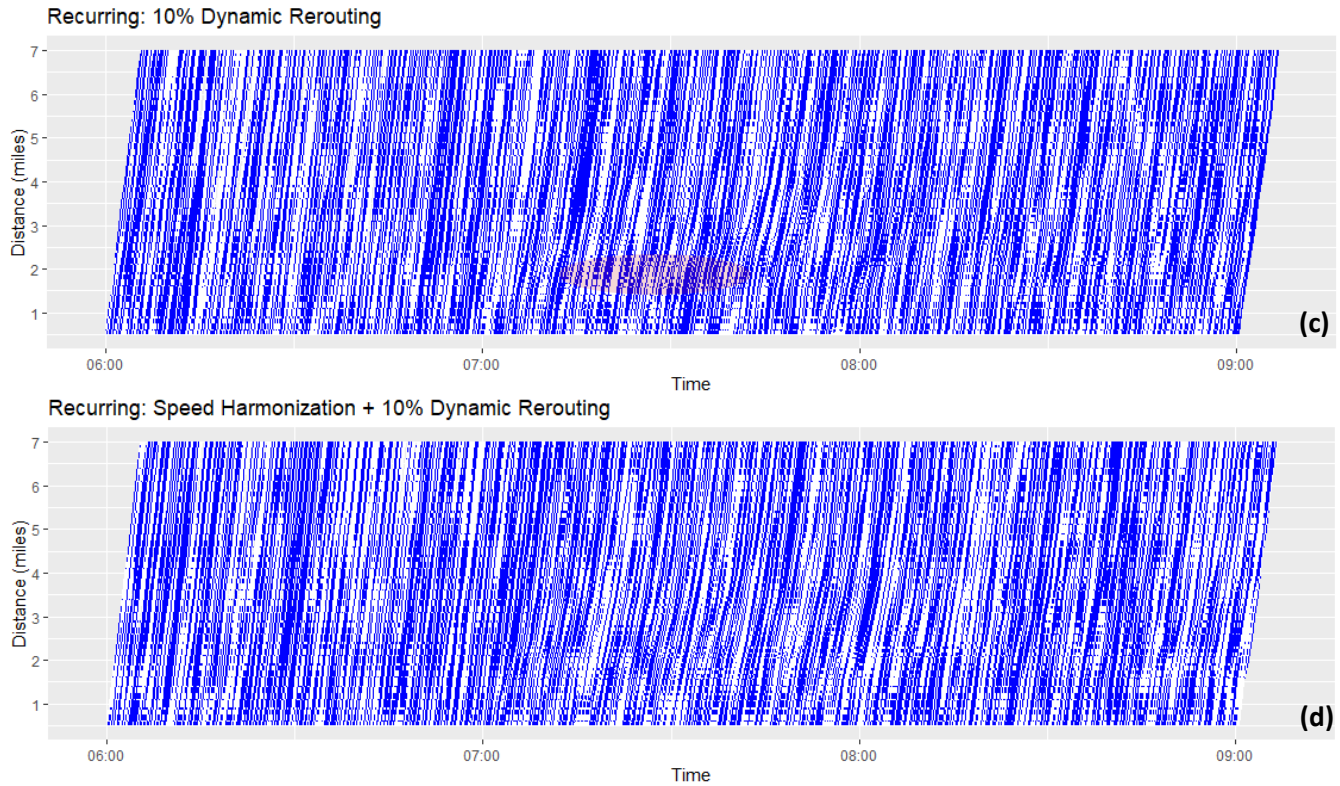


Figure 4-9. Space-time charts showing the impact of mitigation strategies as applied to recurring congestion (red zones indicate congestion)

4.2.3.2. Non-recurring Congestion

No Strategy

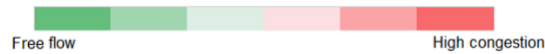
The no strategy reflects the output of the calibrated non-recurring conditions observed on the seed day.

Speed Harmonization

A similar approach to speed harmonization as discussed in the recurring section is followed. The developed congestion algorithm can start identifying non-recurring congestion in segment B-2 by 6:45 AM and a level match (level 4) is achieved by 7:25 AM (Table 4-3). The calibrated seed day simulation model indicated a 7:00 AM starting point for congestion, shown in Table 4-11. Speed advisories are again computed for the bottleneck and upstream sections based on the speed-based algorithm, Equation 4.6.

Table 4-11. Location of incident-related congestion estimated from average section speed on seed day

From	To	65 MPH										55 MPH			
		101_102	102_103	103_104	104_105	105_106	106_107	107_108	108_109	109_110	110_111	111_112	112_113	113_114	114_115
6:30	6:35	70.4	69.5	68.8	66.6	68.8	66.3	67.3	69.5	67.0	69.3	75.4	71.2	75.5	71.4
6:35	6:40	70.5	69.7	68.9	66.9	69.2	66.3	66.7	68.7	66.6	68.8	74.6	70.6	74.8	71.1
6:40	6:45	70.4	69.5	68.6	66.5	69.1	66.3	67.3	69.3	66.9	69.0	75.0	70.9	75.0	71.1
6:45	6:50	70.4	69.4	68.6	66.6	68.5	65.9	67.1	69.2	66.9	68.4	75.0	70.6	75.0	71.0
6:50	6:55	70.5	69.8	68.9	66.7	68.8	66.1	66.6	68.9	67.1	68.8	74.6	70.8	75.0	71.0
6:55	7:00	70.5	69.8	69.0	66.8	69.3	66.6	67.4	69.8	67.2	69.1	75.4	70.5	75.0	71.1
7:00	7:05	69.1	63.9	62.5	35.2	52.5	58.9	68.3	69.7	67.3	69.0	75.0	70.8	74.8	71.0
7:05	7:10	69.1	62.4	30.2	13.2	34.4	43.4	67.2	69.5	67.0	69.3	74.7	70.6	74.9	71.0
7:10	7:15	69.0	43.5	11.1	10.1	31.0	37.8	65.8	69.5	66.8	68.8	73.8	70.3	74.4	70.6
7:15	7:20	68.9	13.3	7.4	10.2	30.1	36.4	65.7	69.6	66.2	68.1	73.8	69.9	74.5	70.7
7:20	7:25	34.6	7.4	7.0	10.0	29.7	35.6	65.5	69.2	66.7	68.9	73.9	69.9	74.4	70.8
7:25	7:30	11.6	5.5	6.9	10.0	29.1	37.2	66.4	69.4	66.2	68.4	74.3	70.0	74.3	70.7
7:30	7:35	6.9	5.3	7.0	10.0	28.9	36.2	66.3	69.7	66.7	68.8	74.1	70.2	74.6	70.8
7:35	7:40	4.9	5.3	7.0	10.0	28.8	36.1	66.0	69.8	66.4	68.8	74.2	70.6	74.6	70.7
7:40	7:45	4.2	5.3	6.9	9.9	28.5	36.8	66.6	69.5	66.4	68.4	74.0	69.9	74.4	70.7
7:45	7:50	4.2	5.3	6.9	10.0	28.4	36.0	66.2	69.6	66.4	68.6	73.9	70.0	74.2	70.5
7:50	7:55	4.4	6.0	9.8	16.7	41.8	50.5	58.8	65.0	61.0	66.4	71.0	69.5	74.2	70.7
7:55	8:00	6.8	11.3	21.5	26.9	32.4	39.6	47.3	59.9	55.7	63.9	67.1	67.7	73.1	70.2
8:00	8:05	9.3	13.7	23.7	27.3	29.8	34.3	41.3	56.5	53.0	61.7	63.9	66.0	72.2	69.5
8:05	8:10	9.7	14.0	23.8	27.5	29.1	31.9	38.3	55.4	51.7	60.5	63.1	64.9	72.0	70.0
8:10	8:15	9.7	14.0	24.1	27.4	28.3	31.8	36.2	54.8	50.7	60.0	62.7	65.2	72.2	69.4
8:15	8:20	9.9	14.2	24.2	27.0	28.2	31.4	36.5	54.6	49.9	58.3	61.6	64.9	71.7	69.6
8:20	8:25	17.5	14.1	24.1	26.9	27.6	31.2	35.6	54.2	50.0	59.1	61.3	64.6	71.6	69.4
8:25	8:30	68.0	18.3	24.0	26.7	27.3	31.4	35.1	54.4	50.1	58.5	61.2	65.2	71.9	69.5
8:30	8:35	69.4	62.6	35.4	27.5	27.7	30.7	35.7	54.6	49.8	59.4	62.3	64.9	71.7	69.4
8:35	8:40	69.7	65.5	65.7	54.4	39.9	33.7	34.8	54.7	50.6	59.9	62.2	65.2	72.0	69.9
8:40	8:45	69.6	65.7	65.7	60.3	62.4	60.7	53.3	60.0	53.8	60.6	62.3	65.5	72.0	69.7
8:45	8:50	69.7	65.9	65.7	59.8	62.5	61.9	63.5	66.3	62.0	66.6	71.4	68.9	73.8	70.6
8:50	8:55	69.7	65.6	65.2	59.9	62.5	61.7	62.8	65.9	62.0	66.9	70.6	69.1	74.0	70.7
8:55	9:00	69.6	65.6	65.9	59.8	62.3	62.0	62.8	66.5	62.7	67.0	71.4	68.7	73.9	70.5



$$u_m(k) = a_m \times \bar{v}_m(k) \tag{4.6}$$

Where,

a_m = established by computing ratio of the posted speed limit to minimum observed speed = $65/35.2 = 1.85$

$\bar{v}_m(k) = (35.2 + 52.5 + 58.9)/3 = 48$ mph

$u_m(k)$ = speed advisory in bottleneck = $48 \times 1.85 = 89$ mph ~ **75 mph** (capped by the maximum allowable speed limit of the facility)

$u_{m-1}(k)$ = speed advisory upstream of bottleneck = $48 / 1.85 = 26$ mph ~ **25 mph**

The established speed advisories are applied in TransModeler. However, as discussed before, only minor improvements to TT are observed from this approach. An iterative approach is used to determine the optimum speed advisories for greatest TT improvement. The best improvements to TT resulted from the same combination of section speed advisories as those of recurring congestion, shown in Table 4-12, applied for a duration of one hour.

Table 4-12. Selected speed advisories for incident-related congestion

Seg ID	102_103	103_104	104_105	105_106	106_107	107_111
Speed advisory (mph)	55	55	50	45	45	65
% TT improvement for 5-10 AM traffic	1.71	1.89	1.91	2.16	0.45	2.20

The overall facility wide improvements to TT resulting from speed harmonization for the peak congestion period (7 AM to 9 AM) and extended morning period (5 AM to 10 AM) are 1.06% and 1.37%, respectively. Section wide breakdown of TT improvements are shown in Table 4-13 and

Table 4-14.

Dynamic Rerouting

Dynamic rerouting is applied for a one-hour period from the first detection of congestion. Traffic volume is aggressively reassigned to the REL in 10%, 20%, and 30% increments. Higher levels of traffic reassignment are possible but are deemed to not be practical due to the capacity limitations of the REL. Peak congestion period traffic for the facility improved by 4.41%, 8.27%, and 12.36%, respectively. Extended morning period traffic also improved by 1.81%, 3.45%, and 5.14%, respectively. Section-wise breakdown of TT improvements, Table 4-13 and

Table 4-14, show significant improvement of traffic conditions close to the incident location.

Dual Strategies

The combination of two mitigation strategies is tested by simultaneously implementing speed harmonization with three varying increments of traffic rerouting, as before. The same increments used in the dynamic rerouting strategy are applied. Peak congestion period traffic for the facility improved by 5.40%, 9.42%, and 13.49%, respectively. Extended morning period traffic also improved by 3.11%, 4.81%, and 6.51%, respectively.

A summary of the applied strategies, their intensities, and percentage improvements to incident traffic conditions are shown in Table 4-13 and

Table 4-14.

Table 4-13. Summary of incident-related TT improvements during 7 AM – 9 AM by section

Strategy Name	Speed limit = 65 MPH										Speed limit = 55 MPH			
	101_102	102_103	103_104	104_105	105_106	106_107	107_108	108_109	109_110	110_111	111_112	112_113	113_114	114_115
Speed Harmonization (SH)	1.90%	2.00%	1.96%	2.02%	1.30%	-2.85%	1.43%	1.96%	0.83%	3.17%	1.14%	-0.07%	0.05%	0.02%
Dynamic re-routing (DR) 10%	17.84%	12.18%	8.06%	4.84%	4.73%	3.85%	3.73%	1.53%	1.79%	1.33%	1.07%	0.56%	0.19%	0.11%
DR 20%	32.08%	23.65%	15.82%	9.45%	9.17%	7.75%	6.16%	2.69%	3.26%	2.00%	2.23%	0.98%	0.34%	0.22%
DR 30%	43.37%	37.85%	25.20%	14.71%	12.31%	11.67%	9.81%	4.14%	4.83%	3.13%	3.40%	1.57%	0.59%	0.42%
SH + DR 10%	18.20%	13.23%	9.63%	5.81%	6.17%	4.78%	4.30%	3.83%	2.71%	3.49%	1.95%	0.83%	0.38%	0.20%
SH + DR 20%	32.26%	24.53%	17.52%	10.78%	10.71%	9.42%	7.54%	5.13%	4.49%	4.26%	3.11%	1.20%	0.51%	0.36%
SH + DR 30%	43.43%	38.38%	26.55%	15.97%	14.51%	13.23%	11.21%	6.73%	6.17%	5.25%	4.29%	1.84%	0.75%	0.52%

Table 4-14. Summary of incident-related TT improvements during 5 AM – 10 AM by section

Strategy Name	Speed limit = 65 MPH										Speed limit = 55 MPH			
	101_102	102_103	103_104	104_105	105_106	106_107	107_108	108_109	109_110	110_111	111_112	112_113	113_114	114_115
Speed Harmonization (SH)	0.78%	1.71%	1.89%	1.91%	2.16%	0.45%	2.28%	2.41%	1.59%	2.50%	1.12%	0.19%	0.12%	0.10%
Dynamic re-routing (DR) 10%	7.42%	5.05%	3.34%	1.96%	1.90%	1.57%	1.57%	0.63%	0.72%	0.54%	0.43%	0.20%	0.05%	-0.01%
DR 20%	13.37%	9.87%	6.63%	3.92%	3.84%	3.17%	2.58%	1.16%	1.40%	0.83%	0.94%	0.39%	0.13%	0.06%
DR 30%	18.07%	15.76%	10.53%	6.12%	5.11%	4.81%	4.10%	1.72%	2.00%	1.27%	1.44%	0.65%	0.22%	0.12%
SH + DR 10%	7.56%	6.32%	5.01%	3.58%	4.10%	3.45%	3.41%	3.23%	2.22%	2.50%	1.25%	0.56%	0.26%	0.10%
SH + DR 20%	13.45%	11.06%	8.34%	5.66%	6.00%	5.43%	4.77%	3.79%	3.05%	2.81%	1.84%	0.71%	0.30%	0.16%
SH + DR 30%	18.10%	16.83%	12.10%	7.82%	7.58%	7.00%	6.33%	4.45%	3.74%	3.23%	2.31%	0.97%	0.40%	0.23%

Figure 4-10 shows the speed profiles of a single vehicle traversing through incident-related congestion under various mitigation strategies. Speed harmonization coupled with dynamic rerouting resulted in the greatest improvement to TTs. This combination, as seen before, proved to be very effective in achieving both TT and safety improvements.

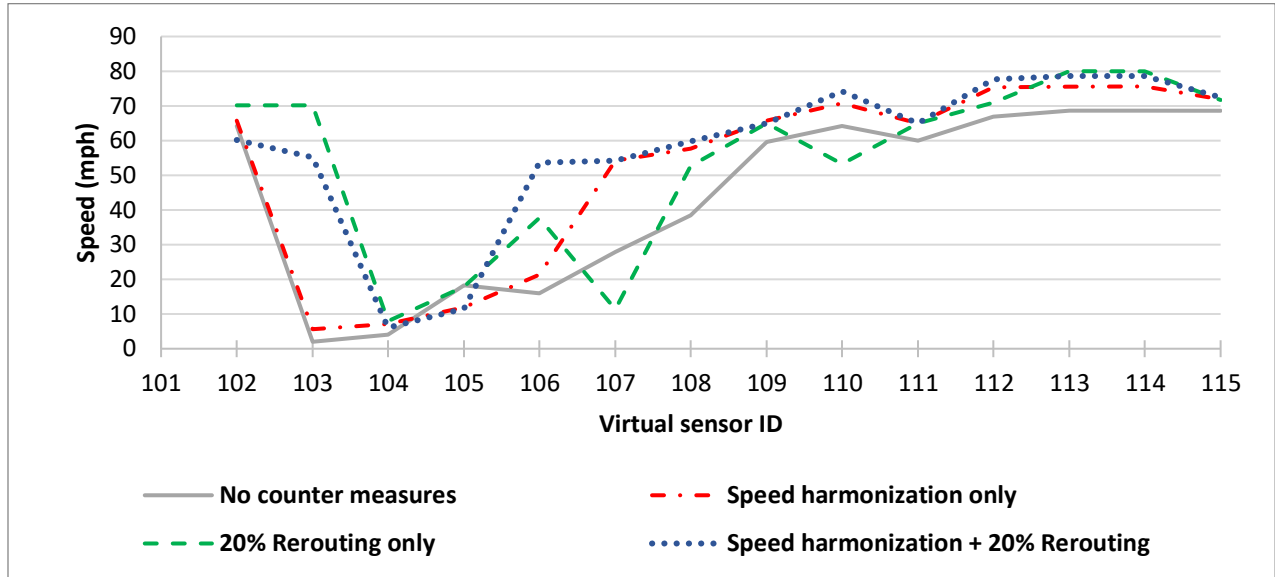
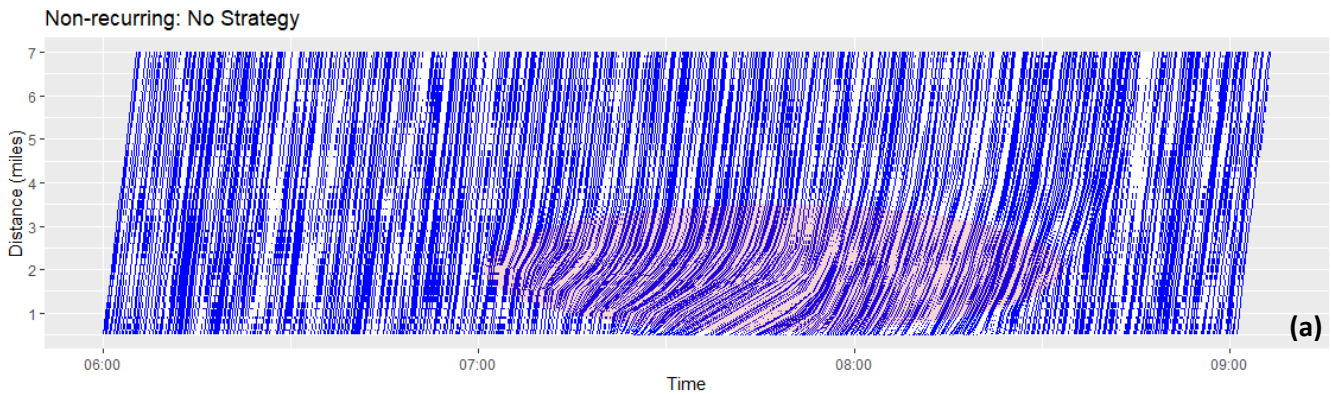


Figure 4-10. Single vehicle speed profiles through various non-recurring congestion mitigation strategies

Figure 4-11 shows space-time charts for a portion of the morning peak travel during an incident. The propagation and intensity of congestion is observed to decrease across Figure 4-11(a) to (d). Combining both speed harmonization and dynamic rerouting acts as the best congestion mitigation strategy within the study area.



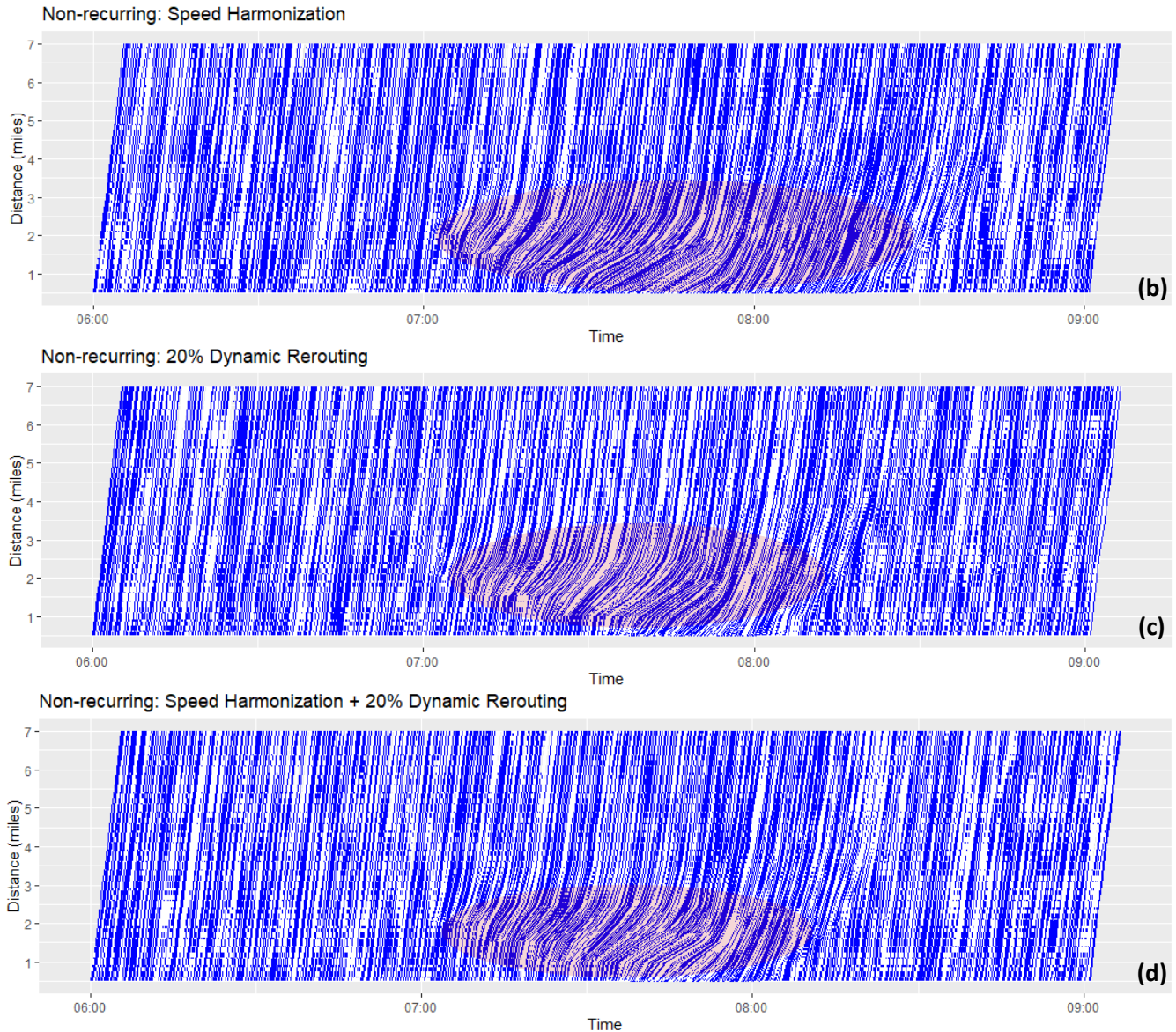


Figure 4-11. Space-time charts showing the impact of mitigation strategies as applied to non-recurring congestion

In conclusion, dual strategies combining speed harmonization and dynamic rerouting provide the most benefit within the congested sections and across the entire facility, as shown in Table 4-15. The same combination of strategies with varying intensities can be used across different types and levels of congestion i.e., recurring (level 2) vs non-recurring (levels 3 and 4). It should be noted that the examined mitigation strategies are specific to the study area (Selmon Expressway in Tampa, FL) and other strategies should be considered depending on the facility requirements.

Table 4-15. Summary of TT improvements obtained from microsimulation models

Strategy	7 – 9 AM	5 – 10 AM
----------	----------	-----------

	Congested sections (101-108)	Entire facility	Congested sections (101-108)	Entire facility
Recurring				
i) Speed Harmonization (SH)	0.39%	0.51%	1.24%	1.09%
ii) Dynamic rerouting (DR) 5%	6.70%	3.84%	2.78%	1.62%
iii) DR 10%	10.51%	6.15%	4.35%	2.53%
iv) DR 15%	13.21%	7.82%	5.47%	3.24%
v) SH + DR 5%	6.03%	3.82%	3.59%	2.49%
vi) SH + DR 10%	8.68%	5.55%	4.70%	3.19%
vii)SH + DR 15%	10.71%	7.00%	5.52%	3.80%
Non-Recurring (incident)				
i) SH	1.11%	1.06%	1.60%	1.37%
ii) DR 10%	7.89%	4.41%	3.26%	1.81%
iii) DR 20%	14.87%	8.27%	6.20%	3.45%
iv) DR 30%	22.13%	12.36%	9.22%	5.14%
v) SH + DR 10%	8.88%	5.40%	4.78%	3.11%
vi) SH + DR 20%	16.11%	9.42%	7.82%	4.81%
vii)SH + DR 30%	23.33%	13.49%	10.82%	6.51%

4.2.4. Approach Limitations

A few limitations of the developed simulation models are discussed below:

- The relatively low CV penetration rates led to assumptions such as applying TTs from last known time periods, thus introducing some errors into the existing conditions and calibrated simulation models. However, the benefits of utilizing relatively short TT segments (0.5-mile long) and possibility of creating even more precise segments, demonstrate the unparalleled merit of CV-based simulation calibration.
- Traffic volumes used for the simulation are obtained from the Iteris dashboard (ClearGuide) and are based on averages by time of day and day of week. In order to generate 5-minute volume estimates Iteris uses the Texas Transportation Institute AADT to volume profile methodology or probe-based data, where available (Iteris, 2021). These volume estimates result in the application of more aggressive calibration measures to replicate existing conditions that might affect the performance of the applied mitigation strategies.
- The developed simulation model is limited to the Westbound traffic flow on the Selmon Expressway and surrounding ramps, without considering impact to surrounding arterials at a meso or macro level. Applying mitigation strategies such as dynamic re-routing could potentially negatively impact the normal traffic flow along the REL. Including the entire REL (currently modeled as an access ramp only) to the geometry can further aid in refining the intensity of the mitigation strategies applied, improving traffic progression and reliability across both the upper and lower decks of the freeway.

5. Conclusions

This project sought to develop a robust proactive congestion detection algorithm. Mitigation strategies applicable to selected study areas are simulated under recurring and non-recurring congestion to explore any improvements to traffic flow and roadway safety.

The methodology applied to the preparation and fusion of the datasets, especially CV data, prove to be efficient in generating the same level of travel time data quality as other more common sources such as Bluetooth, even at low CV market penetration. The versatility of BSM data provides great flexibility for travel time estimation in more aggregate/shorter segment lengths.

The validated congestion detection algorithm shows a mean prediction error of 30.2% and is relatively effective in proactively predicting the onset of congestion and its levels. However, the process followed to compute the prediction error heavily penalizes the algorithm especially in instances where the ground truth cannot be fully verified to the nearest 5-minute time period (i.e., time logs from incident reports could be filed as a derivation of officer arrival time and not actual crash time). This also applies to the estimation of recurring congestion which is based on historical distribution plots and not observed ground truth. The algorithm is expected to have an overall lower prediction error in real world applications.

The developed congestion detection algorithm is robust enough to function using either traditional or CV travel time datasets, thus addressing earlier identified research gaps from the literature. This makes implementation of the methodology relatively easy for transportation agencies upgrading existing traditional infrastructure or those already transitioning to CV technology. To deploy the algorithm, transportation agencies only require access to live travel time estimates of the roadway segments, preferably two miles or shorter in length depending on agency-specific precision requirements for identifying the congestion location and progression. For effective deployment of the congestion detection algorithm in specific locations, optimization of the congestion thresholds can be performed using historical travel time data of the facility, where available.

Finally, this project demonstrated the clear advantage of using CV-based travel time estimates to calibrate simulation models over fixed point-based derivations of travel time from spot speeds. While TransModeler was the microsimulation tool used in the study, the calibration process utilized universal driver behavioral models of car-following and lane changing to ensure replicability across other microsimulation platforms. The ability to calibrate simulation models based on individual sections of shorter lengths (less than or equal to 0.5 miles) allows for a more detailed replication of real-world conditions. CV technology allows for the possibility of deploying multiple mitigation strategies efficiently and in short succession (e.g., CV-based speed advisories), without the need for installing additional roadside infrastructure, such as dynamic message signs and variable speed limits.

6. Future Research

The proposed congestion detection algorithm relies on data from two geographic locations. Adding more geographic variability could help further refine the congestion level thresholds and the overall robustness of the model. Also, implementing a feedback loop to continually evaluate new datasets from locations where the congestion detection algorithm is deployed can aid to train and further improve the accuracy of the established congestion level thresholds.

Further work could extend the simulation geometry to include multiple alternative route choices in order to establish a more holistic impact of congestion intensity and deployed mitigation strategies on these roadways.

Although this project examined speed harmonization, the implementation approach applied a basic speed-based equation. A more refined approach that dynamically re-evaluates the intensity of mitigation strategies based on dissipation of congestion could provide smoother traffic flow.

Finally, more research into driver perception of CV-based HMI alerts especially with respect to the time-lag before compliance (individual/platoon) with the provided speed or rerouting advisories would provide more insights into effective deployment of the congestion mitigation strategies.

References

- Abdel-Aty, M., Pande, A., & Hsia, L. (2010). The concept of proactive traffic management for enhancing freeway safety and operation. *ITE journal*, 80(4), 34.
- Anand, A., Ramadurai, G., & Vanajakshi, L. (2014). Data fusion-based traffic density estimation and prediction. *Journal of Intelligent Transportation Systems: Technology, Planning, and Operations*, 18(4), 367-378. doi:10.1080/15472450.2013.806844
- Anand, R. A., Vanajakshi, L., & Subramanian, S. C. (2011). Traffic density estimation under heterogeneous traffic conditions using data fusion. In (pp. 31-36): IEEE.
- Bauza, R., & Gozalvez, J. (2013). Traffic congestion detection in large-scale scenarios using vehicle-to-vehicle communications. *Journal of Network and Computer Applications*, 36(5), 1295-1307. doi:<https://doi.org/10.1016/j.inca.2012.02.007>
- Caliper-Corporation. (2020). TransModeler 6.0 User Manual. Retrieved from www.caliper.com
- Concas, S., & Kamrani, M. (2019). Development of a Real-Time Roadway Debris Hazard Spotting Tool Using Connected Vehicle Data to Enhance Roadway Safety and System Efficiency.
- Concas, S., Kourtellis, A., & Kamrani, M. (2021). *Connected Vehicle Pilot Deployment Program Performance Measurement and Evaluation Support Plan, Phase 4 – Tampa (THEA)*. Retrieved from
- Concas, S., Kourtellis, A., Kamrani, M., & Dokur, O. (2021). *Connected Vehicle Pilot Deployment Program Performance Measurement and Evaluation– Tampa (THEA) CV Pilot Phase 3 Evaluation Report*. Retrieved from <https://rosap.ntl.bts.gov/view/dot/55818>
- Concas, S., Kourtellis, A., Reich, S. L., & Authority, T. H. E. (2019). *Connected Vehicle Pilot Deployment Program, Performance Measurement and Evaluation Support Plan, Phase 2 UPDATE–Tampa Hillsborough Expressway Authority*. Retrieved from
- Developers, S. (2014). R Package signal: Signal processing. In.
- FDOT-Safety-Office. (2020). *All Crashes: Florida Department of Transportation (FDOT) Open Data Hub*. Florida Crashes. Retrieved from: <https://gis-fdot.opendata.arcgis.com/datasets/fdot::all-crashes/about>
- Friesen, M. R., & McLeod, R. D. (2015). Bluetooth in Intelligent Transportation Systems: A Survey. *International Journal of Intelligent Transportation Systems Research*, 13(3), 143-153. doi:10.1007/s13177-014-0092-1
- Gopalakrishna, D., Cluett, C., Kitchener, F., & Balke, K. (2011). *Developments in weather responsive traffic management strategies*. Retrieved from
- Greenshields, B. D. (1935). A study in highway capacity. *Highway Research Board Proc.*, 1935, 448-477.
- Grumert, E. F., & Tapani, A. (2018). Traffic State Estimation Using Connected Vehicles and Stationary Detectors. *Journal of Advanced Transportation*, 2018, 4106086. doi:10.1155/2018/4106086

- Hale, D., Phillips, T., Raboy, K., Ma, J., Su, P., Lu, X.-Y., . . . Dailey, D. J. (2016). Introduction of Cooperative Vehicle-to-Infrastructure Systems to Improve Speed Harmonization. Retrieved from <https://rosap.ntl.bts.gov/view/dot/35710>
- Hall, F. L. (1996). Traffic stream characteristics. *Traffic Flow Theory. US Federal Highway Administration*, 36.
- Hargrove, S. R., Lim, H., Han, L. D., & Freeze, P. B. (2016). Empirical Evaluation of the Accuracy of Technologies for Measuring Average Speed in Real Time. *Transportation Research Record*, 2594(1), 73-82. doi:10.3141/2594-11
- HCM 2010 : highway capacity manual*. (2010). Fifth edition. Washington, D.C. : Transportation Research Board, c2010-.
- Houbraken, M., Logghe, S., Schreuder, M., Audenaert, P., Colle, D., & Pickavet, M. (2017). Automated Incident Detection Using Real-Time Floating Car Data. *Journal of Advanced Transportation*, 2017, 8241545. doi:10.1155/2017/8241545
- Iteris. (2021). CLEARGUIDE User's Guide. Retrieved from https://clearguide-docs.s3.amazonaws.com/ClearGuide_User_Manual.pdf
- J2735_201603: Dedicated Short Range Communications (DSRC) Message Set Dictionary. (2016). In: SAE International.
- Jacobson, L., Stribiak, J., Nelson, L., & Sallman, D. (2006). *Ramp management and control handbook*. Retrieved from
- Jagtap, S. K., & Uplane, M. (2012). *The impact of digital filtering to ECG analysis: Butterworth filter application*. Paper presented at the 2012 International Conference on Communication, Information & Computing Technology (ICCICT).
- Jolovic, D., Stevanovic, A., Sajjadi, S., & Martin, P. (2016). Assessment of Level-Of-Service for Freeway Segments Using HCM and Microsimulation Methods. *Transportation Research Procedia*, 15, 403-416. doi:10.1016/j.trpro.2016.06.034
- Kamrani, M., Abadi, S. M. H. E., & Golroudbary, S. R. (2014). Traffic simulation of two adjacent unsignalized T-junctions during rush hours using Arena software. *Simulation Modelling Practice and Theory*, 49, 167-179.
- Kamrani, M., Concas, S., & Kourtellis, A. (2021). US11170645.
- Karatsoli, M., Margreiter, M., & Spangler, M. (2017). Bluetooth-based travel times for automatic incident detection – A systematic description of the characteristics for traffic management purposes. *Transportation Research Procedia*, 24, 204-211. doi:<https://doi.org/10.1016/j.trpro.2017.05.109>
- Khan, S. M., Dey, K. C., & Chowdhury, M. (2017). Real-Time Traffic State Estimation With Connected Vehicles. *IEEE Transactions on Intelligent Transportation Systems, Intelligent Transportation Systems, IEEE Transactions on, IEEE Trans. Intell. Transport. Syst.*, 18(7), 1687-1699. doi:10.1109/TITS.2017.2658664
- Kishimoto, K., Yamada, M., & Jinno, M. (2014). Cooperative inter-infrastructure communication system using 700 mhz band. *SEI Technical Review*, 78, 19-23.
- Kondyli, A., Chrysiou, E., & Kummetha, V. (2020). Modeling Driver Behavior and Aggressiveness Using Biobehavioral Methods – Phase II. Retrieved from <https://rosap.ntl.bts.gov/view/dot/54548>
- Kummetha, V., Kamrani, M., & Concas, S. (2021). US Provisional Application No. 63/262,935.
- LeBlanc, D. J. (2006). *Emerging technologies for vehicle-infrastructure cooperation to support emergency transportation operations*.
- Lomax, T., Turner, S., Shunk, G., Levinson, H., Pratt, R., Bay, P., & Douglas, G. (1997). *Quantifying Congestion. Volume 2: User's Guide* (0309060710). Retrieved from
- Mahmassani, H. S., Hou, T., Kim, J., Chen, Y., Hong, Z., Halat, H., & Haas, R. (2014). *Implementation of a weather responsive traffic estimation and prediction system (TrEPS) for signal timing at Utah DOT*. Retrieved from

- Malikopoulos, A. A., Hong, S., Park, B., Lee, J., & Ryu, S. (2019). Optimal Control for Speed Harmonization of Automated Vehicles. *IEEE Transactions on Intelligent Transportation Systems*, 20, 2405-2417.
- Margreiter, M., Spangler, M., Zeh, T., & Carstensen, C. (2015). *Bluetooth-Measured Travel Times for Dynamic Re-Routing*. Paper presented at the Proceedings of the 3rd Annual International Conference ACE 2015.
- May, A. D. (1990). *Traffic flow fundamentals*. Englewood Cliffs, N.J.: Prentice Hall.
- Mirshahi, M., Obenberger, J., Fuhs, C. A., Howard, C. E., Krammes, R. A., Kuhn, B. T., . . . Yung, J. L. (2007). Active traffic management : the next step in congestion management. Retrieved from <https://rosap.ntl.bts.gov/view/dot/16441>
- Pan, J., Khan, M. A., Popa, I. S., Zeitouni, K., & Borcea, C. (2012). Proactive Vehicle Re-routing Strategies for Congestion Avoidance. In (pp. 265-272): IEEE.
- Papacharalampous, A. E., Cats, O., Lankhaar, J.-W., Daamen, W., & Lint, H. v. (2016). Multimodal Data Fusion for Big Events. *Transportation Research Record*, 2594, 118 - 126.
- Pebesma, E. (2018). Simple Features for R: Standardized Support for Spatial Vector Data. *R J.*, 10, 439.
- Puckett, D. D., & Vickich, M. J. (2010). Bluetooth-based travel time/speed measuring systems development. Retrieved from <https://rosap.ntl.bts.gov/view/dot/18163>
- Punzo, V., Borzacchiello, M. T., & Ciuffo, B. (2011). On the assessment of vehicle trajectory data accuracy and application to the Next Generation SIMulation (NGSIM) program data. *Transportation Research Part C: Emerging Technologies*, 19(6), 1243-1262. doi:<https://doi.org/10.1016/j.trc.2010.12.007>
- Qiu, T. Z., Lu, X.-Y., Chow, A. H. F., & Shladover, S. E. (2010). Estimation of Freeway Traffic Density with Loop Detector and Probe Vehicle Data. *Transportation Research Record*, 2178(1), 21-29. Retrieved from <http://ezproxy.lib.usf.edu/login?url=http://search.ebscohost.com/login.aspx?direct=true&db=edo&AN=ejs45673153&site=eds-live>
- Rahman, M., Chowdhury, M., & McClendon, J. (2018). Real time Traffic Flow Parameters Prediction with Basic Safety Messages at Low Penetration of Connected Vehicles. *arXiv: Learning*.
- Roberts, J., & Roberts, T. D. (1978). Use of the Butterworth low-pass filter for oceanographic data. *Journal of Geophysical Research: Oceans*, 83(C11), 5510-5514.
- Salter, R. J. (1976). The relationship between speed, flow and density of a highway traffic stream. In *Highway Traffic Analysis and Design* (pp. 125-134). London: Macmillan Education UK.
- Skycomp, I. (2009). *Traffic Quality on the Metropolitan Washington Area Freeway System, Spring 2009*. Retrieved from <https://www.mwcog.org/documents/2011/10/04/traffic-quality-on-the-metropolitan-washington-area-freeway-system/#>
- Tefft, B. C. (2016). The Prevalence of Motor Vehicle Crashes Involving Road Debris, United States, 2011-2014. *Age (years)*, 20(5.7), 10.11.
- Transportation Research Board, & NASEM, N. A. o. S. E. M. (2014a). *Handbook for Communicating Travel Time Reliability Through Graphics and Tables*. Washington, DC: The National Academies Press.
- Transportation Research Board, & NASEM, N. A. o. S. E. M. (2014b). *Incorporating Travel Time Reliability into the Highway Capacity Manual*. Washington, DC: The National Academies Press.
- Tseng, F., Hsueh, J., Tseng, C., Yang, Y., Chao, H., & Chou, L. (2018). Congestion Prediction With Big Data for Real-Time Highway Traffic. *IEEE Access*, 6, 57311-57323. doi:10.1109/ACCESS.2018.2873569
- Wang, J., Xie, W., Liu, B., Fang, S. e., & Ragland, D. R. (2016). Identification of freeway secondary accidents with traffic shock wave detected by loop detectors. *Safety Science*, 87, 195-201. doi:<https://doi.org/10.1016/j.ssci.2016.04.015>
- Weil, R., Wootton, J., & Garcia-Ortiz, A. (1998). Traffic incident detection: Sensors and algorithms. *Mathematical and computer modelling*, 27(9-11), 257-291.



Appendix A: Algorithm Validation

Table A-1. Recurring congestion manual validation

Date	Confirm Time	Seg ID	Day of Week	Prediction Start Time	Level Match Time	Prediction Error
2/26/2019	6:40	A	Tue	7:55	7:55	1.00
3/13/2019	7:05	A	Wed	6:55	6:55	0.00
3/5/2019	9:30	A	Tue	9:00	9:00	0.00
3/6/2019	8:15	A	Wed	7:20	7:20	0.00
3/25/2019	7:40	A	Mon	NA	NA	1.00
4/1/2019	6:50	A	Mon	7:15	7:15	0.39
4/8/2019	7:35	A	Mon	7:30	7:30	0.00
4/10/2019	8:00	A	Wed	7:00	7:00	0.00
4/18/2019	6:30	A	Thur	6:05	6:05	0.00
5/6/2019	8:10	A	Mon	8:00	8:00	0.00
5/13/2019	7:40	A	Mon	8:05	8:05	0.39
5/15/2019	6:20	A	Wed	6:05	6:05	0.00
5/20/2019	9:10	A	Mon	8:05	8:05	0.00
6/4/2019	6:25	A	Tue	7:25	7:25	1.00
6/21/2019	6:10	A	Fri	NA	NA	1.00
6/28/2019	8:50	A	Fri	7:50	7:50	0.00
7/2/2019	7:20	A	Tue	6:15	6:15	0.00
7/9/2019	8:30	A	Tue	7:50	7:50	0.00
7/22/2019	5:45	A	Mon	6:50	6:50	1.00
8/7/2019	7:50	A	Wed	8:10	8:10	0.33
8/14/2019	7:40	A	Wed	7:30	7:30	0.00
8/15/2019	6:45	A	Thur	6:55	6:55	0.21
8/27/2019	7:25	A	Tue	NA	NA	1.00
8/28/2019	7:45	A	Wed	7:40	7:40	0.00
9/6/2019	7:05	A	Fri	8:25	8:25	1.00
9/9/2019	9:10	A	Mon	8:45	8:45	0.00
9/19/2019	8:20	A	Thur	8:45	8:45	0.39
10/4/2019	7:15	A	Fri	7:05	7:05	0.00
10/16/2019	9:10	A	Wed	9:20	9:20	0.21
10/22/2019	6:45	A	Tue	6:45	6:45	0.00
11/14/2019	6:35	A	Thur	6:00	6:00	0.00
12/3/2019	7:05	A	Tue	NA	NA	1.00
12/11/2019	7:30	A	Wed	7:35	7:35	0.13
12/13/2019	6:25	A	Fri	6:00	6:00	0.00
1/6/2020	7:15	A	Mon	7:30	7:30	0.28

Date	Confirm Time	Seg ID	Day of Week	Prediction Start Time	Level Match Time	Prediction Error
2/21/2019	6:35	B-1	Thur	7:50	7:50	1.00
3/4/2019	6:40	B-1	Mon	6:50	6:50	0.28
3/7/2019	7:15	B-1	Thur	6:55	6:55	0.00
3/21/2019	7:00	B-1	Thur	6:05	6:05	0.00
3/27/2019	7:05	B-1	Wed	6:55	6:55	0.00
4/2/2019	7:05	B-1	Tue	6:50	6:50	0.00
4/29/2019	7:15	B-1	Mon	7:30	7:30	0.28
5/6/2019	6:55	B-1	Mon	7:05	7:05	0.21
6/20/2019	7:00	B-1	Thur	6:55	6:55	0.00
6/26/2019	5:30	B-1	Wed	7:25	7:25	1.00
7/2/2019	6:35	B-1	Tue	6:50	6:50	0.28
7/15/2019	6:20	B-1	Mon	7:50	7:50	1.00
7/17/2019	7:20	B-1	Wed	7:45	7:45	0.39
8/19/2019	7:10	B-1	Mon	7:25	7:25	0.28
8/22/2019	7:25	B-1	Thur	7:30	7:30	0.13
9/4/2019	7:05	B-1	Wed	7:50	7:50	1.00
9/23/2019	7:05	B-1	Mon	7:25	7:25	0.33
10/18/2019	8:40	B-1	Fri	8:00	8:00	0.00
10/30/2019	6:50	B-1	Wed	7:15	7:15	0.39
11/4/2019	6:10	B-1	Mon	6:00	6:00	0.00
11/21/2019	7:25	B-1	Thur	7:40	7:40	0.28
11/26/2019	7:10	B-1	Tue	NA	NA	1.00
12/5/2019	7:00	B-1	Thur	6:50	6:50	0.00
12/6/2019	8:35	B-1	Fri	7:45	7:45	0.00
12/13/2019	7:20	B-1	Fri	7:15	7:15	0.00
12/23/2019	7:40	B-1	Mon	8:45	8:45	1.00
12/30/2019	8:25	B-1	Mon	7:25	7:25	0.00
1/9/2020	7:30	B-1	Thur	6:40	6:40	0.00
1/15/2020	6:35	B-1	Wed	8:15	8:15	1.00
1/21/2020	7:40	B-1	Tue	7:25	7:25	0.00
1/24/2020	7:55	B-1	Fri	7:15	7:15	0.00
1/30/2020	6:55	B-1	Thur	7:25	7:25	1.00
2/6/2020	5:50	B-1	Thur	NA	NA	1.00
2/7/2020	6:20	B-1	Fri	6:40	6:40	0.33
2/13/2020	7:15	B-1	Thur	7:15	7:15	0.00
2/22/2019	6:55	B-2	Fri	7:15	7:15	0.33
3/5/2019	7:30	B-2	Tue	6:50	6:50	0.00
3/18/2019	7:40	B-2	Mon	7:50	7:50	0.21
3/26/2019	6:25	B-2	Tue	7:20	7:20	1.00

Date	Confirm Time	Seg ID	Day of Week	Prediction Start Time	Level Match Time	Prediction Error
4/1/2019	7:20	B-2	Mon	7:30	7:30	0.21
4/5/2019	6:30	B-2	Fri	6:15	6:15	0.00
4/9/2019	7:20	B-2	Tue	7:15	7:15	0.00
4/25/2019	6:55	B-2	Thur	6:45	6:45	0.00
5/3/2019	6:55	B-2	Fri	7:10	7:10	0.28
5/14/2019	6:10	B-2	Tue	6:35	6:35	0.39
5/28/2019	5:25	B-2	Tue	6:50	6:50	1.00
6/6/2019	8:00	B-2	Thur	7:30	7:30	0.00
6/26/2019	7:40	B-2	Wed	7:20	7:20	0.00
7/2/2019	6:45	B-2	Tue	6:50	6:50	0.13
7/15/2019	6:40	B-2	Mon	7:40	7:40	1.00
7/24/2019	7:10	B-2	Wed	7:15	7:15	0.13
7/30/2019	7:25	B-2	Tue	7:15	7:15	0.00
8/12/2019	7:05	B-2	Mon	7:10	7:10	0.13
8/20/2019	7:35	B-2	Tue	7:15	7:15	0.00
8/23/2019	7:35	B-2	Fri	7:15	7:15	0.00
9/4/2019	7:35	B-2	Wed	7:20	7:20	0.00
9/5/2019	7:00	B-2	Thur	6:50	6:50	0.00
9/23/2019	7:15	B-2	Thur	7:10	7:10	0.00
10/14/2019	6:15	B-2	Mon	7:55	7:55	1.00
10/15/2019	7:30	B-2	Tue	6:55	6:55	0.00
11/1/2019	7:20	B-2	Fri	7:30	7:30	0.21
11/15/2019	7:10	B-2	Fri	7:00	7:00	0.00
12/10/2019	6:10	B-2	Tue	6:55	6:55	1.00
1/14/2020	6:55	B-2	Tue	7:00	7:00	0.13
1/28/2020	6:45	B-2	Tue	6:35	6:35	0.00
Mean Error						0.297

Table A-2. Weather-related congestion manual validation

Date	Confirm Time	Seg ID	Day of Week	Prediction Start Time	Level Match Time	Prediction Error
3/12/2019	7:10	A	Tue	6:50	6:50	0.00
5/9/2019	8:00	A	Thur	7:25	7:30	0.00
5/10/2019	16:40	A	Fri	16:10	16:10	0.00
7/10/2019	10:00	A	Wed	10:05	10:05	0.13
8/12/2019	9:10	A	Mon	9:00	9:00	0.00
8/21/2019	5:40	A	Wed	NA	NA	1.00
8/23/2019	18:00	A	Fri	17:30	17:30	0.00
8/29/2019	9:00	A	Thur	8:05	8:05	0.00
9/18/2019	18:00	A	Wed	NA	NA	1.00
10/29/2019	15:50	A	Tue	15:50	15:50	0.00
12/12/2019	17:40	A	Thur	17:45	17:45	0.13
1/16/2020	9:20	A	Thur	8:40	8:40	0.00
1/30/2020	7:00	A	Thur	7:20	7:20	0.33
2/13/2020	15:30	A	Thur	15:25	15:25	0.00
2/20/2020	16:20	A	Thur	15:00	15:00	0.00
2/26/2019	10:30	B-1	Tue	NA	NA	1.00
3/12/2019	6:00	B-1	Tue	5:55	5:55	0.00
4/5/2019	6:50	B-1	Fri	6:15	6:15	0.00
4/12/2019	19:00	B-1	Fri	NA	NA	1.00
5/31/2019	15:20	B-1	Fri	NA	NA	1.00
6/12/2019	14:15	B-1	Wed	NA	NA	1.00
7/12/2019	9:30	B-1	Fri	9:20	9:20	0.00
7/17/2019	13:40	B-1	Wed	13:25	13:30	0.00
8/15/2019	10:30	B-1	Thur	10:10	10:10	0.00
8/14/2019	6:40	B-1	Wed	6:50	6:50	0.21
11/8/2019	17:50	B-1	Fri	NA	NA	1.00
11/14/2019	6:10	B-1	Thur	6:00	6:00	0.00
12/23/2019	15:30	B-2	Mon	NA	NA	1.00
1/7/2020	9:20	B-2	Tue	9:00	9:00	0.00
1/23/2020	7:10	B-2	Thur	6:45	6:45	0.00
3/1/2019	7:10	B-2	Fri	6:55	6:55	0.00
3/27/2019	15:20	B-2	Wed	15:45	15:45	0.39
4/12/2019	17:40	B-2	Fri	17:45	17:45	0.13
5/9/2019	16:30	B-2	Thur	NA	NA	1.00
5/15/2019	6:20	B-2	Wed	6:00	6:00	0.00
5/17/2019	6:20	B-2	Fri	6:00	6:00	0.00
6/3/2019	6:35	B-2	Mon	6:50	6:50	0.28

Date	Confirm Time	Seg ID	Day of Week	Prediction Start Time	Level Match Time	Prediction Error
7/5/2019	12:40	B-2	Fri	NA	NA	1.00
7/10/2019	5:30	B-2	Wed	7:05	NA	1.00
7/26/2019	14:05	B-2	Fri	NA	NA	1.00
8/7/2019	16:55	B-2	Wed	17:05	17:05	0.21
9/25/2019	21:30	B-2	Wed	NA	NA	1.00
11/18/2019	7:00	B-2	Mon	7:10	7:10	0.18
12/9/2019	9:00	B-2	Mon	8:55	8:55	0.00
1/29/2020	8:00	B-2	Wed	7:15	7:15	0.00
Mean Error						0.333

Table A-3. Non-recurring congestion manual validation

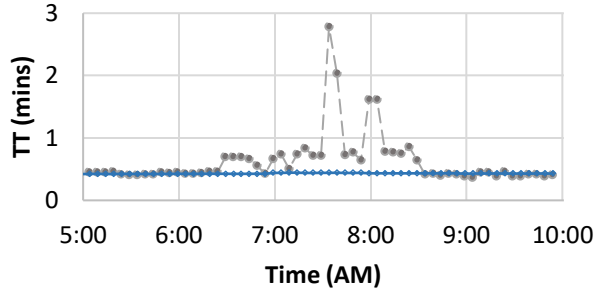
Date	Confirm Time	Seg ID	Day of Week	Prediction Start Time	Level Match Time	Prediction Error
3/11/2019	10:30	A	Mon	NA	10:30	0.00
3/13/2019	15:25	A	Wed	15:25	15:30	0.13
3/18/2019	18:05	A	Mon	18:10	18:15	0.30
3/28/2019	6:50	A	Thur	6:50	6:55	0.13
3/21/2019	5:55	A	Thur	6:05	6:10	0.36
4/8/2019	11:45	A	Mon	11:45	11:50	0.13
4/15/2019	9:55	A	Mon	10:10	NA	0.50
4/24/2019	9:25	A	Wed	9:30	9:30	0.22
5/1/2019	17:50	A	Wed	17:55	17:55	0.22
5/14/2019	16:20	A	Tue	16:25	16:25	0.22
6/5/2019	7:45	A	Wed	7:50	7:55	0.27
6/21/2019	21:00	A	Fri	21:10	NA	0.47
7/22/2019	12:05	A	Mon	12:15	12:20	0.36
8/12/2019	17:05	A	Mon	17:05	17:10	0.13
8/23/2019	17:25	A	Fri	17:30	17:30	0.22
9/3/2019	13:05	A	Tue	13:05	13:05	0.00
9/18/2019	9:15	A	Wed	9:20	9:20	0.22
10/14/2019	18:30	A	Mon	18:30	18:30	0.00
11/4/2019	14:45	A	Mon	14:50	14:50	0.22
11/26/2019	7:25	A	Tue	7:20	7:30	0.11
12/3/2019	15:25	A	Tue	15:30	15:30	0.22
12/13/2019	9:25	A	Fri	9:25	9:25	0.00
12/20/2019	13:05	A	Fri	13:05	13:05	0.13
1/7/2020	7:25	A	Tue	7:30	7:30	0.22
1/22/2020	14:05	A	Wed	14:10	14:10	0.22

Date	Confirm Time	Seg ID	Day of Week	Prediction Start Time	Level Match Time	Prediction Error
3/8/2019	12:35	B-1	Fri	NA	NA	1.00
4/2/2019	15:00	B-1	Tue	NA	NA	1.00
4/25/2019	14:35	B-1	Thur	14:35	14:40	0.13
5/3/2019	16:55	B-1	Fri	17:00	17:00	0.22
6/21/2019	9:30	B-1	Fri	9:40	9:45	0.33
6/24/2019	17:25	B-1	Mon	NA	NA	1.00
7/2/2019	21:05	B-1	Tue	21:20	NA	0.50
7/9/2019	5:55	B-1	Tue	6:05	6:05	0.32
7/15/2019	7:20	B-1	Mon	7:50	NA	0.08
8/8/2019	19:20	B-1	Thur	18:50	19:00	0.00
8/26/2019	6:40	B-1	Mon	6:55	NA	0.50
9/4/2019	15:45	B-1	Wed	NA	NA	1.00
9/12/2019	11:20	B-1	Thur	11:35	NA	0.50
9/24/2019	20:00	B-1	Tue	20:10	NA	0.47
10/8/2019	6:05	B-1	Tue	6:00	NA	0.17
10/9/2019	11:05	B-1	Wed	10:30	10:30	0.00
10/22/2019	20:05	B-1	Tue	20:10	NA	0.44
10/25/2019	8:10	B-1	Fri	8:10	8:10	0.00
11/8/2019	6:25	B-1	Fri	6:35	NA	0.22
11/19/2019	9:30	B-1	Tue	9:35	9:35	0.22
11/27/2019	17:05	B-1	Wed	NA	NA	1.00
12/3/2019	20:15	B-1	Tue	20:30	NA	0.50
1/3/2020	16:25	B-1	Fri	16:30	16:30	0.22
2/4/2020	14:35	B-1	Tue	14:35	14:35	0.00
2/7/2020	10:55	B-1	Fri	11:05	11:10	0.36
4/22/2019	7:55	B-2	Mon	6:55	7:05	0.00
4/22/2019	21:50	B-2	Mon	22:05	NA	0.50
2/28/2019	6:25	B-2	Thur	6:00	6:40	0.06
3/21/2019	7:55	B-2	Thur	7:35	7:35	0.00
3/26/2019	20:45	B-2	Tue	NA	NA	1.00
5/23/2019	7:45	B-2	Thur	7:05	7:15	0.00
6/7/2019	16:50	B-2	Fri	16:55	16:55	0.22
6/11/2019	7:20	B-2	Tue	7:05	7:15	0.00
6/17/2019	7:55	B-2	Mon	7:40	7:40	0.00
6/24/2019	8:00	B-2	Mon	7:55	8:05	0.06
7/10/2019	17:50	B-2	Wed	17:50	17:55	0.08
7/17/2019	7:40	B-2	Wed	7:40	7:40	0.00
7/22/2019	13:15	B-2	Mon	NA	NA	1.00
8/12/2019	10:00	B-2	Mon	9:25	10:15	0.05

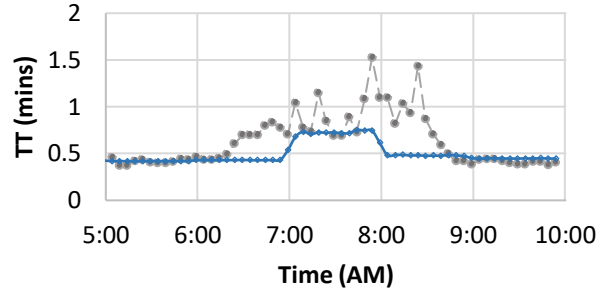
Date	Confirm Time	Seg ID	Day of Week	Prediction Start Time	Level Match Time	Prediction Error
8/21/2019	17:25	B-2	Wed	NA	NA	1.00
9/10/2019	20:10	B-2	Tue	NA	NA	1.00
9/11/2019	6:30	B-2	Wed	6:45	6:45	0.40
9/20/2019	13:50	B-2	Fri	13:55	14:00	0.27
10/4/2019	6:30	B-2	Fri	6:50	6:55	0.50
10/14/2019	8:15	B-2	Mon	7:55	8:00	0.00
10/18/2019	10:30	B-2	Fri	10:30	10:35	0.08
11/4/2019	13:45	B-2	Mon	14:00	NA	0.50
11/22/2019	20:00	B-2	Fri	NA	NA	1.00
12/9/2019	18:50	B-2	Mon	NA	NA	1.00
1/9/2020	6:30	B-2	Thur	6:35	6:40	0.27
				Mean Error		0.322

Appendix B: Recurring Calibration

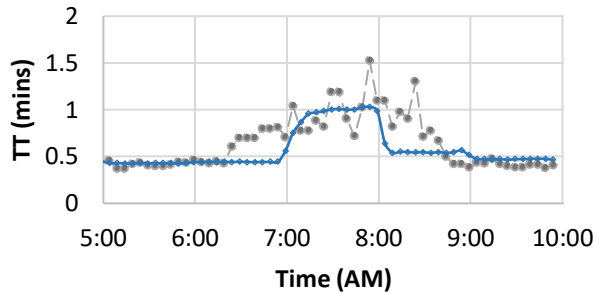
Section 101-102



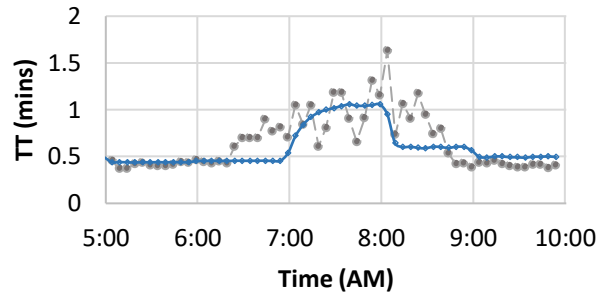
Section 102-103



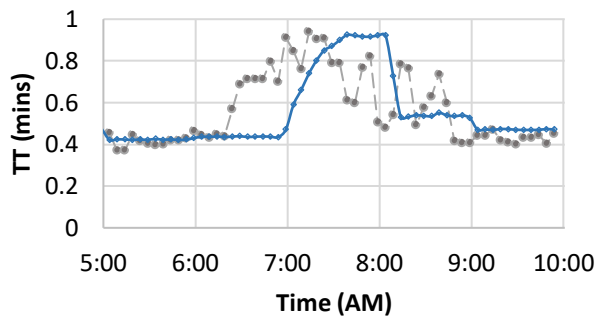
Section 103-104



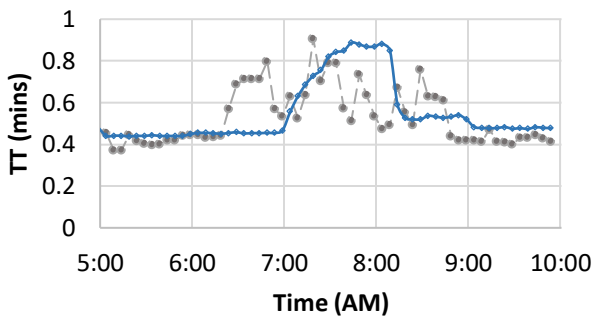
Section 104-105



Section 105-106



Section 106-107



--●-- Observed_TT —◆— Calibrated_TT

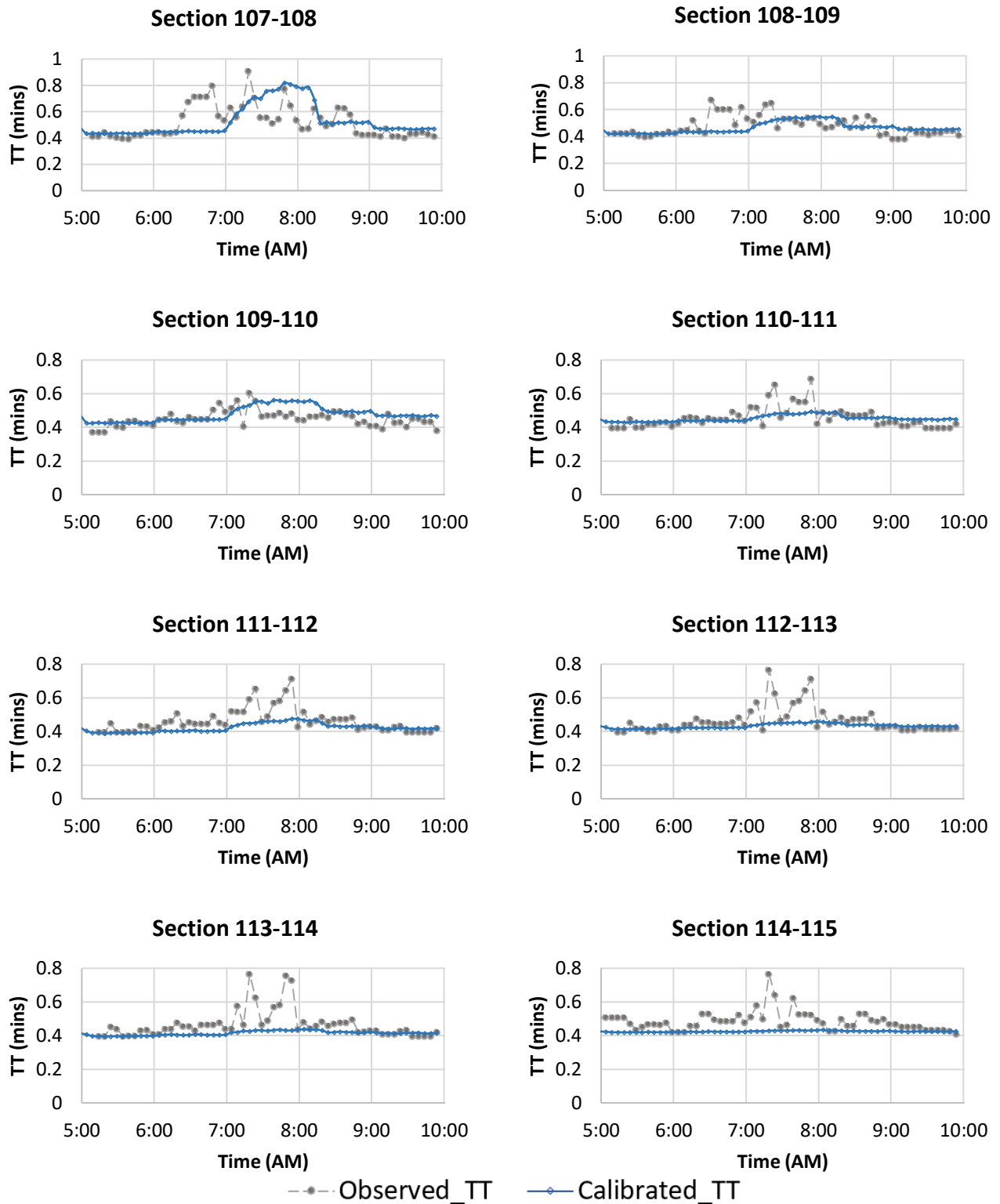
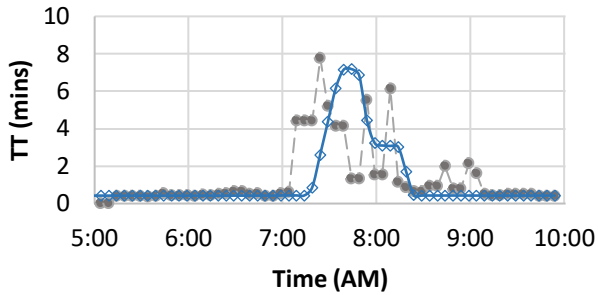


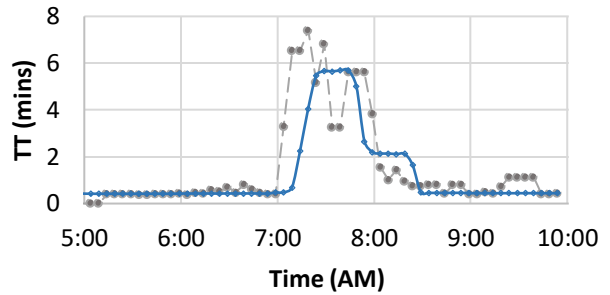
Figure B-1. Section wise comparison of observed and calibrated TTs

Appendix C: Non-recurring Calibration

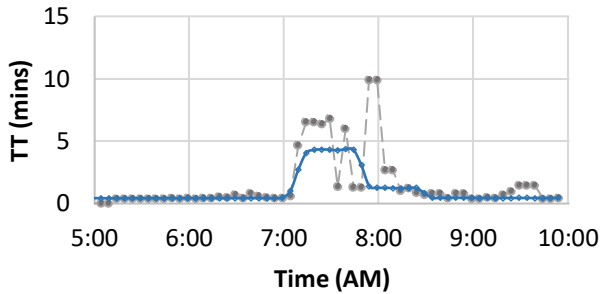
Section 101-102



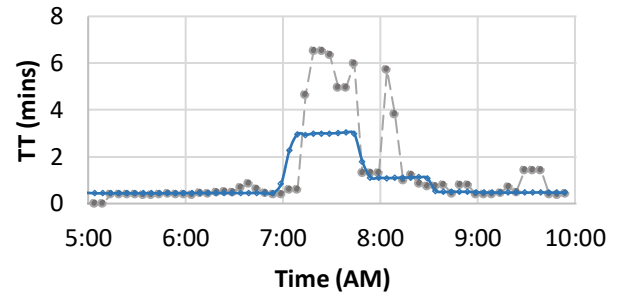
Section 102-103



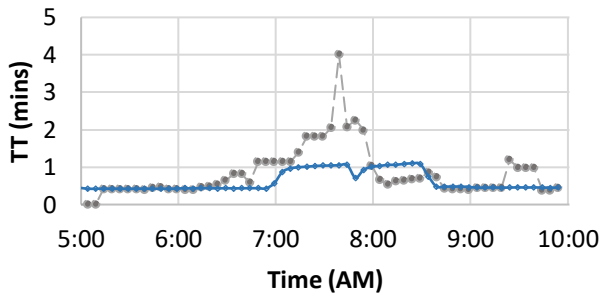
Section 103-104



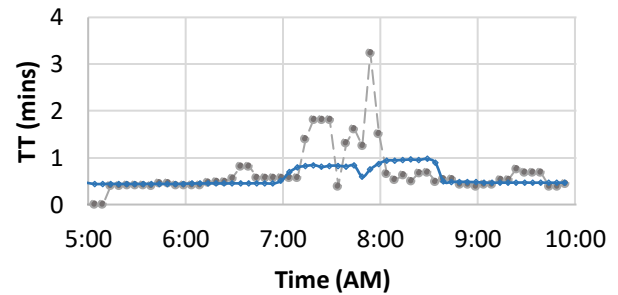
Section 104-105



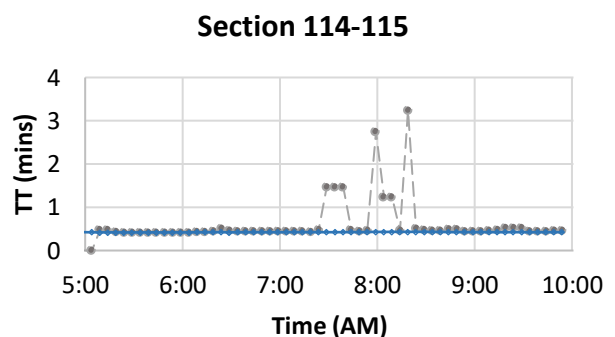
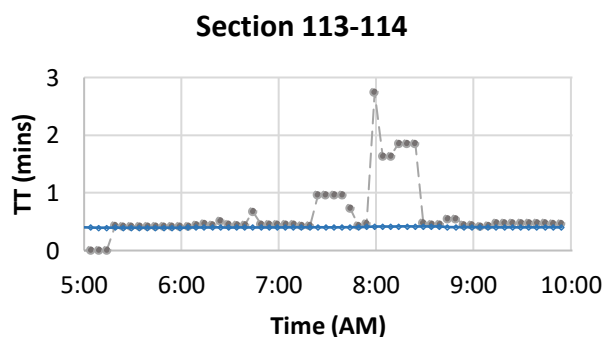
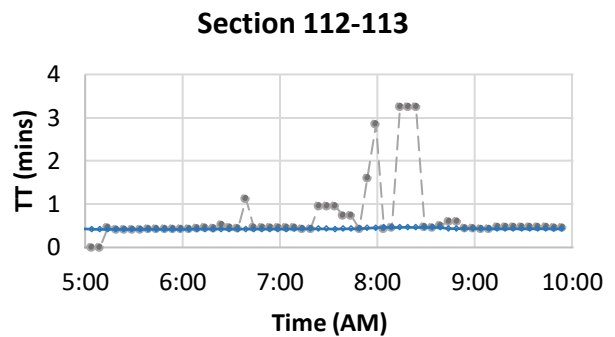
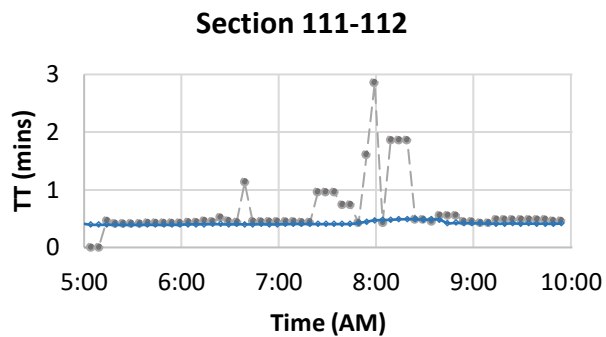
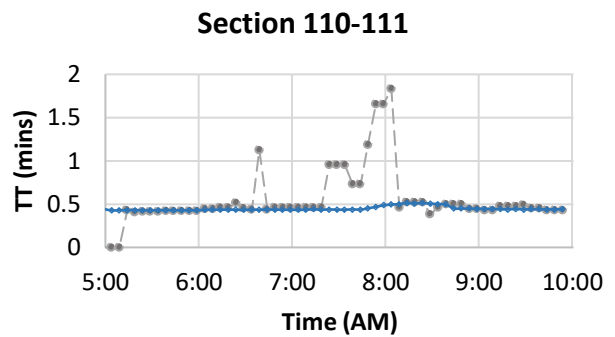
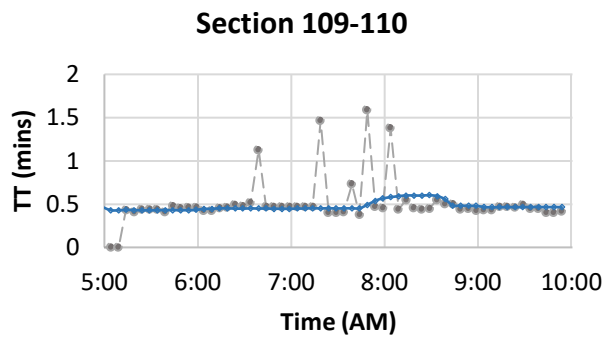
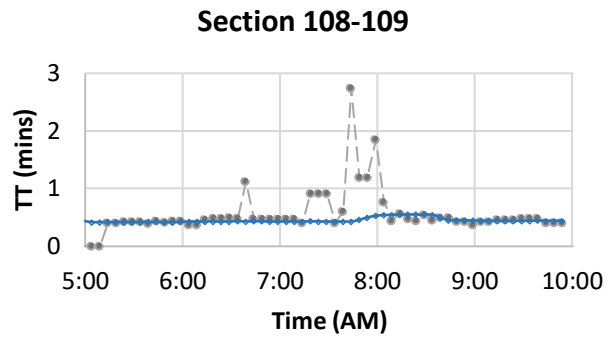
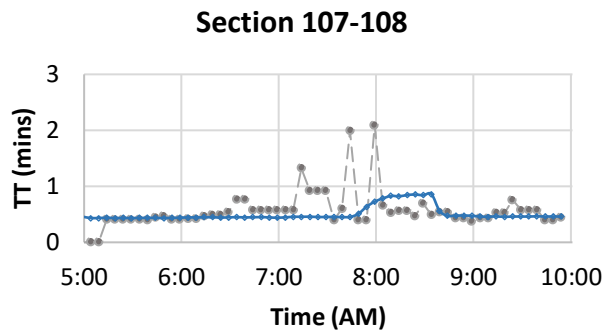
Section 105-106



Section 106-107



--●-- Observed_TT —◆— Calibrated_TT



---●--- Observed_TT —◆— Calibrated_TT

Figure C-1. Section wise comparison of observed and calibrated TTs



NICR

**NATIONAL INSTITUTE FOR
CONGESTION REDUCTION**

The National Institute for Congestion Reduction (NICR) will emerge as a national leader in providing multimodal congestion reduction strategies through real-world deployments that leverage advances in technology, big data science and innovative transportation options to optimize the efficiency and reliability of the transportation system for all users. Our efficient and effective delivery of an integrated research, education, workforce development and technology transfer program will be a model for the nation.



www.nicr.usf.edu